

## Response to Editor

Many thanks to the two reviewers for their detailed and constructive comments on the manuscript. Our revisions include major modifications to the introduction and discussion, new analyses to capture the impact of forest canopy on snow depth, and improvements to the clarity, importance, and target audience of the paper.

As outlined in more detail in our responses to the review comments, the most major revisions are new analyses to test how well the ground results match each other as a function of canopy and ground characteristics. The results reveal distinct snow conditions by vegetation cover (field, coniferous forest, and deciduous forest) as well as slope. We use methods from forest ecology to use our snow-off lidar survey to construct maps of vegetation cover type using a Canopy Height Model (CHM) to distinguish the upper level intact coniferous canopy from other forest cover. Ground and canopy height profiles derived from the lidar dataset are also used to explain differences in lidar derived observations and performance. The use of lidar returns to characterize the forest canopy along side estimates of snow depth is an important strategy for the snow community seeking insight to snow-vegetation interactions and is now highlighted in the revised manuscript.

We also note that Harder et al.'s (2020) UAV lidar manuscript was published on June 15<sup>th</sup> and found by the author team as we were finalizing our comments. The author team has included references to this Harder et al. (2020) in our revisions.

Our response to each comment is outlined below in **bold**. Revised text is in red with line numbers referenced to the manuscript without track changes. We hope these responses are clear, and we look forward to submitting the revised manuscript.

Harder, P., Pomeroy, J. W., and Helgason, W. D.: Improving sub-canopy snow depth mapping with unmanned aerial vehicles: lidar versus structure-from-motion techniques, *The Cryosphere*, 14, 1919-1935, 2020.

## Anonymous Referee #1

*Thank you for the detailed comments and the opportunity to clarify that this article is the first to present snow depth maps measured with UAS-based lidar. We have provided detailed responses to the reviewer following each of the reviewer's comments.*

Received and published: 4 May 2020

Jacobs et al. present snow depth maps measured with a lidar onboard an unmanned aerial system (UAS). The snow depth are calculated as the difference between a snow- on and a snow-off DTM. They study a shallow snowpack with snow depth inferior to 20 cm in a flat open terrain and forested terrain. The lidar snow depth are compared to in situ magnaprobe measurements. They also provide some insights on what controls the lidar precision. The article is innovative as results are obtained with a new combination of sensors and platform which is lidar and UAS. This was, to my knowledge, only suggested by Vander Jagt et al. (2015) but not yet tested. Although this article focuses on shallow

snowpack, it can be inferred that this method is promising for deeper snowpacks in open terrain. I see two points which should be addressed before I would recommend this article for publication.

1. The novelty of this work is not well highlighted. L 95, the authors state: “However, to date there are few previous studies that estimate snow depth using UAS-based lidar (Vander jagt et al., 2013(5!)).”. In my understanding Vander Jagt et al. did not use UAS-based lidar and no other study ever did. The authors should verify the method in Vander Jagt et al. (2015) and cite the “few previous studies” that did similar work, if they exist. If this article is the first to present snow depth maps measured with UAS-based lidar, this should be clearly stated.

**A. We reviewed the earlier manuscript and concur that our manuscript is the first UAS-based lidar snow depth mapping manuscript when it was reviewed and during our revision. Shortly prior to resubmission, on June 15<sup>th</sup>, Harder et al. 2020 was published. There is a notable difference in systems between our study and their study. They also used a considerably more expensive system (~\$300K Canadian). We modified the abstract and the introduction to clarify.**

**Lines 17-19** This paper provides some of the earliest snow depth mapping results on the landscape scale that were measured using lidar on a UAV. The system, which uses modest cost, commercially available components, was assessed in a mixed deciduous and coniferous forest and open field for a thin snowpack (< 20 cm).

**Lines 99-103** However, to date there is only one other published study that estimated snow depth using UAS-based lidar (Harder et al., 2020). However, to date there are no published studies that estimate snow depth using UAS-based lidar. The purpose of this paper is to assess the ability of a UAS platform to provide snow depth using a modest cost UAS-based lidar. The pilot study described here serves as a proof-of-concept for providing a high vertical resolution snowpack dataset in open terrain and forests in the north-eastern United States.

2. The main drawback which should be resolved is the way the “precision” and “accuracy” of the lidar snow depth maps are presented through the article. First, these two terms are not clearly defined. “Precision of the mean snow depth” is found first at L 232 and compared to “one-sided confidence interval”. However, this last term is defined as equivalent to “the uncertainty of the lidar estimate of the snow depth” L181 in a confusing paragraph. Following this, it seems like we end up comparing “accuracy” and “precision” of the snow depth (L232) which I do not think was the initial goal. I rather understood that the authors intend to compare i) the accuracy calculated by comparing lidar and magnaprobe snow depth to ii) the lidar precision defined as the one-sided confidence interval. If I understood correctly, this need to be clearly stated, terms to be defined and consistently used. The definition of precision and accuracy proposed in Eberhard et al. (2020) found in Maune and Naygandhi (2018) might help. Related to this topic, the authors use within-cell standard deviation of the elevation twice: in equation (1) in what seems related to the accuracy of the lidar and L 262 to define “the within-cell variability”. It seems like in the first case, the standard deviation results from error in the

lidar while in the second case, the standard deviation results from the natural variability of the snow pack. As long as this is not clarified, it is hard to understand the point of the paragraph starting L260 in which the authors state that “In addition to the lidar point cloud density, the ability to precisely capture the snow depth also depends on the within cell variability”.

**A. Good point and this comment warranted considerable consideration and clarification for the reader. The reviewer’s interpretation of our intent regarding accuracy is correct. However, our measure of variability is a combination of the instrumentation precision and the sample-to-sample variability within the grid cell (due to variations in surface elevation). Unlike Eberhard et al. (2020), the lidar returns in this study are only a sample of the entire surface. Thus, even if repeated lidar measurements agreed perfectly, there would still be variability within the pixel. We entirely rewrote section 2.6 Snow Depth Uncertainty Assessment. We have revised the definition of “accuracy” and provided a detailed context to the meaning of the confidence intervals of the lidar snow depth maps. Regarding the pooled standard deviation, this is a measure of the variability of the snow on and snow off lidar returns within a grid cell. This variability would depend on both lidar instrument and surface elevation variations. We also clarified the paragraph on L 260 to match the language (now lines 303 to 305). The text has been modified throughout to remove the term precision unless it specifically refers to a measure of the lidar instrumentation variability and to replace it with the “confidence interval”.**

**Lines 219 to 237** The snow depth accuracy was assessed by comparing the lidar snow depth measurements to the magnaprobe measurements. Here, accuracy is the measure of the agreement of the lidar snow depth measurements relative to the in situ measurements (Eberhard et al., 2020; Maune and Nayegandhi, 2018). Error statistics were calculated and the results were summarized by forest and field locations. At each magnaprobe location, the average and standard deviation of the five magnaprobe samples were calculated. The average lidar snow depth was determined for a 0.4 x 0.4 m cell centered on the center magnaprobe location. The mean absolute difference (MAD) and root mean square difference (RMSD) were used to characterize the differences between the magnaprobe snow depths and the lidar snow depths.

The one-sided width of the 95% confidence limits for each cell’s snow depth is a measure of the lidar snow depth variability. Confidence intervals are calculated using a cell’s pooled standard deviation, the number of lidar returns, and the pooled degrees of freedom (Helsel and Hirsh, 1992) to calculate. A cell’s snow depth pooled standard deviation  $\sigma_d$  of the snow on and snow off elevations was calculated as

$$\sigma_d = \sqrt{\sigma_{on}^2 + \sigma_{off}^2} \quad (1)$$

where  $\sigma_{on}$  and  $\sigma_{off}$  are the standard deviation of the snow-on and snow-off lidar return elevations, respectively. This pooled standard deviation is a measure of the variability of the snow on and snow off lidar returns within a grid cell. This variability depends on the lidar instrument’s relative accuracy (Maune and Nayegandhi, 2018), which includes

intra-swath accuracy (i.e., precision or repeatability of measurements) and inter-swath accuracy (i.e., differences in elevations between overlapping swaths), as well as surface elevation variations. The contribution from the individual sources of variability was not assessed.

**Lines 347 to 348** In addition to the lidar point cloud density, the ability to precisely capture the snow depth also depends on the ground surface variability within a cell variability as well as the lidar performance.

Minor comments are listed below. L21 : better repeat snow probe instead of “in situ” L21 : “with” instead of “from” ?

**A. Modified.**

L 34 : Make clear that the albedo is “higher” than the ground albedo not than the deeper snowpacks albedo.

**A. This line was removed when the introductory paragraph was modified significantly to reflect reviewer 2’s comments about shallow snowpack and this reviewer’s more general statement about the value of high-resolution snow depth measurements beyond shallow snowpacks.**

**Lines 30 to 48** Snowpacks are highly dynamic, accumulating and ablating throughout the winter with associated changes in snowpack density, grain size, and albedo (Adolph et al., 2017) as well as ice formation. Wind redistribution, sloughing of snow-off slopes, trapping of snow by vegetation, and forest canopy interception result in a range of spatial features at varying scales (Clark et al., 2011; Mott et al., 2011; Mott et al., 2018). Modest differences in snowpack depth can differentially impact many hydrologic, agricultural, and ecosystem processes. Differences in snowpack meltwaters can alter streamflow volumes (Gichamo and Tarboton, 2019), change the likelihood of spring floods (Tuttle et al., 2017) and intensify overland nutrient transport and soil erosion (Seyfried et al., 1990; Singh et al., 2009).

High-resolution snow depth measurements are also needed to discern processes that depend on the snow state. Insulation by seasonal snow in the Arctic and Antarctic slows sea ice growth (Sturm et al., 2002). High-resolution Arctic snow depths from ICE-Sat2 revealed seasonal snow on ice that would be missed when using coarser snow information (Kwok et al. 2020). Thin, ephemeral snowpacks have limited insulation and allow the underlying soils to freeze more readily in the winter (Groffman et al., 2001; Starkloff et al. 2017; Yi et al. 2019). Soil frost severity impacts soil respiration, carbon sequestration, nutrient retention, and microbial communities as well as a plant root health and tree growth (Aase and Siddoway, 1979; Isard and Schaetzel, 1998; Monson et al., 2006; Henry, 2008; Aanderud et al., 2013; Tucker et al., 2016; Sorensen et al., 2018; Reinmann and Templer, 2018). Detection and mapping of rapid thinning of snowpacks followed by frigid cold during “winter whiplash” events (Casson et al. 2019) is therefore important for understanding ecosystem impacts of soil freezing events, which are otherwise not well quantified (Kraatz et al. 2018; Prince et al. 2019). High vertical resolution snow mapping would greatly improve our understanding of these unique



habitats.

L 55 : precise “point measurements”

**A. Modified.**

L 55-57 : Could you clarify this sentence. Maybe split it in two. Plus, I do not understand the opposition you see between increasing spatial variability and small-scale feature. Finally, is it so sure that spatial variability “naturally increases with spatial scale”? Fig. 4. of Deems et al. (2006) seems to show that spatial variability stops increasing above a typical distance of the order of 10 m.

**A. Thank you for the Deems et al. (2006) reference, which points to a short-range fractal segment and a long-range with a break between 15 and 40 m. The referenced lines were split as recommended to make two separate points as follows:**

**Lines 54 to 57** Using traditional, precise point measurements with a limited sample size, the experimental design requires a balance between the sampling extent and sample spacing (Clark et al. 2011). However, the choice of sampling resolution may yield different measures of snow depth spatial variability when the snow exhibits multifractal behaviour (Deems et al. 2006).

L 63: If you list the methods using difference of surface elevation, you may want to include spaceborne photogrammetry (e.g. Marti et al. 2016, McGrath et al. 2019, Shaw et al. 2019). Otherwise, if you prefer focusing on airborne method, you should remove references to terrestrial laser scanning.

**A. The list of methods was modified to include spaceborne references provided by the reviewer.**

**Lines 61 to 66** Spaceborne photogrammetry (e.g. Marti et al. 2016, McGrath et al. 2019, Shaw et al. 2019), airborne laser scanning (ALS) (Deems et al., 2013; Harpold et al., 2014; Kirchner et al., 2014), terrestrial laser scanning (TLS) (Grünwald et al. 2010; Currier et al. 2019), and structure-from-motion photogrammetry (SfM) (Nolan et al., 2015; Bühler et al., 2016; Harder et al., 2016) have emerged as viable methods to map surface elevations with snow-off and snow-on conditions in order to differentially map snow depths.

L 76 : what is “micro scale” and “field scale” ?

**A. We clarified the scales and now Clark et al.’s definitions where they define point scales as less than 5 m and associated with topographic depressions and trapping or interception by individual vegetation features; hillslope or field scales are 1-100 m and associated with drifting and forest canopy interception and sublimations.**

**Lines 76 to 80** For some snowpack features, the typical vertical accuracies from these platforms, on the order of 10 cm (Kraus et al., 2011; Deems et al., 2013), as well as relatively low return density ( $\sim 10$  returns/m<sup>2</sup>) (Cook et al., 2013) may not be adequate to

observe spatial variations at point scales (0 to 5 m) to hillslope and field scales (1-100 m) or to detect snow depth changes over short time scales.

L 96 : Vander Jagt 2015

**A. We removed the Vander Jagt reference in this statement.**

L 135 : How do such angles occur since the channels are between  $-15/+15^\circ$ ? Is it because of the roll and pitch of the UAS?

Because of degrading accuracy at distances  $>100$  m with the VLP-16, returns acquired outside of  $\pm 30$  degrees of nadir view angles were filtered to limit target distance and improve overall accuracy

**A. We clarified in the text that there are two different field of views on this sensor: 1) the vertical field of view (channels between  $-15/+15^\circ$ ) and 2) the horizontal field of view (rotation angle of channel,  $0-360^\circ$ ). While returns from all vertical field of view channels were used, returns from wide angle views retrieved by each channel (outside of  $\pm 30^\circ$  of nadir) were removed.**

**Lines 131 to 133** The VLP-16 is a 16-channel lidar with a 30-degree vertical field of view with rotating lasers that are spaced evenly between  $-15$  to  $+15$  degrees, with each channel rotating to provide a horizontal field of view of 360-degrees.

**Lines 144 to 146** Because of degrading accuracy at distances  $>100$  m with the VLP-16, returns acquired outside of  $\pm 30$  degrees of nadir view angles in the horizontal field of view were filtered to limit target distance and improve overall accuracy.

L 151 : Please indicate what kind of “non-ground point” you observe in this area. Trees, artifacts.. ?

**A. The progressive morphological filter only identifies ground returns– remaining returns are assumed to be primarily from vegetation (trees and understory shrubs). We clarified this discussion by rewording the first sentence and specified that remaining points are assumed to be from trees and vegetation with minimal artifacts.**

**Lines 159 to 162** The PMF operates iteratively on sets of two parameters, window size and elevation thresholds to erode and dilate point cloud data sets to estimate surface topography as an approach to filter out non-ground returns (i.e. trees, shrubs, and noise) from point cloud data sets (Zhang et al., 2003).

L 153 : Do you further use th and w notations ?

**A. No, these were removed.**

L 154 : “mean” without s?

**A. No. “means” was replaced with “approach”**

L 159 :What do you mean with “Following processing”? The sentence is not clear.

**A. The text was clarified.**

**Lines 167 to 169** Following ground classification for each tile, returns within the 15 m tile buffers were removed, and all resulting 100 m square ground classified tiles were merged. The resulting point clouds for each data set included both the classified ground returns and the non-ground returns.

L 181 : This paragraph is confusing. It seems that lines 181 and 187 are not consistent. Is the “uncertainty” from L181 the same as the one from L187? See main comment about precision and accuracy. L 181 : you state “uncertainty of the lidar estimate of the snow depth” is the “one-sided 95 % confidence interval” L 185 : you define a “pooled standard deviation” not used after. L 187 : you combine “snow depth uncertainty”, “number of lidar return” and “pooled degrees of freedom” to calculate “the one-sided width of the 95 % confidence limits”

**A. This paragraph has been rewritten to address the confusion and word choice after a careful review of the Reviewer’s comments and reading Maune and Nayegandhi (2018). The within cell variability is not negligible. The confidence interval reflects the within cell variability and, when combined with the lidar precision Please see the earlier comment for additional information. Please see the earlier comment for additional information.**

**Lines 226 to 237** The one-sided width of the 95% confidence limits for each cell’s snow depth is a measure of the lidar snow depth variability. Confidence intervals are calculated using a cell’s pooled standard deviation, the number of lidar returns, and the pooled degrees of freedom (Helsel and Hirsh, 1992) to calculate. A cell’s snow depth pooled standard deviation  $\sigma_d$  of the snow on and snow off elevations was calculated as

$$\sigma_d = \sqrt{\sigma_{on}^2 + \sigma_{off}^2} \quad (1)$$

where  $\sigma_{on}$  and  $\sigma_{off}$  are the standard deviation of the snow-on and snow-off lidar return elevations, respectively. This pooled standard deviation is a measure of the variability of the snow on and snow off lidar returns within a grid cell. This variability depends on the lidar instrument’s relative accuracy (Maune and Nayegandhi, 2018), which includes intra-swath accuracy (i.e., precision or repeatability of measurements) and inter-swath accuracy (i.e., differences in elevations between overlapping swaths), as well as surface elevation variations. The contribution from the individual sources of variability was not assessed.

L 185 : Does this assume that the spatial variability within the cell is negligible? See main comment on precision, accuracy.

**A. Please see the response to the previous comment.**

L 191 and following : Please make clear for what resolution these percentages hold.

**A. The resolution was clarified.**

**Lines 241 to 243** The snow-on and snow-off flights lidar ground returns yielded an average point cloud density of 90 and 364 points/m<sup>2</sup> in the forest and field, respectively, with 6.7% of the forest and 0.03% of the 1 m<sup>2</sup> field cells having less than 5 point/m<sup>2</sup>

(Figure 2).

L 198 : You state “0.95 %” of the forest cells are empty for the 1 m resolution grid. Does that correspond to the white areas in the western forest (Fig. 4)? In case it is, this seems to be more than 1 % of the forested area. In case it is not, what are these white areas?

**A. Thank you for catching an issue with the eastern forest boundary. The white areas in the eastern forest are empty cells resulting for a river that runs along the forest. Infrared energy is absorbed by water; therefore, no lidar data were collected over the river. The forest boundaries in Fig 1 and 4 were updated to reflect the eastern forest boundary that was used in the analysis, which excludes the river.**

L 212 : In “(12.2 cm  $\pm$  0.56 cm)”, is 0.56 cm the standard deviation of the population of mean snow depth ? Or is it related to the standard deviation described in L 185?

**A. The 0.56 cm standard deviation is the standard deviation of the in situ Magnaprobe measurements in the field. The mean snow depth was calculated at each in situ sampling location. Then the average and standard deviation of the field locations (N = 11) was calculated. It is not related to the pooled standard deviation described on L 185. The pooled standard deviation described on L185 was used to calculate the 95% confidence intervals of the lidar derived snow depth.**

L 215 : First time the word “tube” is used. Was it the “federal snow sampling tube” (L 172) ?.

A. Yes, it is the federal snow sampling tube.

**Lines 263 to 265 The mean snow depth from the Federal snow tube was (12.9 cm  $\pm$  0.71 cm) and (13.1 cm  $\pm$  1.9 cm) in the field and forest, respectively. There is a notable low bias in the lidar forest snow depth relative to the magnaprobe and snow tube for west forest in particular with exception of one site.**

L 232-233 : “precision” is not defined above. This sentence is thus hard to understand.

**A. See previous response and definition in section 2.5.**

**Lines 233 to 237 This variability depends on the lidar instrument’s relative accuracy (Maune and Nayegandhi, 2018), which includes intra-swath accuracy (i.e., precision or repeatability of measurements) and inter-swath accuracy (i.e., differences in elevations between overlapping swaths), as well as surface elevation variations. The contribution from the individual sources of variability was not assessed.**

L. 260 : " In addition to the lidar point cloud density, the ability to precisely capture the snow depth also depends on the within cell variability. " Why? Is it a statement based on the way you calculate the lidar precision or an assumption which should be justified? See main comment on within-cell variability.

**A. This was clarified in the initial comment on the topic. We modified this sentence to clarify that there are two sources of variability in the cell. “**

**Line 347 to 348 In addition to the lidar point cloud density, the ability to precisely**

capture the snow depth also depends on the ground surface variability within a cell as well as the lidar precision.

L. 260 : this is not mandatory but since you use standard deviation, did you check whether the distribution is normal or not ?

**A. We didn't check normality on a cell-by-cell basis, but did calculate the moments including skew values on a cell-by-cell basis at various scales. At the 10 and 20 cm cell size, there was not a notable skew. Larger cell sizes had increasingly negative skews with skew values typically less than -1.**

L 319 “boresighting”

L 319. Could you explain what boresighting is ? Not sure The Cryosphere readers know what it is.

**A. Considerable additional explanatory text and figures were added to the discussion on boresighting in order to provide a specific example to anyone who is new to airborne lidar. Our goal is to provide a specific example using a snow depth survey that will provide information beyond that available in a standard textbook discussion of boresighting. The new text and revised figure were moved to supplemental material. This location change was in response to Reviewer 2's comment about Figure 7: “OK...but anyone new to airborne lidar will not understand it, and anyone already doing SfM or lidar will not need it. Within the supplemental material we define boresighting.**

**Lines S8 – S9 Boresighting is the process of calculating the differences between the lidar sensor and IMU roll, pitch, and yaw angle measurements to correct those errors in point clouds.**

L. 368 : Could you provide details about the “simple penetration test” ? If this not it, do you think it would be possible to dig a snow pit at the location of the magnaprobe measurement to evaluate probe penetration?

**A. Based on Reviewer 2's comments, this sentence was removed and replaced with additional details about the soil frost depth. In the future, it would be possible to dig a snow pit at the magnaprobe locations to determine. We did not do this during the experiment because we did not observe the bias until the lidar datasets had been post-processed.**

**Line 211 to 217 An independent study collected soil frost depth from three locations at the Thompson Farm Research Observatory using Gandahl-Cold Regions Research and Engineering Laboratory (CRREL) style frost tubes. The frost tubes have flexible, polyethylene inner tubing filled with methylene blue dye whose color change is easy to differentiate when extruded from ice (Gandahl 1957). A nylon string housed inside the polyethylene tubing affixes ice during periods of thaw. The outer tubing consists of PVC pipe installed between 0.4 to 0.5 m below soil surface (Ricard et al., 1976; Sharratt and McCool, 2005). Prior to the January 19<sup>th</sup> and 20<sup>th</sup>, 2019 snowfall event, soil frost was 23.5 to 25.5 cm in the field and 5.5 to 8.5 cm in the west forest.**

L. 389 : “moderately” please give values.

**A. Values were added to the text.**

**Line 508 to 510** Mapped at 1 m<sup>2</sup> cells, a 0.5 to 1 cm snow depth confidence interval was achieved consistently in the field with confidence intervals increasing to within 4 cm in the forest and heavily vegetated areas.

L 510. Missing a carriage return before “Starkloff”

**A. Carriage return was added.**

Fig. 1: what’s the reason for the buffer around the forest polygon, especially why is the forest peninsula out of both zones (east of the field, west of the western forest) ?

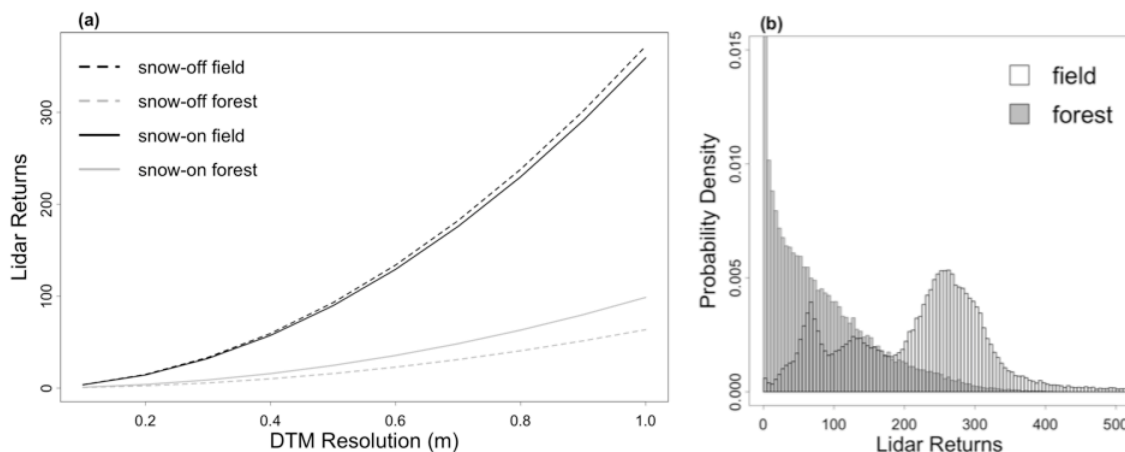
**A. Thank you for the keen eye. The buffer around the forest polygon was removed and the peninsula is now included in the eastern forest. All plots and figures were updated to reflect any changes to the field/forest boundaries.**

Fig. 2.a The number of returns per cell seems to follow a relationship of type  $y=kx^2$  with  $k$  the average density of the point cloud and  $x$  the cell resolution. Could you comment on that? Did you expect that?

**A. Yes, this nonlinear relationship could be expected because the counts are based on area of the DTM (length squared) rather than the resolution (length). For example, if a 1 m x 1 m areas (1m<sup>2</sup>) have 100 returns, then a 2 m x 2 m areas (4m<sup>2</sup>) should have 400 returns.**

Fig. 2.b It is not so easy to distinguish the two distributions. Maybe remove the vertical lines of the bars?

**A. The hatched fill pattern has been removed. Also, the line weight of the field distribution has been increased to more easily distinguish between the two distributions.**



**Figure 2.** (a) Average lidar point cloud density of the ground returns with versus cell size by land cover, and snow-on and snow-off state (top). (b) Probability density function for the lidar ground returns point cloud density for 1 m<sup>2</sup> cell for the forest (gray) and the field (hashed) (bottom).



Fig. 5, what are the gray points/area on panel a. It seems absent in panel b.

**A. The points showed the individual outliers of the distributions. They have now been removed from figure 5a.**

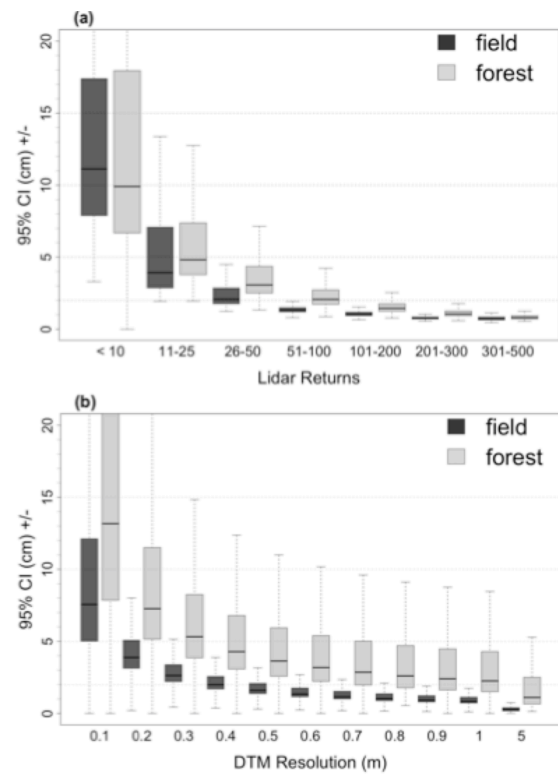


**Figure 5.** One sided confidence intervals of the mean snow depth values in the field and forest at Thompson Farm, Durham, NH on January 23, 2019 from the individual cells for 1 m<sup>2</sup> cells by land cover and point cloud density (top) and for grid resolutions ranging 0.1 to 5 m (bottom). Boxplots show the lower quartile, median, upper quartile, and whiskers.

Fig. 6.a. Isn't that surprising that the STD per cell is the same with snow on and off in the forest? Could you comment on that?

**A. Yes, this is somewhat surprising and we had not seen this effect noted in previous studies. A comment was added to offer an explanation for the difference.**

**Line 350 to 353** Snow cover reduces the within cell variability in field by about 1 cm, but has a limited effect in the forest. It is possible that the modest snowpack was able to flatten the higher grass in the field, while the forest's vegetation and terrain features that dominate the within cell variability are only minimally compacted by the snow.

Fig 7. Label the panels a,b,c,d instead of A/B top/bottom. Zoom in the panel b. Keep a. as it is and add a square showing where b. is. It is really not clear what is shown in A,B. Are we in 2D view from top in A and from profile in B?

**A. Figure was heavily modified, with many clarifications included in the figure caption and the text. All boresighting figures and text are now in supplemental materials part 3.**

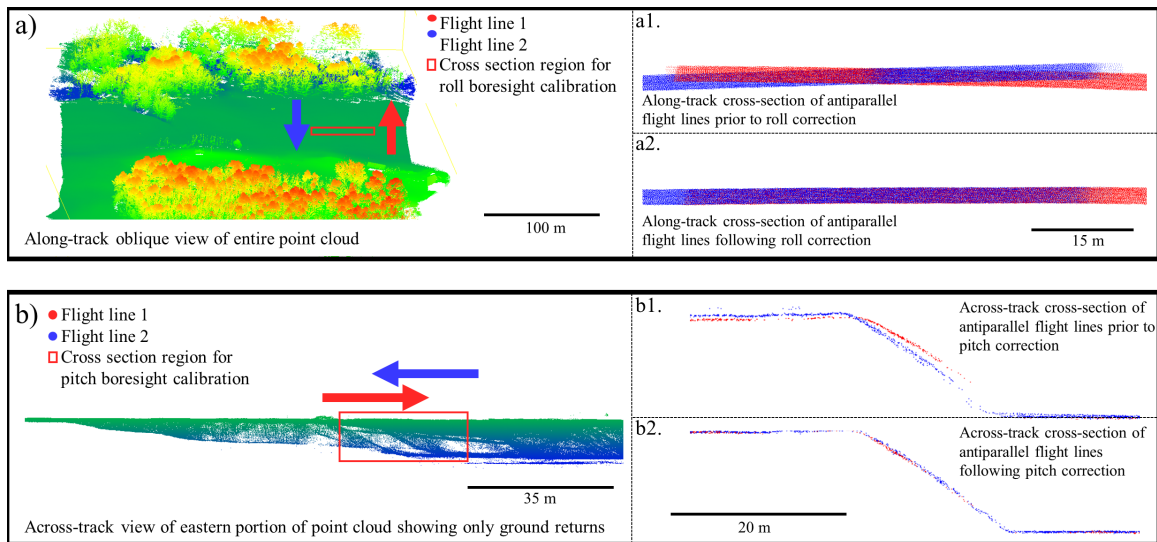


**Figure S3.** Uncalibrated boresight angles between the INS and lidar sensor can result in poorly aligned point clouds (a1 and b1). Arrows in (a) and (b) show approximate flight direction during data acquisition. The lidar returns within the box marked in red in (a) are shown in (a1) and (a2) at an oblique view angle. Figure (a1) shows how boresight errors of roll angles present, while (a2) shows proper boresight alignment for roll. Roll alignment errors present well in anti-parallel flight lines (flight lines flown parallel to each other but in the opposite direction), flown over **flat** terrain. Figure (b) shows the approximate location of returns used for pitch boresight alignment error demonstration (b1) and its correction (b2). Pitch misalignment presents well in anti-parallel flight lines in areas with terrain relief while viewing across the flight track, as opposed to along the flight track as with roll alignment. For (b, a1, a2, b1, and b2), only ground returns are shown for each flight line, while in (a), all returns are shown.

The following references were added to the manuscript based on Reviewer 1's input:

- Deems JS, Fassnacht SR and Elder KJ (2006) Fractal Distribution of Snow Depth from Lidar Data. *J. Hydrometeorol.* 7(2), 285–297 (doi:10.1175/JHM487.1)
- Eberhard LA, Sirguey P, Miller A, Marty M, Schindler K, Stoffel A, Bühler Y (2020) Inter- comparison of photogrammetric platforms for spatially continuous snow depth mapping *Cryosphere Discussions* (<https://doi.org/10.5194/tc-2020-93>)
- Marti R, Gascoin S, Berthier E, De Pinel M, Houet T and Laffly D (2016) Mapping snow depth in open alpine terrain from stereo satellite imagery. *Cryosphere* 10(4), 1361–1380 (doi:10.5194/tc-10-1361-2016)
- Maune DF (Ed.) and Naygandhi A (Ed.) *Digital Elevation Model Technologies and Applications: The DEM Users Manual*, 3rd Edition, 3 ed., 652 pp., 2018.
- McGrath D, Webb R, Shean D, Bonnell R and Marshall HP (2019) Spatially Extensive Ground Penetrating Radar Snow Depth Observations During NASA's 2017 SnowEx Campaign: Comparison With In Situ, Airborne, and Satellite Observations. *Water Resour. Res.* 10 (doi:10.1029/2019WR024907)
- Shaw TE, Gascoin S, Mendoza PA, Pellicciotti F and McPhee J Snow depth patterns in a high mountain Andean catchment from satellite optical tri- stereoscopic remote sensing. *Water Resour. Res.* di (doi:10.1029/2019WR024880)
- Vander Jagt B, Lucieer A, Wallace L, Turner D and Durand M (2015) Snow Depth Retrieval with UAS Using Photogrammetric Techniques. *Geosciences*, 264–285 (doi:10.3390/geosciences5030264)

**Interactive comment on The Cryosphere Discuss., <https://doi.org/10.5194/tc-2020-37>, 2020.**

Anonymous Referee #2

*Thank you for the detailed comments and the opportunity refine the original submission and to consider variations across land-use and terrain. We have provided detailed responses to the reviewer following each of the reviewer's comments.*

Received and published: 5 May 2020

In this study, the investigators mounted a small airborne lidar on a drone and flew several test flights to map snow depths across a small flat farm in New Hampshire that contained fields and forest. They then chose one flight to examine in detail. Most of the paper is concerned with the accuracy of the resultant snow depth maps, with comparison of those derived depths against on-the-ground probing (n=130), and with an extensive analysis of accuracy vs. ground point spacing from the lidar.

My overall impression of the paper is that a single acquisition flight in a single landscape, with a quite limited ground collection campaign, is too thin a reed on which to base a full journal publication. Such a limited comparison leaves open too many questions, like what the results would be if the ground was sloped, how the results would vary if the forest canopy was conifer vs. deciduous, what would happen if the snow had surface relief or other characteristics not tested in this work. In fact, the authors Figure 1 indicates a complex forest with openings and variable canopy density (a snow season air photo here would have been nice), but no attempt has been made to see if the results from one part of the forest look like those from another. No attempt was made to test how well the ground and air results match each other as a function of canopy and ground characteristics. Lastly, while the lidar and ground measurements matched beautifully in the open field, they showed a large discrepancy in the forest, which was then ascribed to over-probing through a duff layer. Perhaps that is the case, but this then ought to have been the focus of more analysis and scrutiny. The conclusion is certainly possible, but Figure 2b suggests there is also lidar sampling bias problem in the forests, and the core depths referred to in the text against which the depth probe depth was compared are never discussed, even to the extent of how many were made.

**A. The reviewer makes a number of reasonable points regarding the long-term value of limited flights over limited landscapes. We entirely agree that this submission leaves open questions, particularly given the strong contrast in performance between the field and the forest. Based on the reviewer's comments, we reconsidered this paper's contribution in light of the early structure from motion (SfM) papers that used a UAS platform to characterize snow depth. A summary of those studies in light of the reviewer's comments appears in Table R1 (below). These recent papers share many commonalities with the current study in that they seek to understand how a recent technological development might contribute to improved understanding of the snow depth. The table shows how the literature and experiments evolved over time. These papers also demonstrate that the experimental design and results from this study equals or exceeds that of these early SfM studies that also sought to demonstrate the value of a new combination of sensors and platform.**

Yr Flown	Location	Area	# flights	Site (# and Description)	Validation	Error	Method Detail	Study
2013	Tasmania, Australia	0.0069 km <sup>2</sup>	1	1. strong gradient in elevation, thick vegetation and various soil/rock	Survey pole 37 measured, N= 20 due to vegetation, survey at snow surface, then ground surface	0.10 m (acc) RMSE = 9.6 cm	Yes & Workflow	(Vander Jagt et al. 2015)
2014	Lombardy region, northern Italy	0.3 km <sup>2</sup>	1	1. sparse grass coverage and rocks, with no tree, firn, or glacier ice.	12 probe measurements horiz. accuracy 2–3 cm.	Bias 0.073 m and aRMSE = 0.14 m	Yes	(De Michele et al. 2016)
2015	Rosthern, Saskatchewan, Canada  Canadian Rocky Mountains	0.65km <sup>2</sup>  0.32 km <sup>2</sup>	22, 18	1. Canadian prairie; tall stubble (35 cm) and short stubble (15 cm) Sparsely vegetated 2. Rocky Mountain alpine ridgetop grasses, shrubs and coniferous trees in gullies	Ruler with 17 snow stakes - horiz.accuracy ±2.5 cm. 34 points  Alpine: 3 to 19 pts per flight. 5 SD measurements in a 0.4 m × 0.4 m square at that point	8.8 cm for a short stubble, 13.7 cm for a tall stubble 8.5 cm alpine mean SD must be > 30 cm	Yes	(Harder et al. 2016)
2015	Davos, Switzerland	0.057 – 0.091 km <sup>2</sup> 0.29 km <sup>2</sup>	3/1	1. Tschuggen: flat alpine meadows and hilly alpine terrain 2. Brämabühl: an exposed location meadow and bushes	60, 95, 95 and 110 (5 pts per site) 5 SD measurements in a 1 m × 1 m square - center pt horiz. accuracy < 10 cm	Overall RMSE = 0.25 m bias = 0.2 m Short grass RMSE 0.07 m bias 0.05 m Bushes/high grass RMSE 0.30 m bias 0.29 m alpine RMSE 0.15 m bias 0.11 m	Yes	(Bühler et al. 2016)
2016	Piedmont region, Italy	0.0067 km <sup>2</sup>	1	1. sparse rocks and grass, with no trees	135 pts and TLS UAS, a multi station survey, and manual probing	RMSE = 0.31 m overall RMSE = 0.17 m areas of likely water accumulation removed	limited	(Avanzi et al. 2017)
2016	Canada	0.02 km <sup>2</sup>	13/16	1 and 2. G Gatineau: N. Shrubs up to 1m. S. Shrubs and sm. forested area southwest corner S. 3 to 5. Acadia A. grass (< 5 cm) and stumps (< 20 cm). B stumps (< 20 cm) and brush and shrubs (< 1 m). C 1 – 5 m balsam fir	Transects of ~ 50 m in length; 12 48" × 2" × 1" wooden stakes; no horiz. accuracy	2 to 11 cm RMSD for SD change	Yes	(Fernandes et al. 2018)

Table R1. Review of early structure from motion papers

### References

- Adams, M.S., Bühler, Y., & Fromm, R. (2018). Multitemporal accuracy and precision assessment of unmanned aerial system photogrammetry for slope-scale snow depth maps in Alpine terrain. *Pure and Applied Geophysics*, 175, 3303-3324
- Avanzi, F., Bianchi, A., Cina, A., De Michele, C., Maschio, P., Pagliari, D., Passoni, D., Pinto, L., Piras, M., & Rossi, L. (2017). Measuring the snowpack depth with Unmanned Aerial System photogrammetry: comparison with manual probing and a 3D laser scanning over a sample plot. *The Cryosphere Discuss.*, <https://doi.org/10.5194/tc-2017-57>
- Bühler, Y., Adams, M.S., Bösch, R., & Stoffel, A. (2016). Mapping snow depth in alpine terrain with unmanned aerial systems (UASs): potential and limitations. *The Cryosphere*, 10, 1075-1088
- De Michele, C., Avanzi, F., Passoni, D., Barzaghi, R., Pinto, L., Dosso, P., Ghezzi, A., Gianatti, R., & Della Vedova, G. (2016). Using a fixed-wing UAS to map snow depth distribution: an evaluation at peak accumulation. *Cryosphere*, 10, 511-522
- Fernandes, R., Prevost, C., Canisius, F., Leblanc, S.G., Maloley, M., Oakes, S., Holman, K., & Knudby, A. (2018). Monitoring snow depth change across a range of landscapes with ephemeral snowpacks using structure from motion applied to lightweight unmanned aerial vehicle videos. *The Cryosphere*, 12, 3535-3550
- Harder, P., Schirmer, M., Pomeroy, J., & Helgason, W. (2016). Accuracy of snow depth estimation in mountain and prairie environments by an unmanned aerial vehicle. *The Cryosphere*, 10, 2559
- Vander Jagt, B., Lucieer, A., Wallace, L., Turner, D., & Durand, M. (2015). Snow depth retrieval with UAS using photogrammetric techniques. *Geosciences*, 5, 264-285



In brief, Table R1 indicates that the studies that used SfM to map SD were first published in 2015 and 2016. In those early studies, the number of flights was extremely limited, the surveyed area was typically quite small, there was often only a single site, and the cover conditions were typically relatively short grass, stubble, with limited shrubs and no or limited trees. Studies that estimate SfM SDs in sites having significant tree canopies were published approximately three years after the initial studies. These SfM papers are an example where the early papers use targeted, focused studies to provide the broader community with an approach that is now embraced, and which has been subsequently refined and used to explore a range of landscapes, terrain, and forest canopy.

The submitted manuscript, as noted by Reviewer 1, “is the first to present snow depth maps measured with UAS-based lidar” and the novel contribution is its results that were obtained with a new combination of sensors and platform. Our manuscript also sets the stage for further research by including results that demonstrate a sharp contrast between the field and the forest findings as well as considerable variability of metrics within in the forests. We expect the broader community will contribute the additional studies that the reviewer desires, with more extensive campaigns over a wide range of landscapes, following a similar trajectory of UAV-based SfM in the embracement of new technology. Note that Harder et al.’s (2020) UAV lidar manuscript was published on June 15<sup>th</sup>. The author team has included references to this study.

We revised the manuscript to be clearer about the contribution including in the abstract, the last paragraph of the introduction, and the conclusion. Specifically, we have added context of our work in the Discussion to emphasize the refinement of methodology and new questions that emerged from our work. Our work highlights, unknown at the time of study implementation, sampling and collection finding that are useful for planning for future snow depth studies.

Regarding the lidar sampling bias problem in the forests, the reviewer makes a number of reasonable points including that ascribing the errors to over-probing is likely a gross simplification of the complexity of measuring forest SD. Based on this comment, the discussion section that discusses these issues has been revised, the snow core observation information has been expanded in Section 2.4 (renamed “*In Situ* Observations”) and in Section 4 (renamed “Challenges and Recommended Improvements to UAS Lidar Snow Depth Mapping”, last paragraph), and a preliminary assessment of variations in forest canopy has been added. Even with high ground return lidar that is collected with a UAS, forest canopies still generate collection issues that complicate interpretation and characterization of snow. When collecting data over a region, forest type and canopy characteristics and their impacts on a lidar snow depth survey may not known in advance. We have added a section in the Discussion that describes issues found with forests in our study, including reduced total and ground return density in forests compared to open fields, and we make suggestions on how data collection strategies might be modified for forested areas. Additionally, we suggest that further studies may be warranted to understand how forest vegetation (e.g. canopy species, understory vegetation density, and duff layer quality) contributes to snow depth measurement bias, while pointing to recent

## evidence in the literature of challenges inherent to sampling mixed land-use landscapes with airborne lidar sensors.

### Lines 378 to 425 4.1 *In Situ* and UAS Sampling

While UAS-based lidar surveys can measure snow depth to within a centimeter at high spatial resolutions, validation of those observations is challenging. A time consuming collection of high accuracy GNSS survey points was required to co-locate magnaprobe and lidar observations. Surveying in sample locations prior to the winter season might reduce this effort. It is also challenging to make *in situ* snow depth measurements that provide centimeter accuracy. In this study, the magnaprobe *in situ* snow depth observations made in the forest were considerably higher than the lidar observations as compared to the open field where the magnaprobe and lidar measurements were within 1 cm. Previous studies also found that snow depth observations from ALS measurements are biased lower than those from snow-probe observations in the forest (Hopkinson et al., 2004, Currier et al., 2019; Harder et al., 2020). In past studies, the causes of these differences have been partially attributed to the snow probe's ability to penetrate the soil and vegetation, human observers tending to make snow depth measurements in locations with relatively high snow (Sturm and Holmgren, 2018) and the reduced accuracy of the GNSS. Our study suggests additional issues in forest sampling including enhanced terrain variability in forested areas relative to adjacent field areas and reduced lidar returns in forested areas as compared to field areas combine with sampling issues to contribute to the higher uncertainty in the forest snow depths observed in our study.

In this study, the cold temperatures and snow-free conditions prior to the January 19<sup>th</sup> and 20<sup>th</sup> snowfall event resulted in deeper frozen soils (23.5 to 25.5 cm) in the field and shallower soil frost depth (5.5 to 8.5 cm) in the west forest, which would have limited the probe penetration into soils at both sites. However, the forest has a 1-4 cm thick organic leaf litter layer that may have been penetrated by the magnaprobe. The average Federal snow sampler tube depths (13.1 cm) were not as deep as the magna probe (15.2 cm) and thus more closely match the lidar snow depth (7.8 cm; see Figure 3), though a considerable low bias (~5.3 cm) similar to that found by Harder et al. (2020) persists in the lidar snow depth relative to the federal snow sampler snow depths. Additional factors such as downed logs, thick understory, and fine-scale topographic features (ie: small boulders and hummocky terrain) as well as reduced ground return density may contribute to the lidar snow depth errors in a forest, whereas these factors are absent in the field.

An improved understanding of forest canopies impacts on lidar returns is also warranted. Recent work has demonstrated that lidar pulses are “lost” at a much higher rate in forest canopies than open ground terrain due to interception, absorption, and scattering through canopy transmission, with the loss ratio largely influenced by the range of the target from the sensor (Liu et al., 2020). The data that we presented in this paper were acquired using constant flight speed and at consistent altitude above target areas. Because of this, it is feasible that forest canopy conditions and variable understory vegetation density may have resulted in lost pulses and increased uncertainty in our data set. Indeed, we did observe lower return densities for both ground and all returns in forested areas in our data set (Figure 4).

One possible outcome of these lidar sampling issues in forests was a significant difference in snow depth confidence intervals between field and forest types and among slope groups.

Confidence intervals were highest in conifer stands and on steep slopes and lowest in the field. While this result is not entirely surprising, it is likely partially the result of lower ground return density in forests due to the combined effects of lost pulses and canopy occlusion in forested areas. Additionally, this observation may be driven by increased variability in snow depth due to pockets of duff and woody debris, and due to higher variability in subnivean terrain in the forested areas of the study site. Areas of high terrain relief are expected to have more variability in ground return elevations over shorter distances, which would partially drive higher confidence intervals of ground surface elevation for pixels located in high relief areas. High relief areas of the study site were more common in forested areas of the study site, and the uncertainty resulting around high slopes also carries through snow depth estimation. Snow depth was significantly different between field and forested areas, as well as between conifer and deciduous forest types, despite the relatively high uncertainty. This indicates the possible influence of tree canopies on snow accumulation due to enhanced snow interception in forests, and particularly in conifer stands, but also could be the result of an under-sampled ground surface in forested areas relative to field areas. Snow depth also was significantly different among the three slope groups, possibly due to wind-driven snow displacement and sloughing on slopes during accumulation.

**A. The core depth procedures originally described briefly in Section 2.4 were expanded. The core accuracy values appeared in section 3.2.**

**Lines 206 to 209** Along the same forest and field transects, a federal snow sampler was used to collect a single sample of snow depth and snow water equivalent at each magnaprobe sample location for a total of 12 field samples and 16 forest samples. Snow depth was measured by inserting the aluminium tube vertically into the snowpack and a core was extracted and weighed using a spring scale.

The other problem with the paper is that it is too equipment/system specific. Not everyone reading this paper will have the same drone, the same lidar etc., so what does the paper offer them? It is perhaps necessary to be equipment-specific in this type of paper to some extent, but to maximize its use to the wider community, the authors need to strive to separate what is inherent in the methodology used with the specific equipment test to what might be more universal. They try this in the discussion section with some lessons-learned statements, but these too general and read a bit like “be careful when you drive” rules. I am not sure what would be best in this regard, but some improvement is definitely needed.

**A. We have embraced the reviewer’s comment “the authors need to strive to separate what is inherent in the methodology used with the specific equipment test to what might be more universal.” and have rewritten the discussion section to more keenly focus on what we believe are the most useful lessons learned, broken them into more manageable units and clearly indicated what are generalizable lessons versus those that are instrument specific. The first paragraph in the discussion and sections 4.2 and 4.3 respond to the reviewer’s comments.**

**Lines 307 to 487 4. Challenges and Recommended Improvements to UAS Lidar Snow Depth Mapping**

Despite UAS-based lidar's increasing use in the natural sciences and capacity to make high-resolution snow maps, there are many operational and technical challenges that require consideration prior to successfully conducting UAS-based lidar surveys that produce research grade, high-resolution snow depth data. Even though the UAVs are modest in size (i.e., weighing less than 25 kg), the hardware and supporting software analysis tools can be expensive and require trained pilots and lidar data analysis specialists. In this section, we present some general considerations regarding validation of the lidar snow depth maps, selection and deployment of a lidar sensor on a UAV for snow depth mapping as well as specific insights that we experienced when using our system.

#### 4.1 *In Situ* and UAS Sampling

While UAS-based lidar surveys can measure snow depth to within a centimeter at high spatial resolutions, validation of those observations is challenging. A time consuming collection of high accuracy GNSS survey points was required to co-locate magnaprobe and lidar observations. Surveying in sample locations prior to the winter season might reduce this effort. It is also challenging to make *in situ* snow depth measurements that provide centimeter accuracy. In this study, the magnaprobe *in situ* snow depth observations made in the forest were considerably higher than the lidar observations as compared to the open field where the magnaprobe and lidar measurements were within 1 cm. Previous studies also found that snow depth observations from ALS measurements are biased lower than those from snow-probe observations in the forest (Hopkinson et al., 2004, Currier et al., 2019; Harder et al., 2020). In past studies, the causes of these differences have been partially attributed to the snow probe's ability to penetrate the soil and vegetation, human observers tending to make snow depth measurements in locations with relatively high snow (Sturm and Holmgren, 2018) and the reduced accuracy of the GNSS. Our study suggests additional issues in forest sampling including enhanced terrain variability in forested areas relative to adjacent field areas and reduced lidar returns in forested areas as compared to field areas combine with sampling issues to contribute to the higher uncertainty in the forest snow depths observed in our study.

In this study, the cold temperatures and snow-free conditions prior to the January 19<sup>th</sup> and 20<sup>th</sup> snowfall event resulted in deeper frozen soils (23.5 to 25.5 cm) in the field and shallower soil frost depth (5.5 to 8.5 cm) in the west forest, which would have limited the probe penetration into soils at both sites. However, the forest has a 1-4 cm thick organic leaf litter layer that may have been penetrated by the magnaprobe. The average Federal snow sampler tube depths (13.1 cm) were not as deep as the magna probe (15.2 cm) and thus more closely match the lidar snow depth (7.8 cm; see Figure 3), though a considerable low bias (~5.3 cm) similar to that found by Harder et al. (2020) persists in the lidar snow depth relative to the federal snow sampler snow depths. Additional factors such as downed logs, thick understory, and fine-scale topographic features (ie: small boulders and hummocky terrain) as well as reduced ground return density may contribute to the lidar snow depth errors in a forest, whereas these factors are absent in the field.

An improved understanding of forest canopies impacts on lidar returns is also warranted. Recent work has demonstrated that lidar pulses are “lost” at a much higher rate in forest canopies than open ground terrain due to interception, absorption, and scattering through canopy transmission, with the loss ratio largely influenced by the range of the target from the sensor (Liu et al., 2020). The data that we presented in this paper were acquired using constant flight speed and at

consistent altitude above target areas. Because of this, it is feasible that forest canopy conditions and variable understory vegetation density may have resulted in lost pulses and increased uncertainty in our data set. Indeed, we did observe lower return densities for both ground and all returns in forested areas in our data set (Figure 4).

One possible outcome of these lidar sampling issues in forests was a significant difference in snow depth confidence intervals between field and forest types and among slope groups. Confidence intervals were highest in conifer stands and on steep slopes and lowest in the field. While this result is not entirely surprising, it is likely partially the result of lower ground return density in forests due to the combined effects of lost pulses and canopy occlusion in forested areas. Additionally, this observation may be driven by increased variability in snow depth due to pockets of duff and woody debris, and due to higher variability in subnivean terrain in the forested areas of the study site. Areas of high terrain relief are expected to have more variability in ground return elevations over shorter distances, which would partially drive higher confidence intervals of ground surface elevation for pixels located in high relief areas. High relief areas of the study site were more common in forested areas of the study site, and the uncertainty resulting around high slopes also carries through snow depth estimation. Snow depth was significantly different between field and forested areas, as well as between conifer and deciduous forest types, despite the relatively high uncertainty. This indicates the possible influence of tree canopies on snow accumulation due to enhanced snow interception in forests, and particularly in conifer stands, but also could be the result of an under-sampled ground surface in forested areas relative to field areas. Snow depth also was significantly different among the three slope groups, possibly due to wind-driven snow displacement and sloughing on slopes during accumulation.

#### 4.2 Flight Planning

Because larger UAVs that can carry heavier payloads have challenges that may differ from small UAVs, a well-formulated flight plan that addresses weather conditions, logistics of flying at proposed site, flight lines, UAS equipment, and personnel is clearly needed. Weather impacts operations. UAS surveys cannot be conducted when there is any type of precipitation or in dense fog/clouds because moisture can cause electronic components to malfunction and moisture build-up on the propellers can also adversely affect lift production. Depending on the UAV, wind speeds exceeding 7 to 10 m/s may make flights more difficult. This project's Eagle XF high lift capacity UAS cannot be flown comfortably in winds greater than 8 m/s. At the study site, wind speeds often exceeded this threshold in the days immediately following snowfall except early in the morning. High wind speeds can also significantly reduce battery life as well as impact the accuracy of sensor observations. Low air temperatures can cause batteries to rapidly discharge. For winter UAS surveys, all flight and operational batteries were kept warm in a building, vehicle, or insulated cooler prior to the UAS survey. This also applies to the computer used to upload flight lines and relay telemetry information. A MIL-STD-810 certified Panasonic Toughbook was used in this study to handle the anticipated cold temperatures. Additionally, cold temperatures can severely limit the dexterity of the person manipulating the flight controls.

High lift UAVs capable of carrying a lidar sensor package have the potential to cause significant damage to person and property. The selection of a survey site not only needs to meet the scientific objectives of the UAV survey, but also must have the proper attributes for safe and legal UAV operation including permission to operate the UAV at the site. Visual line of sight

(VLOS) of the UAV needs to be maintained throughout the flight. When it is difficult to maintain VLOS (e.g., flying over forested or mountainous sites), spotters can be used if there is constant two-way communication between the spotters and the person operating the flight controls. For this study, an on-site, walk up tower with a spotter was necessary while the UAV was flown over the forest.

The deployment of a UAV lidar system requires additional flight patterns designed for boresighting to ensure that point clouds are aligned (Painter et al., 2016). Provided that GNSS data are accurate, the most common reason for misalignment of point clouds is boresight angle errors (Li et al., 2019). Boresighting is the process of calculating the differences between lidar sensor and IMU roll, pitch, and yaw angle measurements to correct those errors in point clouds. Due to battery flight time limitations, we were unable to complete the flight pattern that is commonly used for boresighting alignment. Because of this, we leveraged our first two antiparallel flight lines for boresighting calibration. Additional details on boresighting calibration, our technique due to the flight time limitations, and examples of roll and pitch alignment errors observed during this field campaign appear in the supplemental materials.

#### 4.3 UAS Sampling Strategies

While lidar calibration and data post-processing requirements are quite similar for UAS and airborne surveys, the UAS lidar surveys presented in this study have key differences from previous ALS surveys. As noted above, UAS flight durations are considerably shorter, resulting in limited spatial coverage as compared to previous ALS snow depth surveys. An advantage of UAS over ALS surveys is that the average point cloud density is much higher and has fewer missing pixels in the forest. This study's sampling densities and the proportion of areas with no ground returns are quite different from previous airborne lidar SD studies. This study had ground returns of 90 and 364 points/m<sup>2</sup> in the forest and field, respectively, and had no ground returns in only 0.086% and 0.95% of the 1 m resolution field and forest cells, respectively. In contrast, ALS surveys typically report surface model densities between 8 to 16 points/m<sup>2</sup> (Broxton et al., 2015; 2019; Carrier et al., 2019; Kirchner et al., 2014) and ground returns between 3 and 6 points/m<sup>2</sup> (Broxton et al., 2019; Kirchner et al., 2014). ALS derived snow depth maps have a much greater proportion of areas that are masked due to no ground returns, particularly under trees, with masking areas ranging from less to 10% to more than 23% (Harpold et al., 2014; Mazzotti et al., 2019). While gap filling is possible, interpolation using measured snow depth values to fill under tree can overestimate snow depth (Zheng et al., 2016). Based on our work comparing field and forest lidar collections from a UAS, we suggest testing alternative flight plans, including reduced flight speed over forest canopies to account for lost pulses and canopy returns to produce ground return density that is comparable to field ground return density and to further reduce the number of missing pixels in an acquisition area.

A well understood challenge exists when developing a spatial sampling strategy in which, for given resources, there is a trade-off between spatial extent and sampling density (Clark et al. 2011). Increasing flight altitude can expand the spatial extent of an aerial survey. However, flying at higher altitudes results in a decreased point density. In theory, a higher point density could be achieved by slower speeds and increased swath overlap. The targeted spatial extent of an aerial survey dictates whether a manned aircraft or a UAV platform should be used. If the targeted area has a limited domain then using a manned airborne platform is probably overkill



and inefficient for many studies and the use of a UAV would be more cost effective. However, as the domain increases in size, additional batteries would be required, much of the battery power would be used to reach the outer limits of the domain, and the ability to maintain the required line of sight could be difficult. Thus, there are end-members for survey site or regions where it is self-evident as to whether a UAV or an airborne platform should be used, but that leaves considerable gray areas where an appropriate choice of UAV platform with a well designed mission could stretch the domain. Future research and technological advances are needed to offer insights for snow science observation platforms and trade-offs.

If the comment that the paper is “too equipment/system specific” is intended to mean that we should reduce the description of the equipment, we would push back because the authors strongly believe that the audience who is interested in replicating the experiment should be provided with adequate details to be able to do so. Authors who are interested in conducting similar studies with different instrumentation should be able to understand difference due to instrumentation versus those due to snow differences. Similarly, every experiment is equipment specific and most experiments across research groups do not use identical equipment. This author team has found papers very informative when methods and equipment are described in detail and not just overall results. When new methods and equipment are deployed in studies, the ability to recreate a study or examine the methods is important. This knowledge allows for repeatability, criticism of the experiment, and also can save a research team many hours when learning a new method or developing an experimental plan with technological equipment. Early SfM, airborne lidar, and UAS optical work included specific equipment details and methodologies.

We have slightly reduced our equipment description in the body of the text and reference supplemental material with a new table of technical specifications. We hope that this will balance out the reviewer’s concern.

Table S1. Technical specifications of the project UAS

<b>UAS</b>	
UAS type	quadcopter
Manufacturer/Model	UAV-America / Eagle X8
Diameter	130 cm
Height	70 cm
Number of rotors	4
Rotor diameter	27.5 in (~70cm)
Motor Manufacturer/Model	KDE Direct / 7208
RPM/Volt (KV rating)	110 KV
Aircraft empty weight	8 kg
Aircraft weight at take-off (with payload)	16 kg
Flight time at take-off weight	~7 minutes
Tolerable wind speed (with payload)	5 m/s
Flight controller	Pixhawk PX4
Flight Batteries	22,000 mAh 6 Cell Lipo (2X)
<b>Sensor Payload</b>	
Gimble	Gremsy H7

IMU/GPS	Applanix APX-15
Lidar	Velodyne VLP-16
Payload weight	3 kg

Lastly, considerable space in the text is given to thin, shallow snow covers, and other lidar and airborne methods of mapping snow. While clearly when there is a fixed error in snow depth mapping (e.g.,  $\pm 3$  cm), it is a more serious problem in thin snow. Ultimately this is a methods paper, and nothing described in the accuracy and operation of the lidar is limited or specific to thin snow.

**A. The reviewer makes a reasonable point that this work is more about pushing the envelope by reducing SD errors as opposed to thin snow per se and is relevant to any research that needs snow depth with a high vertical resolution. Based on the reviewer's comment, we have broadened the motivation to include a range of scenarios where an improved vertical resolution of SD beyond the existing 10+ cm resolution would be welcome. We have also discussed where the lidar observations are likely specific to thin snow.**

**Lines 30 to 57** Snowpacks are highly dynamic, accumulating and ablating throughout the winter with associated changes in snowpack density, grain size, and albedo (Adolph et al., 2017) as well as ice formation. Wind redistribution, sloughing of snow-off slopes, trapping of snow by vegetation, and forest canopy interception result in a range of spatial features at varying scales (Clark et al., 2011; Mott et al., 2011; Mott et al., 2018). Modest differences in snowpack depth can differentially impact many hydrologic, agricultural, and ecosystem processes. Differences in snowpack meltwaters can alter streamflow volumes (Gichamo and Tarboton, 2019), change the likelihood of spring floods (Tuttle et al., 2017) and intensify overland nutrient transport and soil erosion (Seyfried et al., 1990; Singh et al., 2009).

High-resolution snow depth measurements are also needed to discern processes that depend on the snow state. Insulation by seasonal snow in the Arctic and Antarctic slows sea ice growth (Sturm et al., 2002). High-resolution Arctic snow depths from ICE-Sat2 revealed seasonal snow on ice that would be missed when using coarser snow information (Kwok et al. 2020). Thin, ephemeral snowpacks have limited insulation and allow the underlying soils to freeze more readily in the winter (Groffman et al., 2001; Starkloff et al. 2017; Yi et al. 2019). Soil frost severity impacts soil respiration, carbon sequestration, nutrient retention, and microbial communities as well as a plant root health and tree growth (Aase and Siddoway, 1979; Isard and Schaetzel, 1998; Monson et al., 2006; Henry, 2008; Aanderud et al., 2013; Tucker et al., 2016; Sorensen et al., 2018; Reinmann and Templer, 2018). Detection and mapping of rapid thinning of snowpacks followed by frigid cold during “winter whiplash” events (Casson et al. 2019) is therefore important for understanding ecosystem impacts of soil freezing events, which are otherwise not well quantified (Kraatz et al. 2018; Prince et al. 2019). High vertical resolution snow mapping would greatly improve our understanding of these unique habitats.

Distributed modeling and mapping of snowpacks can increasingly provide output at fine spatiotemporal scales but snow state change validation typically relies on in situ observations (Gichamo and Tarboton 2019; Starkloff et al., 2017). Despite importance, few spatially continuous high-resolution snowpacks datasets are available to support modelling, and mapping

efforts. Because snowpacks have considerable spatiotemporal variability, a large number of snow depth measurements are often needed to characterize the snowpack (Dickinson and Whiteley, 1972). Using traditional, precise point measurements with a limited sample size, the experimental design requires a balance between the sampling extent and sample spacing (Clark et al. 2011). However, the choice of sampling resolution may yield different measures of snow depth spatial variability when the snow exhibits multifractal behaviour (Deems et al. 2006).

I am going to recommend that this paper be returned for major revisions and specifically the inclusion of more extensive testing across a wider set of snow and terrain conditions. In revision, I would suggest that the focus of the paper be honed to be squarely focused on the methodology and not waste journal space on issues related to thin snow covers, for which no real new information was presented.

Recommendation: Return for major revisions and strengthen with more flights over a wider range of terrain and vegetation.

**Thank you for the recommendations here and in the following sections. We have refined the focus and the thin snow covers discussion is now only one aspect of the broader motivation for a new combination of sensors and platform to provide higher vertical resolution SD measurements. Please see the previous comment and response.**

**The reviewer requested consideration of canopy and terrain variations. At this site, there are notable variations in slope as well as forest type. We conducted a new analysis to better quantify the canopy variations and to determine if the mean snow depth and the confidence intervals differ by slope or land-use. We found statistically significant differences for all combinations. Land-use differences include a new delineation of the forest by coniferous or deciduous trees. A new methods section 2.4 Slope and Vegetation Cover Classification and Analysis was added. The findings are reported in results section 3.3 Snow Depth Maps from UAS Lidar with an additional figure showing boxplots.**

#### **Lines 172 to 194 2.4 Slope and Vegetation Cover Classification and Analysis**

The snow-off DTM was used to develop a 1 m resolution map of slope (Horn, 1981). Vegetation cover type (field/forest) was determined from the known boundaries of field and forest. The forested area was further classified as coniferous or deciduous for the study region using the following methodology (Figure 1). Within the forested area (Figure 1), a Canopy Height Model (CHM) was used to distinguish the intact upper canopy from other forest cover using our snow-off survey, collected with leaf off in the spring (Sullivan et al., 2017). The CHM was generated by subtracting the DTM produced using ground-classified points from the DSM produced using all lidar points. This results in a digital model consisting solely of canopy heights with no terrain or topography. The CHM generation used raster images with a 1 m resolution. A 3 by 3 maximum convolve filter was used to enhance the edges of canopy crowns and expand smaller regions that might have just one pixel of an intact canopy or a whole in a larger canopy (Palace et al., 2008). A 15 m threshold was used to differentiate between the upper level intact coniferous canopy. CHM pixels that were below this threshold were deemed deciduous canopies (see supporting information for intermediate figures). The 5.6 ha forested area has a forest type that is 65% deciduous and 35% coniferous.

Once the vegetation forest type was classified, the raster binary image was vectorized. Within the forest and field regions of our study, a subsample was created from the entire image of 5000 random points in the field and 5000 random points each of the eastern and western forested areas (Palace et al., 2017). At each of these random points, slope, vegetation type (field, deciduous, coniferous), and snow depth and snow depth confidence interval values were extracted. Because of missing values in the raster images, not all random points extracted values and resulted in different numbers of samples points for the forest and forest types. Slope was assigned to one of three categories: 0-10 degrees, 10-20 degrees, and greater than 20 degrees. Because the extracted datasets (i.e., snow depth, confidence interval, and slope) were not normally distributed, the non-parametric Steel-Dwass Method test was used to test for differences. This non-parametric method is useful when sample numbers are large and groups are small, because it allows type I errors to be controlled (Dolgun and Demirhan, 2017).

### **Lines 290 to 317 3.3 Snow Depth Maps from UAS Lidar**

The UAS-mapped snow depth, mapped by subtracting snow-off DTMs from snow-on DTMs, reveals a shallow snowpack whose depth ranges from less than 2 cm to over 18 cm (Figure 5). The mean lidar snow depth was 10.3 cm in the field and 6.0 cm in the forest. Despite the shallow conditions, spatially coherent patterns are readily discernible. The field snowpack depth has higher spatial variability than the west forest snowpack and more spatial organization. In the field, the deepest snow is in the low-lying northeast areas that are sheltered from westerly winds. A relatively moderate and consistent snowpack occurs in southern part of the east field and west of the small pond. The shallowest snowpack is found in the center portion of the field, which is slightly elevated and, unlike most of the field, was not mowed. Lower snow depth at the forest edge distinguishes the field to forest transition. A non-parametric Steel-Dwass test found significant variation for the mean snow depth among the two forest types and field ( $p < 0.0001$ ) (Figure 6a). A pairwise Steel-Dwass test showed that snow depths were significantly different between the three pairs of field and forest types ( $p < 0.0001$ ). When comparing just field and forest as categories, the test also found significant differences for snow depth ( $p < 0.0001$ ). Snow depth was also determined to be significantly different among the three slope group categories using the Steel-Dwass test where regions with a limited slope (Group 1) had more decidedly different snow than steeper regions ( $p < 0.0001$ ) (Figure 6b).

The one-sided confidence interval values of the mean snow depth estimate are remarkably consistent in the field and typically are between 0.5 to 1 cm regardless of snow depth (Figure 5b). Modestly larger confidence intervals occur adjacent to the north-south road where the fields were not mowed prior to winter as well as the northern and southern extents of the flight lines likely due to the reduced sampling density. The forest had an average one-sided confidence interval of 3.5 cm, which is considerably higher than the field. Where the forest is predominantly comprised of deciduous trees, the typical one-sided confidence intervals of the mean snow depth were as low as 1 to 2 cm. The largest one-sided confidence interval values occur in the middle of the field where there is dense shrubbery, at the edge of the fields, and in clusters within the forest where the forest sections are dominated by coniferous trees. The nexus of flight lines in the take-off and landing area resulted in a local area with very high confidence. A non-parametric Steel-Dwass test found significant variation for confidence intervals of the mean snow depth among the two forest types and field ( $p < 0.0001$ ) (Figure 6c). A pairwise Steel-Dwass test showed that

confidence intervals were significantly different between the three pairs of field and forest types and ( $p < 0.0001$ ). Confidence intervals were also significantly different among the three slope categories as determined using a Steel-Dwass test ( $p < 0.0001$ ) (Figure 6d).

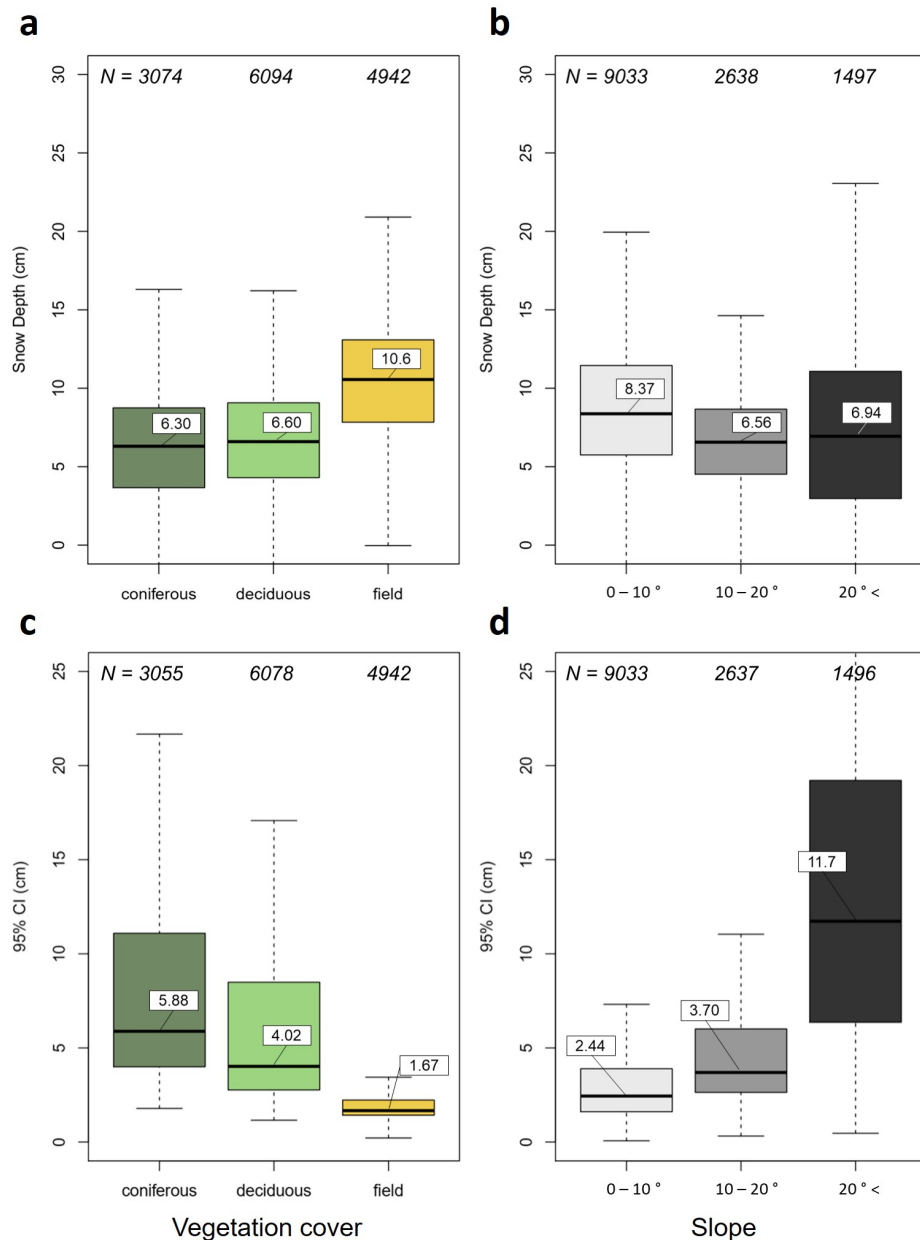


**Figure 6.** Snow depths (a,b) and their one sided confidence intervals (c,d) from the random sample points of the field and forest at Thompson Farm, Durham, NH on January 23, 2019 from the individual cells for 1 m<sup>2</sup> cells by vegetation cover (a,c) and slope group (b,d). Boxplots show the lower quartile, median, upper quartile, and whiskers with the median value noted. Because of missing values in the raster images, not all random points extracted values and resulted in different numbers of samples points for vegetation cover classes.

**While more extensive testing across a wider set of snow and terrain conditions would**

certainly be welcome, the previous literature with SfM SD shows that there is a place in the literature for limited, targeted, early studies and that these papers provide tremendous value as evidenced by their heavy citation rate and how they have informed subsequent research. Also, most of the early SfM SD papers were published in The Cryosphere. The additional analysis on snow depth variations by land cover and slope add novel results for this region. There are very few snow depth studies in the northeast region that attempt to quantify the contribution of land cover and slope in the thin and ephemeral snowpacks that are increasingly characteristic of this region.

Our manuscript closely follows the model used by the early SfM studies and provides early guidance on methods for surveying and ground-based sampling as well as early results that provide insights to potential outcomes, performance and challenges. The requested additional datasets would very much change this submission and, as the request would require an additional winter field season, delay the communication of these early findings by over a year.

We hope our responses and explanations on why this paper is novel and a contribution to the field of shallow snowpack estimation using remotely sensed data warrants consideration of publication. We believe that our work presented in this manuscript is valuable for the community of researcher who are increasingly likely to consider including lidar UAS systems in experiments, with timely information to support decisions regarding whether to proceed with UAS lidar observations, to inform equipment purchases, and to plan field campaigns.

#### Detailed Comments

Abstract: First three sentences could be deleted.

Lines 1 to 98 could readily be deleted with no loss to the topic of the paper (thin snow discussion).

**A. Based on the reviewer's comment, we have revised the motivation to include a range of scenarios where an improved vertical resolution of SD beyond the 10+ cm resolution would be welcome. Beyond shallow snowpacks, lines 54 forward provide a review of the methods used to measure SD and their limitations. A review of this literature is important to put this current new technology and methods in context. Based on the reviewer's comments the introduction section was entirely rewritten.**

**Lines 30 to 66** Snowpacks are highly dynamic, accumulating and ablating throughout the winter with associated changes in snowpack density, grain size, and albedo (Adolph et al., 2017) as well as ice formation. Wind redistribution, sloughing of snow-off slopes, trapping of snow by vegetation, and forest canopy interception result in a range of spatial features at varying scales (Clark et al., 2011; Mott et al., 2011; Mott et al., 2018). Modest differences in snowpack depth can differentially impact many hydrologic, agricultural, and ecosystem processes. Differences in snowpack meltwaters can alter streamflow volumes (Gichamo and Tarboton, 2019), change the likelihood of spring floods (Tuttle et al., 2017) and intensify overland nutrient transport and soil erosion (Seyfried et al., 1990; Singh et al., 2009).



High-resolution snow depth measurements are also needed to discern processes that depend on the snow state. Insulation by seasonal snow in the Arctic and Antarctic slows sea ice growth (Sturm et al., 2002). High-resolution Arctic snow depths from ICE-Sat2 revealed seasonal snow on ice that would be missed when using coarser snow information (Kwok et al. 2020). Thin, ephemeral snowpacks have limited insulation and allow the underlying soils to freeze more readily in the winter (Groffman et al., 2001; Starkloff et al. 2017; Yi et al. 2019). Soil frost severity impacts soil respiration, carbon sequestration, nutrient retention, and microbial communities as well as a plant root health and tree growth (Aase and Siddoway, 1979; Isard and Schaetzel, 1998; Monson et al., 2006; Henry, 2008; Aanderud et al., 2013; Tucker et al., 2016; Sorensen et al., 2018; Reinmann and Templer, 2018). Detection and mapping of rapid thinning of snowpacks followed by frigid cold during “winter whiplash” events (Casson et al. 2019) is therefore important for understanding ecosystem impacts of soil freezing events, which are otherwise not well quantified (Kraatz et al. 2018; Prince et al. 2019). High vertical resolution snow mapping would greatly improve our understanding of these unique habitats.

Distributed modeling and mapping of snowpacks can increasingly provide output at fine spatiotemporal scales but snow state change validation typically relies on in situ observations (Gichamo and Tarboton 2019; Starkloff et al., 2017). Despite importance, few spatially continuous high-resolution snowpacks datasets are available to support modelling, and mapping efforts. Because snowpacks have considerable spatiotemporal variability, a large number of snow depth measurements are often needed to characterize the snowpack (Dickinson and Whiteley, 1972). Using traditional, precise point measurements with a limited sample size, the experimental design requires a balance between the sampling extent and sample spacing (Clark et al. 2011). However, the choice of sampling resolution may yield different measures of snow depth spatial variability when the snow exhibits multifractal behaviour (Deems et al. 2006).

Over the past two decades, remote sensing methods, providing spatially continuous, high-resolution snow depth maps at local and regional scales, have greatly advanced the ability to characterize the spatiotemporal variability of snow depth over earlier work using snow probes (see reviews in Deems et al., 2013; López-Moreno et al., 2017). Spaceborne photogrammetry (e.g. Marti et al. 2016, McGrath et al. 2019, Shaw et al. 2020), airborne laser scanning (ALS) (Deems et al., 2013; Harpold et al., 2014; Kirchner et al., 2014), terrestrial laser scanning (TLS) (Grünwald et al. 2010; Currier et al. 2019), and structure-from-motion photogrammetry (SfM) (Nolan et al., 2015; Bühler et al., 2016; Harder et al., 2016) have emerged as viable methods to map surface elevations with snow-off and snow-on conditions in order to differentially map snow depths.

Figure 1: Nice graphic. . .very clear.

**A. Thank you.**

Line 84: Ground control points are mentioned, but I don't see any indication that they used control points for the SfM maps beyond the 200hz measurement rate, and I don't understand how that works.

**A. We are not sure what the reviewer means. We did not create any SfM maps for this paper. Line 84 is the literature review not methods. The 200hz referred to in the methods**

**and conclusion is the sampling rate of the inertial navigation system (INS), which measures the position of the UAS during acquisition flights. Those data are then used to calculate the location of lidar returns. We do use GCPs in the same sentence as 200hz once, and it is to point out that one of the benefits of our lidar payload over SfM approaches is that a payload that relies on an INS does not require GCPs, while SfM does.**

Line 158: DTM not defined, which reflects a certain unevenness in the technical level of the paper. Who is this paper for? The new practitioner or the veteran GIS and UAV group? There are many acronyms in the paper all of which should when first presented be defined.

**A. The acronyms were reviewed and defined. We apologize for the original omission of the definition of digital terrain model (DTM) and now include it.**

**Lines 164 to 167 PMF was parameterized using a set of window sizes of 1, 3, 5, and 9 m, and elevation thresholds of 0.2, 1.5, 3, and 7 m, which were determined by varying value sets and assessing digital terrain models (DTMs) to determine the parameter sets that produced a visually smooth surface over a dense grid (*sensu* Muir et al., 2017).**

Line 166: Ground probe sampling method was a 5-sample cross pattern, with a GNSS GPS point in the center of the cross, but the authors wait until line 175 to tell us they averaged these 5 samples. What was the logic behind the sampling protocol and why only 5 points per 0.4 m sampling pixel, when the lidar was producing between 25 and 90? Surely more could have been measured? Also, later in the paper a core tube (Federal sampler?) is mentioned but no other details about it. About here in the paper it would also be good to mention the nature of the ground surface and depth of freeze, instead of later when trying to explain the discrepancy between the forest and field measurements errors.

**A. Because the lidar observations were anticipated to give very high-resolution observations, we used an approach that would provide very high spatial precision for the in situ observation coordinates. The ground sampling protocol was informed by the methods used to validate SfM SDs. Harder (2016), Bühler et al. (2016), and Adams et al. (2018) used the same 5-sample cross pattern with a GNSS GPS point in the center of the cross. Our in situ SD observations were measured using the magna probe and then the center point was surveyed to a horizontal uncertainty of 2.51cm and 4.17cm for the field and forest, respectively, that meets or exceeds previous studies. The downside is that this procedure limits the number of in situ validation points.**

**The federal snow sampling tube was originally described on lines 172 and 173 (2.4 Snow Depth Ground Truth) and the later reference to the “tube” has been clarified. The section 2.4 Snow Depth Ground Truth section has been modified to 2.4 *In Situ* Observations. This section now includes requested a discussion of the ground surface and depth of freeze as well as additional details on the sampling methods.**

**Lines 195 to 217 2.5 *In Situ* Observations**

**A 1.2-m Global Positioning System (GPS)-equipped magnaprobe (Sturm and Holmgren, 2018) was used to compare to the unmanned aerial system (UAV) lidar surveys (hereafter noted as ALS measurements) over two transects. The first transect consisted of 12 sample locations in the field and 5 locations in the eastern forest of our study site. The second transect consisted of 11**

sample locations in the western forest. Sample locations were separated by approximately 10 m. The field transect follows the prevailing westerly wind direction with its west side at the foot of a modest depression (approximately 2 m below the land further to the west) and the east side transitioning into a wooded area. Following (Harder et al. 2016) and (Bühler et al. 2016), each sample location includes 5 samples in a cross pattern with the four ordinal directions sampled approximately 20 cm from the center sampling location in the cross. The five samples are used to provide a measure of SD central tendency and variation over a 0.4 x 0.4 m pixel. Because the magnaprobe GPS has an absolute accuracy of 8 m, a Trimble<sup>®</sup> Geo7X GNSS Positioning Unit with Zephr<sup>™</sup> antenna was used to collect each sampling location's center point with an estimated horizontal uncertainty of 2.51cm (standard deviation  $\sigma$  0.95 cm) and 4.17cm ( $\sigma$  4.60 cm) for the field and forest, respectively after differential correction. Along the same forest and field transects, a federal snow tube sampler was used to collect a single sample of snow depth and snow water equivalent at each magnaprobe sample location for a total of 12 field samples and 16 forest samples. Snow depth was measured by inserting the aluminium tube vertically into the snowpack and a core was extracted and weighed using a spring scale.

An independent study collected soil frost depth from three locations at the Thompson Farm Research Observatory using Gandahl-Cold Regions Research and Engineering Laboratory (CRREL) style frost tubes. The frost tubes have flexible, polyethylene inner tubing filled with methylene blue dye whose color change is easy to differentiate when extruded from ice (Gandahl 1957). A nylon string housed inside the polyethylene tubing affixes ice during periods of thaw. The outer tubing consists of PVC pipe installed between 0.4 to 0.5 m below soil surface (Ricard et al., 1976; Sharratt and McCool, 2005). Prior to the January 19<sup>th</sup> and 20<sup>th</sup>, 2019 snowfall event, soil frost was 23.5 to 25.5 cm in the field and 5.5 to 8.5 cm in the west forest.

Line 240-Figure 4: The maps look quite good, and the inclusion of the confidence map is to be commended. But several aspects shown on this figure go unremarked. Specifically, how was the location of the ground validation determined, and why so few ground data? It is unfortunate that for the field ground data, other data from the shallower area bracketing the road wasn't obtained so that a second thinner field comparison could be made. As for the confidence map, the very high confidence area in the center of western forest is at the nexus of all the flight lines. . . is that why the confidence is high there? Conversely, comparing Fig. 1 to 4a and 4b, there are gaps and openings in the trees in both east and west forest where the confidence drops considerably, yet one might have expected these to function like the open field. Why does it drop?

**A. Thank you. Additional remarks about this figure were added based on the reviewer's comments including the point about the nexus of flight lines resulting in high confidence. The forest locations having a marked decreased confidence are locations where there is a dense canopy and limited lidar penetration combined with increased pulse loss. The higher variability in confidence in the forest is likely due to the heterogeneity of the forest structure, not canopy gaps as this is a continuous forest canopy. Instead, what the reviewer perceives to be gaps are more likely areas with more deciduous trees and variable terrain. A new analysis was conducted and added to the paper to examine the variability within the forest. The areas with marked decreased confidence are locations where there is a dense canopy and limited lidar penetration.**

We were intrigued by the reviewer's comments about the confidence in the forests and revisited the forest locations. A new analysis of the forest canopy profiles and the ground versus nonground returns in the forest and field for both snow on and snow-off conditions was added.

**Lines 312 to 314** The nexus of flight lines in the take-off and landing area resulted in a local area with very high confidence.

**Lines 266 to 278** To provide insight to differences between the forest and field observations, mean height profiles were calculated for a 25 m<sup>2</sup> square region centered on forest and field study plots from lidar data (Figure 4). To do this, all lidar returns were extracted from the bounding box of each plot, then the mean elevation of ground returns was calculated within each plot. Return heights for each plot were determined by subtracting the mean ground elevation of the plot, then the normalized return elevations were binned in 0.1 m height increments. Within forests, an average of 2142 and 2889 returns were classified as ground and non-ground in snow-free conditions per 25 m<sup>2</sup> plot, respectively with 2218 ground returns and 1721 non-ground returns in snow-on conditions. In field plots, an average of 5666 ground returns and 154 non-ground returns in snow-free conditions were obtained per 25 m<sup>2</sup> plot, with 7567 ground returns and 25 non-ground returns in snow-on conditions. Figure 4 also shows that there is a greater range of ground return elevations in the forest as compared to the field. In forest plots, ground return elevations had an average standard deviation of 0.157 m and 0.154 m in snow-free and snow-on conditions, respectively, while in field plots, ground return elevations had standard deviations of 0.058 m and 0.050 m in snow-free and snow-on conditions, respectively.

The limited number of ground sampling points is discussed in the response to the previous section. We agree it is unfortunate that our field data didn't capture more of the variability. Unfortunately, because lidar post-processing takes some time, it is not possible to develop a sampling plan based on the lidar observations because the field data needs to be collected at nearly the same time as the lidar data. Similarly, field data collection occurs after the lidar acquisition because snow sampling and movement of people across the landscape alters the snow field.

Regarding how was the location of the ground validation determined: Our working hypothesis that informed the ground sampling design was that there would be limited local variations in precipitation in the field and that wind redistribution would drive variations in snow depth across the field. The field transect was set up along the prevailing wind direction with the west side at the foot of a modest depression (approximately 3-4 m below the land further to the west) and the east side transitioning into a wooded area in an effort to capture wind driven variations. The results instead showed limited SD variations along the transect as compared to notable SD variations and patterns that were readily evident from the lidar SD maps. This suggests opportunities for further research and will inform future in situ sampling strategies. We updated the methods to describe how the field transect was located.

**Lines 199 to 201** The field transect follows the prevailing westerly wind direction with its west side at the foot of a modest depression (approximately 3-4 m below the land further to the west) and the east side transitioning into a wooded area.

Figure 7: OK...but anyone new to airborne lidar will not understand it, and anyone already doing SfM or lidar will not need it. Think of who you are writing for.

**A. This is a reasonable point and was also noted by Reviewer #1. We moved this to supplemental materials and modified the text. Because our target audience will likely include readers who are new to airborne lidar, this figure has been revised and the supporting text have been rewritten to make this important information for accessible to that audience. Additional explanatory text and figures were added to the discussion on boresighting in order to provide a specific example to anyone who is new to airborne lidar. Our goal is to provide a specific example using a snow depth survey that will provide information beyond that available in a standard textbook discussion of boresighting. We hope that the placement in supplementary material will allow readers who are new to lidar to have a specific example that is linked to this analysis, but will remove the material from the main body of the paper for those who do not need it.**

## **S2 Boresight Calibration**

The deployment of a lidar system mounted on a UAV platform for snow depth monitoring requires flight patterns designed for calculating boresight alignment and post-processing to ensure that point clouds are properly aligned (Painter et al., 2016). Provided that GNSS data are accurate, the most common reason for misalignment of point clouds is boresight angle errors (Li et al., 2019). Boresighting is the process of calculating the differences between lidar sensor and IMU roll, pitch, and yaw angle measurements to correct those errors in point clouds. Traditionally, boresighting calibration is performed using antiparallel flight lines in addition to a perpendicular flight line (Keyetieu and Seube, 2019). Due to battery flight time limitations, it was not possible to complete the flight pattern that is commonly used for boresighting alignment. Because of this, the first two antiparallel flight lines were leveraged for boresighting calibration. Offsets between sensor and IMU are calculated by observing misalignments between lidar data collected from different flight lines, and iteratively adjusting roll, pitch, and yaw angles of the IMU data to produce sub-datasets into the same planes. To determine roll offset, broad (10 m) along-path cross-sections over flat terrain were assessed, and to determine pitch offset narrow (1 m) across-path cross-sections in sloped terrain where the point clouds overlapped were used (Figure S3). Though not shown here, unique features were leveraged within the data acquisition region, including barn roofs and deciduous tree branches, to assess the resulting boresight angles (Kumari et al., 2011; Li et al., 2005). For this particular study, boresight calibration was performed manually and iteratively. Methods often require extensive user input (Li et al., 2005), however boresight calibration is an increasingly automated process with wide variation in algorithms and approaches (e.g. Maas, 2000; Kumari et al., 2011; Zhang et al., 2019). In future work, automated boresight calibration methods to improve the accuracy of point cloud data sets will be explored.

Figure S2 shows two examples of ground return point clouds before and after calibration in this study's field region. Uncalibrated boresight angles between the INS and lidar sensor can result in

poorly aligned point clouds (i and iii). Red and blue arrows in (A) and (B) show approximate flight direction during data acquisition superimposed on the LAS point cloud. Roll alignment errors present well in anti-parallel flight lines (flight lines flown parallel to each other but in the opposite direction) over flat terrain. The top panel in Figure S3 addresses roll misalignment with (a) showing the LAS point cloud and the two flight lines flown in opposite directions. The lidar returns within the box marked in red in (a) are shown in (a1) and (a2) at an oblique view angle. Figure (a1) shows how boresight errors of roll angles present, while (a2) shows proper boresight alignment for roll. Figure (b) shows the approximate location of returns and flight lines used for pitch boresight alignment error demonstration (b1) and its correction (b2). Pitch misalignment presents well in anti-parallel flight lines in areas with terrain relief while viewing across the flight track, as opposed to along the flight track as with roll alignment.

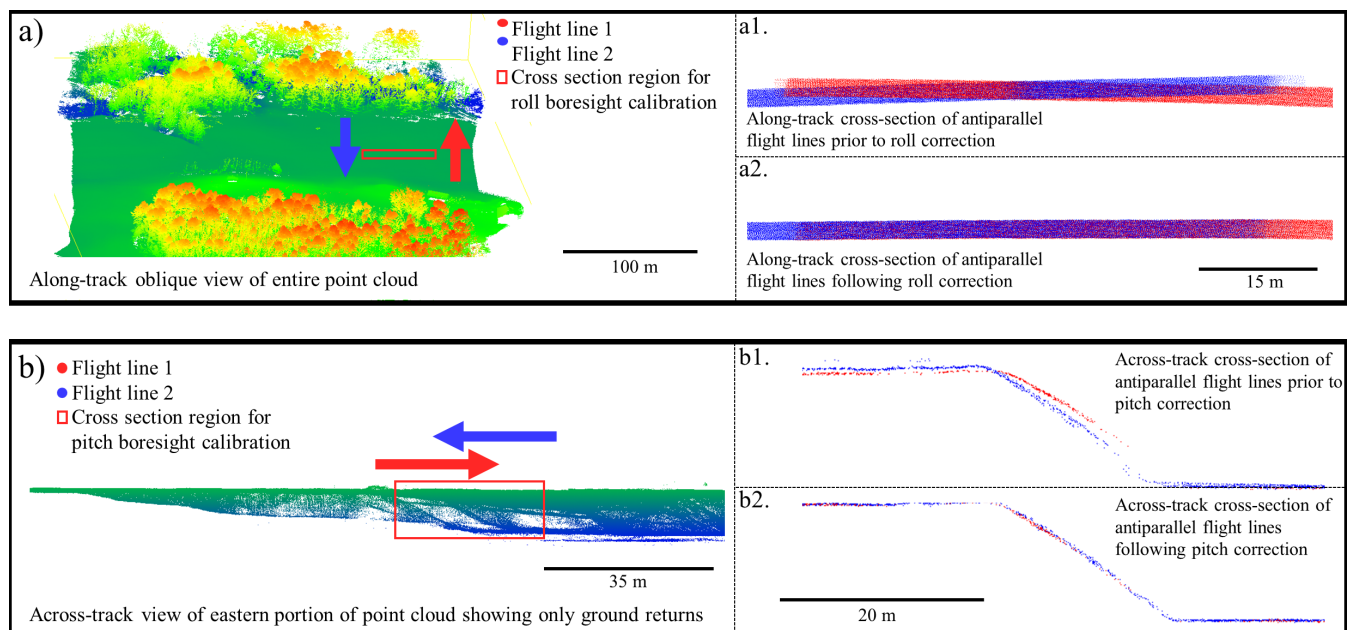


**Figure S2.** Boresight examples that show how uncalibrated boresight angles between the INS and lidar sensor can result in poorly aligned point clouds (a1 and b1). Arrows in (a) and (b) show approximate flight direction during data acquisition. The lidar returns within the box marked in red in (a) are shown in (a1) and (a2) at an oblique view angle. Figure (a1) shows how boresight errors of roll angles present, while (a2) shows proper boresight alignment for roll. Figure (b) shows the approximate location of returns used for pitch boresight alignment error demonstration (b1) and its correction (b2). Pitch misalignment presents well in anti-parallel flight lines in areas with terrain relief while viewing across the flight track, as opposed to along the flight track as with roll alignment. For (b, a1, a2, b1, and b2), only ground returns are shown for each flight line, while in (a), all returns are shown.

Line 286 to 316: This is the first time that large vs. small UAVs are differentiated, though the weight of the lidar package would suggest a larger UAV was in use. But a quick scan of the web suggest that the drone used can handle about 14 kg. . .and recent some heavy lift drones are getting near 100 kg. Much of the discussion here seems like lessons learned that anyone trying to fly these larger drones probably already knows. It could be helpful, but they aren't detailed



enough to really guide a newcomer to a successful mission. See the general point of trying to write a paper that is generic rather than specific. . . . which for rapidly changing tech can be challenging.

**A. Agreed that additional details are needed to support the target audience. We envision an important audience of this research to be researchers who have used off the shelf systems such as the DJI Phantom IV and are considering instrumentation that would increase the UAV payload beyond that carrying light weight sensors such as optical sensors. We added a table of specifications to the supplemental materials and clearly differentiated this UAV from those used previously in SfM SD studies.**

Table S1. Technical specifications of the project UAS

<b>UAS</b>	
UAS type	quadcopter
Manufacturer/Model	UAV-America / Eagle X8
Diameter	130 cm
Height	70 cm
Number of rotors	4
Rotor diameter	27.5 in (~70cm)
Motor Manufacturer/Model	KDE Direct / 7208
RPM/Volt (KV rating)	110 KV
Aircraft empty weight	8 kg
Aircraft weight at take-off (with payload)	16 kg
Flight time at take-off weight	~7 minutes
Tolerable wind speed (with payload)	5 m/s
Flight controller	Pixhawk PX4
Flight Batteries	22,000 mAh 6 Cell Lipo (2X)
<b>Sensor Payload</b>	
Gimble	Gremsy H7
IMU/GPS	Applanix APX-15
Lidar	Velodyne VLP-16
Payload weight	3 kg

**There is a total 55lb (~25 kg) limit on UAVs with our specific license. Heavier than that requires additional licensing. Our effort is to provide information on UAVs that can carry a lidar, GPS, and IMU appropriate for shallow snow depth retrieval. Because our work is intended to be helpful to new researchers and even seasoned UAV groups, we have tended on the side of presenting additional equipment attributes and settings.**

**We entirely rewrote the discussion section and separated it into three distinct sections (4.1 *In Situ* and UAS Sampling, 4.2 Flight Planning, and 4.3 UAS Sampling Strategies. Regarding the material on flight planning, this section is now much tighter.**

#### **Lines 425 to 455 4.2 Flight Planning**

Because larger UAVs that can carry heavier payloads have challenges that may differ from small UAVs, a well-formulated flight plan that addresses weather conditions, logistics of flying at proposed site, flight lines, UAS equipment, and personnel is clearly needed. Weather impacts

operations. UAS surveys cannot be conducted when there is any type of precipitation or in dense fog/clouds because moisture can cause electronic components to malfunction and moisture build-up on the propellers can also adversely affect lift production. Depending on the UAV, wind speeds exceeding 7 to 10 m/s may make flights more difficult. This project's Eagle XF high lift capacity UAS cannot be flown comfortably in winds greater than 8 m/s. At the study site, wind speeds often exceeded this threshold in the days immediately following snowfall except early in the morning. High wind speeds can also significantly reduce battery life as well as impact the accuracy of sensor observations. Low air temperatures can cause batteries to rapidly discharge. For winter UAS surveys, all flight and operational batteries were kept warm in a building, vehicle, or insulated cooler prior to the UAS survey. This also applies to the computer used to upload flight lines and relay telemetry information. A MIL-STD-810 certified Panasonic Toughbook was used in this study to handle the anticipated cold temperatures. Additionally, cold temperatures can severely limit the dexterity of the person manipulating the flight controls.

High lift UAVs capable of carrying a lidar sensor package have the potential to cause significant damage to person and property. The selection of a survey site not only needs to meet the scientific objectives of the UAV survey, but also must have the proper attributes for safe and legal UAV operation including permission to operate the UAV at the site. Visual line of sight (VLOS) of the UAV needs to be maintained throughout the flight. When it is difficult to maintain VLOS (e.g., flying over forested or mountainous sites), spotters can be used if there is constant two-way communication between the spotters and the person operating the flight controls. For this study, an on-site, walk up tower with a spotter was necessary while the UAV was flown over the forest.

The deployment of a UAV lidar system requires additional flight patterns designed for boresighting to ensure that point clouds are aligned (Painter et al., 2016). Provided that GNSS data are accurate, the most common reason for misalignment of point clouds is boresight angle errors (Li et al., 2019). Boresighting is the process of calculating the differences between lidar sensor and IMU roll, pitch, and yaw angle measurements to correct those errors in point clouds. Due to battery flight time limitations, we were unable to complete the flight pattern that is commonly used for boresighting alignment. Because of this, we leveraged our first two antiparallel flight lines for boresighting calibration. Additional details on boresighting calibration, our technique due to the flight time limitations, and examples of roll and pitch alignment errors observed during this field campaign appear in the supplemental materials.

Lines 333 to 334: Heavy payload=short flight duration=small area mapped, hence better ground point density. While that makes sense, can't that be achieved by slower speed, closer passes etc.? And mapping extent, of course can be larger if more missions are used. So, I was puzzled what this paragraph was really trying to say.

**A. This is a reasonable comment led to a modification of section 4.3 UAS Sampling Strategies to include a brief paragraph which appears at the end of the response.**

**This comment reflects a general challenge that occurs when developing a spatial sampling strategy in which, for given resources, there is a trade-off between spatial extent and sampling density. An additional point is that the survey height can also be varied with higher altitudes increasing the spatial extent with trade-offs between the point density and**



number of missions. The main point was intended to provide the reader with the means to contrast this study's sampling densities and the proportion of areas that are masked due to no ground returns with those from previous airborne lidar SD studies.

A second point was added to a separate section to respond to the reviewer's insights that regarding the trade-offs between using a UAV versus an airborne platform. While we agree in theory that "Heavy payload=short flight duration=small area mapped, hence better ground point density." could be achieved by "slower speed, closer passes etc." by an airborne platform, if the mapped area has a limited domain then using an airborne platform is probably overkill and inefficient for many studies. Similarly, the "mapping extent, of course can be larger if more missions are used", but as the domain increases in size, much of the battery power would be used to reach the outer limits of the domain and the ability to maintain the required line of sight could also limit the domain. Thus, there are end-members for survey site or regions where it is self-evident as to whether a UAV or an airborne platform should be used, but that leaves considerable gray areas where an appropriate choice of UAV platform and a well designed mission could stretch the domain. Future research and technological advances is needed to offer insights for snow science observation platforms and trade-offs.

Finally, slower flights and lower altitude do increase the point density, but further limit the area covered. We used three sets of batteries and flew over 2 hr period to collect our images. Limitations on battery cost and time to fly restrict data collection. Flights over multiple days are not appropriate because snowpacks can change within 24 hours.

Lines 475 to 486 A well understood challenge exists when developing a spatial sampling strategy in which, for given resources, there is a trade-off between spatial extent and sampling density (Clark et al. 2011). Increasing flight altitude can expand the spatial extent of an aerial survey. However, flying at higher altitudes results in a decreased point density. In theory, a higher point density could be achieved by slower speeds and increased swath overlap. The targeted spatial extent of an aerial survey dictates whether a manned aircraft or a UAV platform should be used. If the targeted area has a limited domain then using a manned airborne platform is probably overkill and inefficient for many studies and the use of a UAV would be more cost effective. However, as the domain increases in size, additional batteries would be required, much of the battery power would be used to reach the outer limits of the domain, and the ability to maintain the required line of sight could be difficult. Thus, there are end-members for survey site or regions where it is self-evident as to whether a UAV or an airborne platform should be used, but that leaves considerable gray areas where an appropriate choice of UAV platform with a well designed mission could stretch the domain. Future research and technological advances are needed to offer insights for snow science observation platforms and trade-offs.

**The following references were added to the manuscript based on Reviewer 2's input:**

Adams, M.S., Bühler, Y., & Fromm, R. (2018). Multitemporal accuracy and precision assessment of unmanned aerial system photogrammetry for slope-scale snow depth maps in Alpine terrain. *Pure and Applied Geophysics*, 175, 3303-3324

Bühler, Y., Adams, M.S., Bösch, R., & Stoffel, A. (2016). Mapping snow depth in alpine terrain with unmanned aerial systems (UASs): potential and limitations. *The Cryosphere*, 10, 1075-1088

Harder, P., Schirmer, M., Pomeroy, J., & Helgason, W. (2016). Accuracy of snow depth estimation in mountain and prairie environments by an unmanned aerial vehicle. *The Cryosphere*, 10, 2559

# Snow depth mapping with unpiloted aerial systems lidar observations: A case study in Durham, New Hampshire, United States

5 Jennifer M. Jacobs<sup>1,2</sup>, Adam G. Hunsaker<sup>1,2</sup>, Franklin B. Sullivan<sup>2</sup>, Michael Palace<sup>2,3</sup>, Elizabeth A. Burakowski<sup>2</sup>, Christina Herrick<sup>2</sup>, Eunsang Cho<sup>1,2</sup>

<sup>1</sup>Department of Civil and Environmental Engineering, University of New Hampshire, Durham, NH, 03824, USA

<sup>2</sup>Earth Systems Research Center, Institute for the Study of Earth, Oceans, and Space, University of New Hampshire, Durham, NH, 03824, USA

10 <sup>3</sup>Department of Earth Sciences, University of New Hampshire, Durham, NH, 03824, USA

Correspondence to: Jennifer M. Jacobs (Jennifer.jacobs@unh.edu)

**Abstract.** Terrestrial and airborne laser scanning and structure from motion techniques have emerged as viable methods to map snow depths. While these systems have advanced snow hydrology, these techniques have noted limitations in either horizontal or vertical resolution. Lidar on an unpiloted aerial vehicle (UAV) is also a potential method to observe field and slope scale variations at the vertical resolutions needed to resolve local variations in snowpack depth and to quantify snow depth when snowpacks are shallow. This paper provides some of the earliest snow depth mapping results on the landscape scale that were measured using lidar on a UAV. The system, which uses modest cost, commercially available components, was assessed in a mixed deciduous and coniferous forest and open field for a thin snowpack (< 20 cm). The lidar classified point clouds had an average of 90 and 364 points/m<sup>2</sup> ground returns in the forest and field, respectively. In the field, in-situ and lidar mean snow depths, at 0.4 m resolution, had a mean absolute difference of 0.96 cm and a root mean squared error of 1.22 cm. At 1 m resolution, the field snow depth confidence intervals were consistently less than 1 cm. The forest and heavily vegetated areas had modestly reduced performance with typical confidence intervals within 4 cm. Although the mean snow depth was only 10.3 cm in the field and 6.0 cm in the forest, a pairwise Steel-Dwass test showed that snow depths were significantly different between the coniferous forest, the deciduous forest, and the field land covers ( $p < 0.0001$ ). Snow depths were shallower and snow depth confidence intervals were higher in areas with steep slopes. Results of this study suggest that performance depends on both the point cloud density, which can be increased or decreased by modifying the flight plan over different vegetation types, and the within cell variability that depends on site surface conditions.

## 30 1 Introduction

Snowpacks are highly dynamic, accumulating and ablating throughout the winter with associated changes in snowpack density, grain size, and albedo (Adolph et al., 2017) as well as ice formation. Wind redistribution, sloughing of snow-off slopes, trapping of snow by vegetation, and forest canopy interception result in a range of spatial features at varying scales (Clark et al., 2011; Mott et al., 2011; Mott et al., 2018). Modest differences in snowpack depth can differentially impact many hydrologic, agricultural, and ecosystem processes. Differences in snowpack meltwaters can alter streamflow volumes (Gichamo and Tarboton, 2019), change the likelihood of spring floods (Tuttle et al., 2017) and intensify overland nutrient transport and soil erosion (Seyfried et al., 1990; Singh et al., 2009).

High-resolution snow depth measurements are also needed to discern processes that depend on the snow state. Insulation by seasonal snow in the Arctic and Antarctic slows sea ice growth (Sturm et al., 2002). High-resolution Arctic snow depths

Jennifer Jacobs 7/13/2020 11:24 AM

Formatted: Space Before: 6 pt

Jennifer Jacobs 7/13/2020 11:08 AM

Deleted: Shallow snow depth mapping with unmanned

Jennifer Jacobs 7/13/2020 11:09 AM

Deleted: Shallow snowpack conditions, which occur throughout the year in many regions as well as during accumulation and ablation periods in all regions, are important in water resources, agriculture, ecosystems, and winter recreation.

Jennifer Jacobs 7/13/2020 11:10 AM

Deleted: (manned and unmanned)

Jennifer Jacobs 7/13/2020 11:10 AM

Deleted: (SfM)

Jennifer Jacobs 7/13/2020 11:12 AM

Deleted: unmanned aerial vehicle

Jennifer Jacobs 7/13/2020 11:12 AM

Deleted: of shallow snowpacks

Jennifer Jacobs 7/13/2020 11:12 AM

Deleted: This paper describes an unmanned aerial lidar system, which uses commercially available components, for snow depth mapping on the landscape scale. The system was

Jennifer Jacobs 7/13/2020 11:13 AM

Deleted: shallow

Hunsaker, Adam G 7/22/2020 11:58 AM

Deleted: grou

Hunsaker, Adam G 7/22/2020 11:58 AM

Deleted: nd

Jennifer Jacobs 7/13/2020 11:14 AM

Deleted: yielded

Jennifer Jacobs 7/13/2020 11:15 AM

Deleted: Comparisons of snow probe and lidar mean snow depths i

Hunsaker, Adam G 7/22/2020 12:00 PM

Deleted: snow magnaprobe

Jennifer Jacobs 7/13/2020 11:17 AM

Deleted: difference

Jennifer Jacobs 7/13/2020 11:16 AM

Deleted: In the forest, the *in situ* mean snow depth was nearly twice that from the lidar from mean absolute difference of 9.6 cm and root mean squared difference of 10.5 cm. These differences in forests are likely due, in part, to limitations of sampling using a snow probe.

Jennifer Jacobs 7/13/2020 11:16 AM

Deleted: precision was

Jennifer Jacobs 7/13/2020 11:18 AM

Deleted: values

Jennifer Jacobs 7/13/2020 11:18 AM

Deleted: precision

Jennifer Jacobs 7/13/2020 11:17 AM

Deleted: Performance depends on both the point cloud density, which can be increased or decreased by changing the flight plan, and the within cell variability that depends on site surface conditions.

from ICE-Sat2 revealed seasonal snow on ice that would be missed when using coarser snow information (Kwok et al. 2020). Thin, ephemeral snowpacks have limited insulation and allow the underlying soils to freeze more readily in the winter (Groffman et al., 2001; Starkloff et al. 2017; Yi et al. 2019). Soil frost severity impacts soil respiration, carbon sequestration, nutrient retention, and microbial communities as well as a plant root health and tree growth (Aase and Siddoway, 1979; Isard and Schaetzel, 1998; Monson et al., 2006; Henry, 2008; Aanderud et al., 2013; Tucker et al., 2016; Sorensen et al., 2018; Reinmann and Templer, 2018). Detection and mapping of rapid thinning of snowpacks followed by frigid cold during “winter whiplash” events (Casson et al. 2019) is therefore important for understanding ecosystem impacts of soil freezing events, which are otherwise not well quantified (Kraatz et al. 2018; Prince et al. 2019). High vertical resolution snow mapping would greatly improve our understanding of these unique habitats.

Distributed modeling and mapping of snowpacks can increasingly provide output at fine spatiotemporal scales but snow state change validation typically relies on in situ observations (Gichamo and Tarboton 2019; Starkloff et al., 2017). Despite importance, few spatially continuous high-resolution snowpacks datasets are available to support modelling, and mapping efforts. Because snowpacks have considerable spatiotemporal variability, a large number of snow depth measurements are often needed to characterize the snowpack (Dickinson and Whiteley, 1972). Using traditional, precise point measurements with a limited sample size, the experimental design requires a balance between the sampling extent and sample spacing (Clark et al. 2011). However, the choice of sampling resolution may yield different measures of snow depth spatial variability when the snow exhibits multifractal behaviour (Deems et al. 2006).

Over the past two decades, remote sensing methods, providing spatially continuous, high-resolution snow depth maps at local and regional scales, have greatly advanced the ability to characterize the spatiotemporal variability of snow depth over earlier work using snow probes (see reviews in Deems et al., 2013; López-Moreno et al., 2017). Spaceborne photogrammetry (e.g. Marti et al. 2016, McGrath et al. 2019, Shaw et al. 2020), airborne laser scanning (ALS) (Deems et al., 2013; Harpold et al., 2014; Kirchner et al., 2014), terrestrial laser scanning (TLS) (Grünwald et al. 2010; Currier et al. 2019), and structure-from-motion photogrammetry (SfM) (Nolan et al., 2015; Bühler et al., 2016; Harder et al., 2016) have emerged as viable methods to map surface elevations with snow-off and snow-on conditions in order to differentially map snow depths.

Over the past two decades, remote sensing methods, providing spatially continuous, high-resolution snow depth maps at local and regional scales, have greatly advanced the ability to characterize the spatiotemporal variability of snow depth over earlier work using snow probes (see reviews in Deems et al., 2013; López-Moreno et al., 2017). Spaceborne photogrammetry (e.g. Marti et al. 2016, McGrath et al. 2019, Shaw et al. 2020), airborne laser scanning (ALS) (Deems et al., 2013; Harpold et al., 2014; Kirchner et al., 2014), terrestrial laser scanning (TLS) (Grünwald et al. 2010; Currier et al. 2019), and structure-from-motion photogrammetry (SfM) (Nolan et al., 2015; Bühler et al., 2016; Harder et al., 2016) have emerged as viable methods to map surface elevations with snow-off and snow-on conditions in order to differentially map snow depths.

ALS and TLS both rely on well-established lidar (light detection and ranging) technology. TLS, applied from a fixed ground position, is able to measure snow depth with high vertical accuracy (Fey et al., 2019), and has the advantage of being relatively low-cost and portable, making repeat observations possible. However, TLS uncertainties are caused by large incident angles, occlusion from hills and trees that can cause data gaps in forested domains (Currier et al., 2019; Palace et al., 2016), and challenges providing a stable scanner position for the tripod in snow-on conditions (Schweizer et al., 2003). ALS technology such as that deployed on the Airborne Snow Observatory (ASO) (Painter et al., 2016) has the advantage of being

Jennifer Jacobs 7/27/2020 5:22 PM

**Deleted:** -In many regions, shallow snowpacks, i.e., snow depth less than 20 cm, are typical throughout the winter. Even in mountainous regions with deep seasonal snowpacks, snowpacks can be shallow and nonuniform during the accumulation and melt periods as well as in areas with high winds. Shallow snowpacks impact many hydrologic, agricultural, and ecosystem processes. Shallow snowpack characteristics effect the location and condition of suitable habitats in animal populations (Friggens et al., 2018). Meltwaters from shallow snowpacks can be a major contributor to streamflow and spring floods in many regions (Tuttle et al., 2017) and intensify overland nutrient transport and soil erosion (Seyfried et al., 1990; Singh et al., 2009). Thin, ephemeral snowpacks allow the underlying soils to freeze more readily in the winter because they lack the insulating properties of deeper packs and the shallower snow's higher albedo may increase deep-freezing (Starkloff et al. 2017). Soil frost severity impacts soil respiration, carbon sequestration, nutrient retention, and microbial communities as well as a plant root health and tree growth (Aase and Siddoway, 1979; Isard and Schaetzel, 1998; Monson et al., 2006; Henry, 2008; Aanderud et al., 2013; Tucker et al., 2016; Sorensen et al., 2018; Reinmann and Templer, 2018). When the frozen soils impede meltwater infiltration, flooding and erosion may increase (Watanabe and Osada, 2016). Winter recreation is also affected by shallow snowpacks. In some regions, minimum snow depth restrictions for recreational activities are required (e.g., 30.5 cm for snowmobiling on US Forest Service lands) or being considered to reduce impacts to sensitive ecosystems (Hatchett and Eisen, 2019).

... (1)

Jennifer Jacobs 7/13/2020 11:20 AM

**Deleted:** airborne

Jennifer Jacobs 7/13/2020 11:20 AM

**Deleted:** A

able to cover large areas, but it is extremely expensive and has limited availability and flexibility of deployment, which impacts its use for most studies. ALS also has issues with observation gaps in forested regions (Broxton et al., 2015; Currier and Lundquist, 2018; Mazzotti et al., 2019) but possibly to a lesser extent than TLS (Currier et al., 2019). For some snowpack features, the typical vertical accuracies from these platforms, on the order of 10 cm (Kraus et al., 2011; Deems et al., 2013), as well as relatively low return density (~10 returns/m<sup>2</sup>) (Cook et al., 2013) are not adequate to observe spatial variations at point scales (0 to 5 m) to hillslope and field scales (1-100 m) and to detect snow depth changes over short time scales.

SfM can create a digital surface model (DSM) from photographs taken using a standard consumer-grade digital camera. When deployed on an unmanned aerial system (UAS) platform, SfM is a low-cost method that has the capacity for routine snow depth monitoring (Adams et al., 2018; Bühler et al., 2016; De Michele et al., 2016; Harder et al., 2016; Vander Jagt et al., 2015). Reported accuracies range from 8 to 30 cm using UAS SfM (Adams et al., 2018; Bühler et al., 2016; Goetz and Brenning, 2019; Harder et al., 2016; Meyer and Skiles, 2019; Harder et al., 2020). The primary drawbacks of UAS SfM as compared to lidar for mapping snow depth are that the DSM needs to be georeferenced using ground control points (GCPs) with known coordinates and may require significant manual steps (Tonkin et al., 2016; Meyer and Skiles, 2019), although new techniques are emerging that may reduce field data collection time (Gabrlík et al., 2019; Meyer and Skiles, 2019). Dense canopy or vegetation can reduce performance when snow compresses the vegetation relative to the snow-off imagery or when above-canopy vegetation is falsely interpreted to be the snow surface (Bühler et al., 2017; Cimoli et al., 2017; De Michele et al., 2016; Fernandes et al., 2018; Harder et al., 2016; Nolan et al., 2015). Canopy effects impact SfM snow mapping capability in regions where snowpacks are masked by dense forest canopies. The inability to sense portions of the ground/snow surface beneath dense canopies results in fine scale variations in snow depth, such as tree wells, not being accurately represented in UAS SfM snow depth products (Harder et al., 2020).

UAS-based lidar has been widely used in forest-related research (e.g. canopy height and forest change detection) (Wallace et al., 2012; 2014) and appears to offer the advantages of both the UAS SfM and lidar for snow depth mapping. A UAS platform also eliminates many of the drawbacks that arise from ALS and TLS systems discussed earlier. However, to date there is only one previous study that estimates snow depth using UAS-based lidar (Harder et al., 2020). The purpose of this paper is to assess the ability of a UAS platform to provide snow depth using a modest cost UAS-based lidar. The pilot study described here serves as a proof-of-concept for a high vertical resolution snowpack dataset production in open terrain and forests in the north-eastern United States. Snow depth magnitude and variability are mapped and analyzed for differences by land use and terrain. The study highlights results from the 2019 winter season that provide insights as to the potential for UAS lidar mapping of snow depth as well as details about the system, its deployment and operational and validation challenges. We explore the capability of UAS through the comparison of contemporary field-based snow depth measurements collected in a landscape containing fields and forests.

Jennifer Jacobs 7/13/2020 11:25 AM

Deleted: shallow

Jennifer Jacobs 7/13/2020 11:26 AM

Deleted: s

Jennifer Jacobs 7/27/2020 4:46 PM

Deleted: and

Jennifer Jacobs 7/13/2020 11:27 AM

Deleted: from micro to field scales of shallow snowpacks.

Jennifer Jacobs 7/27/2020 4:45 PM

Deleted: costlow-cost

Hunsaker, Adam G 7/22/2020 1:04 PM

Deleted: shallow

Hunsaker, Adam G 7/22/2020 1:04 PM

Deleted: like the northeastern United States

Jennifer Jacobs 7/27/2020 4:49 PM

Deleted: .

Hunsaker, Adam G 7/22/2020 1:09 PM

Deleted:

Jennifer Jacobs 7/13/2020 11:28 AM

Deleted: there are few previous studies that estimate snow depth using UAS-based lidar (Vander jagt et al., 2013).

Jennifer Jacobs 7/13/2020 11:28 AM

Deleted: shallow

Hunsaker, Adam G 7/22/2020 1:30 PM

Deleted: northeastern

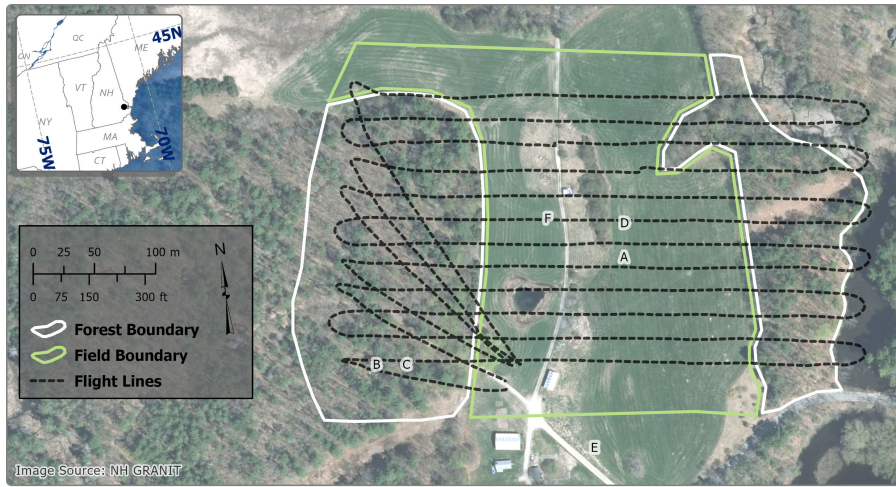


Image Source: NH GRANIT



**Figure 1.** 2015 imagery of Thompson Farm, Durham NH showing both forest and field region with lidar flight lines (top). Ground imagery (a to f), collected in December 2019, locations are noted on the top map and show the surface and leaf off forest conditions (bottom panels).

## 2 Site, Data, and Methods

### 2.1 Site

The test flights were conducted at the University of New Hampshire Thompson Farm Research Station in southeast New Hampshire, United States (N 43.10892°, W 70.94853°, 35 m above sea level, ASL), which was chosen for its mixed hardwood forest and open field land covers (Burakowski et al., 2015; Burakowski et al., 2018) that are characteristic of the region (Figure 1). Thompson Farm has an area of 0.83 km<sup>2</sup> and little topographic relief (Perron et al., 2004). The agricultural fields are actively managed for pasture grass. The mixed deciduous and coniferous forest is composed primarily of white pine (*Pinus strobus*), northern red oak (*Quercus rubra*), red maple (*Acer rubrum*), shagbark hickory (*Carya ovata*), and white oak (*Quercus alba*) (Perron et al., 2004). There are two “wood roads” that run north-south through the pasture and into the western forest section.

Hunsaker, Adam G 7/22/2020 1:32 PM

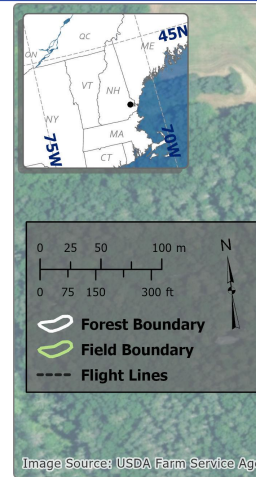
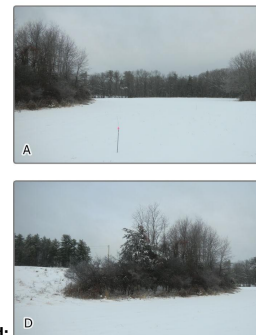


Image Source: USDA Farm Service Agency



Deleted:

Unknown

Formatted: Font:9 pt, Bold, Font color:

Unknown

Formatted: Font color: Black

Jennifer Jacobs 7/13/2020 11:30 AM

Deleted: (18 to 36 m ASL)



## 2.2 UAS Laser Scanning

A series of UAS lidar surveys were conducted over approximately a 0.1 km<sup>2</sup> (9.8 hectares) area (430 by 225 m) within the farm during the winter of 2018/2019 (Figure 1). Here, we focus on the snow-on flight conducted on January 23, 2019 and the snow-off flight conducted on April 11, 2019. We selected the January 23 flight because it had snowed approximately 11.5 cm with 1.8 cm of snow water equivalent from January 19<sup>th</sup> to January 20<sup>th</sup> and the air temperature was persistently below freezing prior to the flight. For the April 11, 2019 snow-off flight, the deciduous component of the canopy and understory were both dormant.

We used an Eagle X8 UAS manufactured by UAV America, which carried a small, light-weight lidar sensor (Velodyne VLP-16) suitable for UAS deployment (see Table S1 in supporting information). The VLP-16 is a 16-channel lidar sensor with a 30-degree vertical field of view with rotating lasers that are spaced evenly between -15 to +15 degrees. Each channel rotates to provide a horizontal field of view of 360-degrees. The VLP-16 collects up to 300,000 points per second with an accuracy of +/- 3 cm at a range of 100 m. The sensor was mounted with the vertical field of view parallel with the ground. The payload is equipped with an Applanix APX-15 UAV inertial navigation system (INS), which has 2-5 cm positional, 0.025-degree roll and pitch, and 0.08-degree true heading uncertainties following post-processing. The INS has a measurement rate of 200 Hz, allowing for a timestamp to associate each lidar pulse with the closest data for latitude, longitude, altitude, and perspective information (roll/pitch/yaw), which is required for georeferencing returns.

Flights were conducted to maximize spatial coverage while conserving batteries due to the limited flight time of the Eagle X8 (approx. 9 minutes flight time to discharge to 3.6 V per cell). Because of the limited flight time, flights were conducted at an altitude of 81 m for greater spatial coverage and multiple return flight lines were necessary for battery exchanges (Figure 1). Automated flights were conducted using UgCS flight planning software. Flight speed was 7 m/s, with a total of 12 parallel flight lines with targeted overlap of 40 percent. Because of degrading accuracy at distances >100 m with the VLP-16, returns acquired outside of +/- 30 degrees of nadir view angles in the horizontal field of view were filtered to limit target distance and improve overall accuracy.

Applanix APX-15 INS data were post-processed to a Smoothed Best-Estimate Trajectory (SBET) file using POSPac MMS UAV (v. 8.2.1), resulting in approximately 3 cm positional accuracy for both the snow-on and snow-off flights. Lidar returns were matched to post-processed INS data and georeferenced using Headwall Photonics, Inc.'s Lidar Tools software. Boresighting calibration was performed using returns from the first two flight lines that were collected in antiparallel directions. A roll offset was determined using 10 m cross sections along the flight lines over flat terrain, and a pitch offset was determined using 1 m cross sections across the flight lines over terrain with moderate relief (see Figure S2 in supporting information). Resulting LAS (LASer) point clouds were generated for the entire study area and projected in WGS84 UTM Zone 19N (EPSG 32619). Flight and filtering parameters of the raw point cloud resulted in return densities of approximately 150 returns/m<sup>2</sup> for each of the two flights.

## 2.3 Lidar Classification and Gridding

Three-dimensional point clouds were processed using the progressive morphological filter algorithm (PMF), in the lidR package (<https://github.com/Jean-Romain/lidR>) of R (v. 3.4, Team, 2018) to identify ground returns. The PMF operates iteratively on sets of two parameters, window size and elevation thresholds, to erode and dilate point cloud data sets to estimate surface topography as an approach to filter out non-ground returns (i.e. trees, shrubs, and noise) from point cloud data sets (Zhang et al., 2003). For ground classification, point clouds were chunked into 100 m square tiles with a 15 m buffer on all sides using catalog options in lidR to ensure returns near tile edges were classified. Processing was distributed

Jennifer Jacobs 7/13/2020 11:32 AM

**Deleted:** (590 g) VLP-16 lidar (Velodyne, Inc.) suitable for UAS deployment

Jennifer Jacobs 7/13/2020 11:33 AM

**Deleted:** , with each channel rotating 360-degrees

Jennifer Jacobs 7/13/2020 11:35 AM

**Deleted:** with

Jennifer Jacobs 7/13/2020 11:35 AM

**Moved down [1]:** Automated flights were conducted using UgCS flight planning software.

Jennifer Jacobs 7/13/2020 11:36 AM

**Deleted:** our flight plan included multiple return flight lines for the three battery exchanges

Jennifer Jacobs 7/13/2020 11:35 AM

**Moved (insertion) [1]**

Jennifer Jacobs 7/13/2020 11:36 AM

**Deleted:** Our f

Jennifer Jacobs 7/13/2020 11:39 AM

**Deleted:** The payload is equipped with an Applanix APX-15 UAV inertial navigation system (INS), which has 2-5 cm positional, 0.025-degree roll and pitch, and 0.08-degree true heading uncertainties following post-processing. The INS has a measurement rate of 200 Hz, allowing for a timestamp to associate each lidar pulse with the closest data for latitude, longitude, altitude, and perspective information (roll/pitch/yaw), which is required for georeferencing returns. ... [2]

Jennifer Jacobs 7/13/2020 11:37 AM

**Deleted:** Data

Jennifer Jacobs 7/13/2020 11:38 AM

**Deleted:** We performed b

Jennifer Jacobs 7/13/2020 11:38 AM

**Deleted:** R

Jennifer Jacobs 7/13/2020 11:39 AM

**Deleted:** Our f

Jennifer Jacobs 7/13/2020 11:40 AM

**Deleted:** were classified as ground and non-ground points

Jennifer Jacobs 7/13/2020 11:40 AM

**Deleted:** (w)

Jennifer Jacobs 7/13/2020 11:41 AM

**Deleted:** (th)

Jennifer Jacobs 7/13/2020 11:41 AM

**Deleted:** as a means to filter out non-ground returns



across 8 computing cores to improve efficiency. PMF was parameterized using a set of window sizes of 1, 3, 5, and 9 m, and elevation thresholds of 0.2, 1.5, 3, and 7 m, which were determined by varying value sets and assessing digital terrain models (DTMs) to determine the parameter sets that produced a visually smooth surface over a dense grid (*in sensu* Muir et al., 2017). Following ground classification for each tile, returns within the 15 m tile buffers were removed, and all resulting 100 m square ground classified tiles were merged. The resulting point clouds for each data set included both the classified ground returns and the non-ground returns. Snow-on and snow-off ground point clouds were gridded at 0.1, 0.2, 0.4, 0.5, and 1.0 m spatial resolutions using the average of all grid points within each grid cell (Currier et al., 2019). Gridded products for each data set were forced to the same coordinate grid to generate DTMs as raster files.

#### 2.4 Slope and Vegetation Cover Classification and Analysis

The snow-off DTM was used to develop a 1 m resolution map of slope (Horn, 1981). Vegetation cover type (field/forest) was determined from the known boundaries of field and forest. The forested area was further classified as coniferous or deciduous for the study region using the following methodology (Figure 1). Within the forested area (Figure 1), a Canopy Height Model (CHM) was used to distinguish the intact upper canopy from other forest cover using our snow-off survey, collected with leaf off in the spring (Sullivan et al., 2017). The CHM was generated by subtracting the DTM produced using ground-classified points from the DSM produced using all lidar points. This results in a digital model consisting solely of canopy heights with no terrain or topography. The CHM generation used raster images with a 1 m resolution. A 3 by 3 maximum convolve filter was used to enhance the edges of canopy crowns and expand smaller regions that might have just one pixel of an intact canopy or a hole in a larger canopy (Palace et al., 2008). A 15 m threshold was used to differentiate between the upper level intact coniferous canopy. CHM pixels that were below this threshold were deemed deciduous canopies (see Figure S3 in supporting information for intermediate figure). The 5.6 ha forested area has a forest type that is 65% deciduous and 35% coniferous.

Once the vegetation forest type was classified, the raster binary image was vectorized. Within the forest and field regions of our study, a subsample was created from the entire image of 5000 random points in the field and 5000 random points in each of the eastern and western forested areas (Palace et al., 2017). At each of these random points, slope, vegetation type (field, deciduous, coniferous), snow depth, and snow depth confidence interval values were extracted. Because of missing values in the raster images, not all random points extracted values. Slope was assigned to one of three categories: 0-10 degrees, 10-20 degrees, and greater than 20 degrees. Because the extracted datasets (i.e., snow depth, confidence interval, and slope) were not normally distributed, the non-parametric Steel-Dwass Method test was used to test for differences. This non-parametric method is useful when sample numbers are large and groups are small, because it allows type I errors to be controlled (Dolgun and Demirhan, 2017).

#### 2.5 In Situ Observations

A magnaprobe (Sturm and Holmgren, 2018) was used to compare to the JAS lidar surveys (hereafter noted as ALS measurements) over two transects. The first transect consisted of 12 sample locations in the field and 5 locations in the eastern forest of our study site. The second transect consisted of 11 sample locations in the western forest. Sample locations were separated by approximately 10 m. The field transect follows the prevailing westerly wind direction with its west side at the foot of a modest depression (approximately 3-4 m below the land further to the west) and the east side transitioning into a wooded area. Following (Harder et al. 2016) and (Bühler et al. 2016), each sample location includes 5 samples in a cross pattern with the four ordinal directions sampled approximately 20 cm from the center sampling location in the cross. The five samples are used to provide a measure of snow depth, central tendency and variation over a 0.4 x 0.4 m pixel. Because the magnaprobe GPS has an absolute accuracy of 8 m, a Trimble® Geo7X GNSS Positioning Unit with Zephyr™ antenna was

Jennifer Jacobs 7/13/2020 11:41 AM

Deleted: We used

Jennifer Jacobs 7/13/2020 11:42 AM

Deleted: DTMs

Jennifer Jacobs 7/13/2020 11:42 AM

Deleted: Following processing, buffers were removed, and tiles were merged to output final classified point clouds for each data set.

Hunsaker, Adam G 7/22/2020 3:53 PM

Deleted: and resulted in different numbers of samples points for the forest and forest types.

Jennifer Jacobs 7/13/2020 11:43 AM

Deleted: 2.4 Snow Depth Ground Truth

Jennifer Jacobs 7/27/2020 4:52 PM

Deleted: 1.2-m Global Positioning System (GPS)-equipped Magnaprobe

Jennifer Jacobs 7/13/2020 11:44 AM

Deleted: unmanned aerial system (UAV)

Hunsaker, Adam G 7/22/2020 4:02 PM

Deleted: SD

Jennifer Jacobs 7/13/2020 11:45 AM

Deleted: Each sample location includes 5 samples in a cross pattern with the four ordinal directions sampled approximately 20 cm from the center sampling location in the cross.

Hunsaker, Adam G 7/22/2020 1:47 PM

Deleted: m

355 used to collect each sampling location's center point with an estimated horizontal uncertainty of 2.51 cm (standard deviation  
σ 0.95 cm) and 4.17 cm (σ 4.60 cm) for the field and forest, respectively after differential correction. Along the same forest  
and field transects, a federal snow tube sampler was used to collect a single sample of snow depth and snow water equivalent  
(SWE) at each magnaprobe sample location for a total of 12 field samples and 16 forest samples. SWE was measured by  
inserting the aluminium tube vertically into the snowpack and a core was extracted and weighed using a spring scale.

360 An independent study collected soil frost depth from three locations at the Thompson Farm Research Observatory using  
Gandahl-Cold Regions Research and Engineering Laboratory (CRREL) style frost tubes. The frost tubes have flexible,  
polyethylene inner tubing filled with methylene blue dye whose color change is easy to differentiate when extruded from ice  
(Gandahl 1957). A nylon string housed inside the polyethylene tubing affixes ice during periods of thaw. The outer tubing  
365 consists of PVC pipe installed between 0.4 to 0.5 m below soil surface (Ricard et al., 1976; Sharratt and McCool, 2005).  
Prior to the January 19<sup>th</sup> and 20<sup>th</sup>, 2019 snowfall event, soil frost was 23.5 to 25.5 cm in the field and 5.5 to 8.5 cm in the  
west forest.

## 2.6 Snow Depth Uncertainty Assessment

370 The snow depth accuracy was assessed by comparing the lidar snow depth measurements to the magnaprobe measurements.  
Here, accuracy is the measure of the agreement of the lidar snow depth measurements relative to the in-situ measurements  
(Eberhard et al., 2020; Maune and Nayegandhi, 2018). Error statistics were calculated and the results were summarized by  
forest and field locations. At each magnaprobe location, the average and standard deviation of the five magnaprobe samples  
were calculated. The average lidar snow depth was determined for a 0.4 x 0.4 m cell centered on the center magnaprobe  
location. The mean absolute difference (MAD) and root mean square deviation (RMSD) were used to characterize the  
375 differences between the magnaprobe snow depths and the lidar snow depths.

The one-sided width of the 95% confidence limits for each cell's snow depth is a measure of the lidar snow depth variability.  
Confidence intervals were calculated using a cell's pooled standard deviation, the number of lidar returns, and the pooled  
degrees of freedom (Helsel and Hirsh, 1992) to calculate. A cell's snow depth pooled standard deviation  $\sigma_d$  of the snow-on  
380 and snow-off elevations was calculated as

$$\sigma_d = \sqrt{\sigma_{on}^2 + \sigma_{off}^2} \quad (1)$$

where  $\sigma_{on}$  and  $\sigma_{off}$  are the standard deviation of the snow-on and snow-off lidar return elevations, respectively. This pooled  
standard deviation is a measure of the variability of the snow-on and snow-off lidar returns within a grid cell. This variability  
depends on the lidar instrument's relative accuracy (Maune and Nayegandhi, 2018), which includes intra-swath accuracy  
385 (i.e., precision or repeatability of measurements) and inter-swath accuracy (i.e., differences in elevations between  
overlapping swaths), as well as surface elevation variations. The contribution from the individual sources of variability was  
not assessed.

## 3 Results and discussion

### 3.1 Snow Depth Survey

390 The snow-on and snow-off lidar ground returns yielded an average point cloud density of 90 and 364 points/m<sup>2</sup> in the forest  
and field, respectively, with 6.7% of the 1 m<sup>2</sup> forest cells and 0.03% of the 1 m<sup>2</sup> field cells having less than 5 point/m<sup>2</sup>  
(Figure 2). There is a wide range of the point cloud densities (Figure 2b). The highest point cloud density occurred for those  
cells sampled by both the regular flight lines and the multiple return flight lines conducted for the three battery exchanges.

Hunsaker, Adam G 7/22/2020 4:03 PM

Deleted: m

Hunsaker, Adam G 7/22/2020 4:11 PM

Deleted:

Hunsaker, Adam G 7/22/2020 4:10 PM

Deleted: Snow depth

Jennifer Jacobs 7/13/2020 11:45 AM

Deleted: a federal snow sampler was used to collect a single sample of snow depth and snow water equivalent at each location.

Jennifer Jacobs 7/27/2020 4:55 PM

Deleted: 5

Hunsaker, Adam G 7/22/2020 4:05 PM

Deleted: m

Hunsaker, Adam G 7/22/2020 4:06 PM

Deleted:

Hunsaker, Adam G 7/22/2020 4:06 PM

Deleted: m

Hunsaker, Adam G 7/22/2020 4:06 PM

Deleted: m

Hunsaker, Adam G 7/22/2020 4:06 PM

Deleted: m

Hunsaker, Adam G 7/22/2020 4:06 PM

Deleted: m

Jennifer Jacobs 7/13/2020 11:47 AM

Deleted: Error statistics were calculated and the results were summarized by forest and field locations. At each magnaprobe location, the average and standard deviation of the five magnaprobe samples were calculated. The average lidar snow depth was determined for a 0.4 x 0.4 m cell centered on the center magnaprobe location. The mean absolute difference (MAD) and root mean square difference (RMSD) were used to characterize the differences between the magnaprobe snow depths and the lidar snow depths. ...[3]

Hunsaker, Adam G 7/22/2020 4:26 PM

Deleted: snow on

Hunsaker, Adam G 7/22/2020 4:26 PM

Deleted:

Hunsaker, Adam G 7/22/2020 4:26 PM

Deleted: snow on

Hunsaker, Adam G 7/22/2020 4:26 PM

Deleted:

Jennifer Jacobs 7/13/2020 11:47 AM

Deleted: The snow depth uncertainty was combined with the number of lidar returns and the pooled degrees of freedom (Helsel and Hirsh, 1992) to calculate the one-sided width of the 95% confidence limits for each cell.

Hunsaker, Adam G 7/22/2020 4:35 PM

Deleted: flights

The vast majority of field cells (82%) have more than 100 points/m<sup>2</sup>. Only 1% of the field cells had less than 25 points/m<sup>2</sup> and most of those cells were in shrubbery or dense vegetation surrounding the small pond in the center of the study site (Figure 1). In contrast, 41% of the forest cells had more than 100 points/m<sup>2</sup> and nearly 20% of the forest cells had less than 25 points/m<sup>2</sup> with 8% having fewer than 10 points/m<sup>2</sup> (Figure 2b). Only 0.086% and 0.95% of the 1 m resolution field and forest cells, respectively, had no ground returns. The number of points per cell decreases with decreasing cell size (Figure 2a). In the field, reducing the gridded resolution from 1 m to 0.5 m lowers the mean cell return count to 91 points per cell on average. Thus a 0.5 m field cell has approximately the same number of returns as a 1 m forest cell. At a 0.2 m spatial resolution, the mean number of ground returns is 14.6 and 3.6 in the field and forest, respectively.

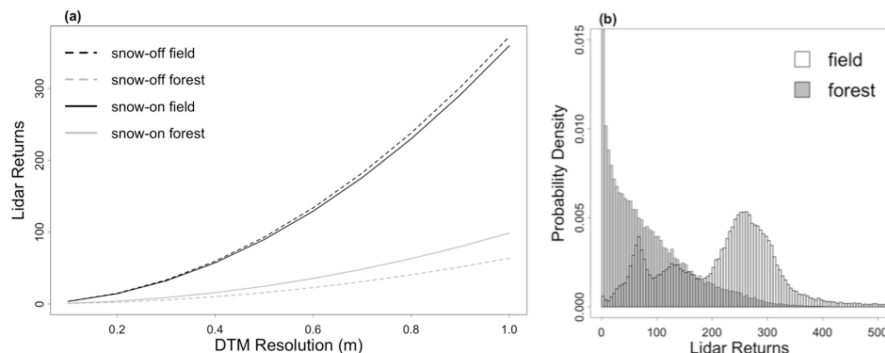


**Figure 2.** (a) Average lidar point cloud density of the ground returns versus cell size by land cover, and snow-on and snow-off state (top). (b) Probability density function for the number of lidar ground returns by square meter for the forest (gray) and the field (white) (bottom).

### 3.2 Lidar and In Situ Snow Depth Comparison

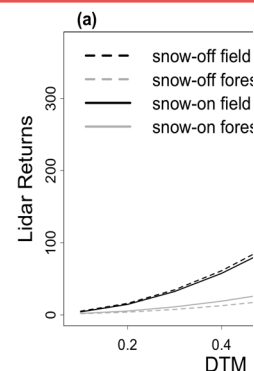
Based on the magnaprobe snow depth and UAS-mapped snow depth measurements, the accuracy of lidar snow depth measurements differed between field and forest cells (Figure 3). In the field, the mean snow depth from the magnaprobe (12.2 cm ± 0.56 cm) was only slightly greater than that from the lidar (11.2 cm ± 0.72 cm) and the MAD and RMSD values were 0.96 cm and 1.22 cm, respectively. In the forest, the mean snow depth from the magnaprobe (15.2 cm ± 2.3 cm) was twice as large as the lidar snow depths (7.8 cm ± 6.3 cm) and the MAD and RMSD were 9.6 cm and 10.5 cm, respectively. The mean snow depth from the snow tube was (12.9 cm ± 0.71 cm) and (13.1 cm ± 1.9 cm) in the field and forest, respectively. There is a notable low bias in the lidar forest snow depth relative to the magnaprobe and snow tube for west forest in particular with exception of one site.

To provide insight to differences between the forest and field observations, mean height profiles were calculated for a 25 m<sup>2</sup> square region centered on forest and field study plots from lidar data (Figure 4). To do this, all lidar returns were extracted from the bounding box of each plot, then the mean elevation of ground returns was calculated within each plot. Return height profiles for each plot were determined by subtracting the mean ground elevation of the plot from each return, then the normalized return elevations were binned in 0.1 m height increments. Within the forests, an average of 2142 and 2889 returns were classified as ground and non-ground in snow-free conditions for each 25 m<sup>2</sup> plot, respectively. Snow-on conditions had a comparable number of ground returns (2218), but fewer non-ground returns (1721). In field plots, an average of 5666 ground returns and 154 non-ground returns in snow-free conditions were obtained per 25 m<sup>2</sup> plot, with 7567

Jennifer Jacobs 7/13/2020 11:48 AM  
Deleted: the small water body.

Hunsaker, Adam G 7/22/2020 4:39 PM  
Deleted: the

Jennifer Jacobs 7/13/2020 11:49 AM



Deleted:

Unknown

Formatted: Font color: Black

Hunsaker, Adam G 7/22/2020 4:40 PM

Deleted: with

Hunsaker, Adam G 7/22/2020 4:43 PM

Deleted: point cloud density for 1 m<sup>2</sup> cell

Hunsaker, Adam G 7/22/2020 4:44 PM

Deleted: hashed

Jennifer Jacobs 7/27/2020 5:02 PM

Deleted: .

Jennifer Jacobs 7/13/2020 11:50 AM

Deleted: Snow Depth

Hunsaker, Adam G 7/22/2020 4:06 PM

Deleted: m

Hunsaker, Adam G 7/22/2020 4:06 PM

Deleted: m

Hunsaker, Adam G 7/22/2020 4:07 PM

Deleted: m

Hunsaker, Adam G 7/22/2020 4:07 PM

Deleted: m

Jennifer Jacobs 7/27/2020 5:03 PM

Formatted: Border:Top: (No border), Bottom: (No border), Left: (No border), Right: (No border), Between : (No border)

Hunsaker, Adam G 7/22/2020 5:03 PM

Deleted: s

Jennifer Jacobs 7/27/2020 5:00 PM

Deleted: the

ground returns and 25 non-ground returns in snow-on conditions. Figure 4 also shows that there is a greater range of ground return elevations in the forest as compared to the field. In forest plots, ground return elevations had an average standard deviation of 0.157 m and 0.154 m in snow-free and snow-on conditions, respectively, while in field plots, ground return elevations had standard deviations of 0.058 m and 0.050 m in snow-free and snow-on conditions, respectively.

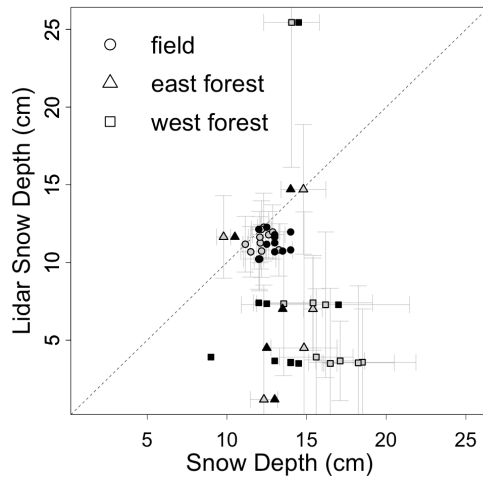


**Figure 3.** Comparison between the [magnaprobe](#) (gray fill) and snow tube (black fill) versus the lidar snow depth measurements by location. The mean and 95% confidence intervals were calculated using the five [magnaprobe](#) snow depths and the lidar snow depths averaged over a 0.4 x 0.4 m grid cell. Single snow tube snow depth measurements are shown without confidence intervals.

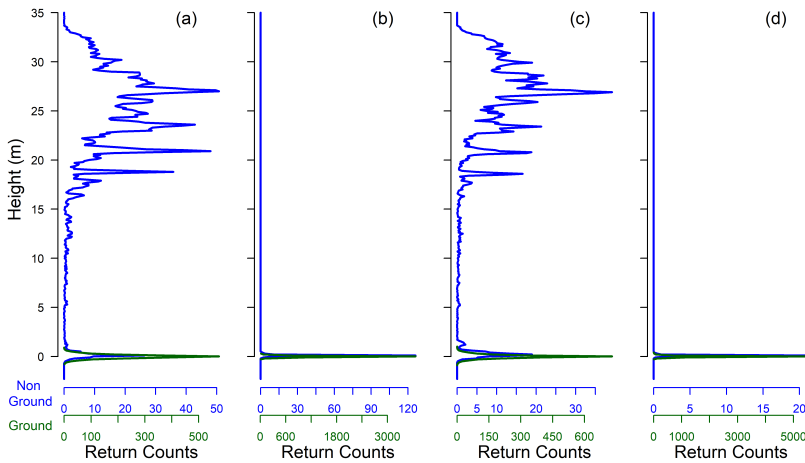


**Figure 4.** Mean height profiles for all ground (green) and non-ground (blue) returns within a 5 m x 5 m region centered on each transect plot in snow-free conditions (a, b) and snow-on conditions (c, d) in forest (a, c) and field (b, d) study plots.

### 3.3 Snow Depth Maps from UAS Lidar

The UAS-mapped snow depth, mapped by subtracting snow-off DTMs from snow-on DTMs, reveals a shallow snowpack whose depth ranges from less than 2 cm to over 18 cm (Figure 5). The mean lidar snow depth was 10.3 cm in the field and 6.0 cm in the forest. Despite the shallow conditions, spatially coherent patterns are readily discernible. The field snowpack depth has higher spatial variability than the west forest snowpack and more spatial organization. In the field, the deepest snow is in the low-lying northeast areas that are sheltered from westerly winds. A relatively moderate and consistent snowpack occurs in southern part of the east field and west of the small pond. The shallowest snowpack is found in the center portion of the field, which is slightly elevated and, unlike most of the field, was not mowed. Lower snow depth at the forest edge distinguishes the field to forest transition. A non-parametric Steel-Dwass test found significant variation for the mean snow depth among the two forest types and field ( $p < 0.0001$ ) (Figure 6a). A pairwise Steel-Dwass test showed that snow depths were significantly different between the three pairs of field and forest types ( $p < 0.0001$ ). When comparing just field and forest as categories, the test also found significant differences for snow depth ( $p < 0.0001$ ). Snow depth was also determined to be significantly different among the three slope group categories using the Steel-Dwass test where regions with a limited slope (Group 1) had more decidedly different snow than steeper regions ( $p < 0.0001$ ) (Figure 6b).

The one-sided confidence interval values of the mean snow depth estimate are remarkably consistent in the field and typically are between 0.5 to 1 cm regardless of snow depth (Figure 5b). Modestly larger confidence intervals occur adjacent to the north-south road where the fields were not mowed prior to winter as well as the northern and southern extents of the flight lines likely due to the reduced sampling density. The forest had an average one-sided confidence interval of 3.5 cm, which is considerably higher than the field. Where the forest is predominantly comprised of deciduous trees, the typical one-sided confidence intervals of the mean snow depth were as low as 1 to 2 cm. The largest one-sided confidence interval values occur in the middle of the field where there is dense shrubbery, at the edge of the fields, and in clusters within the forest where the forest sections are dominated by coniferous trees. The nexus of flight lines in the take-off and landing area resulted in a local area with very high confidence. A non-parametric Steel-Dwass test found significant variation for confidence intervals of the mean snow depth among the two forest types and field ( $p < 0.0001$ ) (Figure 6c). A pairwise Steel-Dwass test showed that confidence intervals were significantly different between the three pairs of field and forest types and ( $p < 0.0001$ ). Confidence intervals were also significantly different among the three slope categories as determined using a Steel-Dwass test ( $p < 0.0001$ ) (Figure 6d).

### 3.4 Point Cloud Density and Spatial Resolution

Confidence intervals for the mean snow depths by grid cell were examined in light of the point cloud density and the spatial resolution at which lidar returns were aggregated. The confidence interval width for a mean snow depth of a  $1 \text{ m}^2$  area increases dramatically as the lidar point cloud density increases (Figure 7a). Except for the cells with fewer than  $10 \text{ point/m}^2$ , forest cells have larger confidence intervals for the mean depths than field cells for a given sample size. When the density exceeds  $25 \text{ point/m}^2$  in the field and  $50 \text{ point/m}^2$  in the forest, confidence intervals are typically 2 cm. The cells with the highest point cloud densities have one-sided confidence intervals of about 1 and 1.5 cm for the field and forest cells, respectively. The field cells with more than  $50 \text{ point/m}^2$  did not have noticeably smaller confidence intervals, but the increased density did reduce the number of cells with anomalously small confidence intervals. Given the high lidar point cloud density for the field cells, it is possible that reasonable estimates of snow depth can be made at scales finer than 1 m (Figure 5b).

Jennifer Jacobs 7/13/2020 11:52 AM  
Moved (insertion) [2]

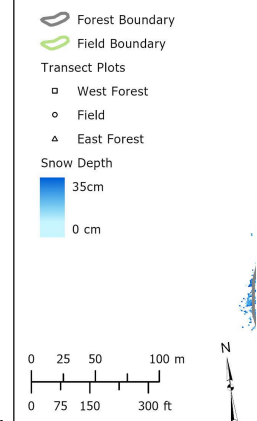
Jennifer Jacobs 7/13/2020 11:52 AM  
Deleted: 4...). The mean lidar snow depth ... [4]

Jennifer Jacobs 7/13/2020 11:56 AM  
Deleted: In the field, the precision of the mean snow depth estimate is...remarkably consiste... [5]

Jennifer Jacobs 7/13/2020 12:00 PM  
Moved (insertion) [3]

Jennifer Jacobs 7/13/2020 12:00 PM  
Deleted: Snow depth precision was ...xam... [6]

Jennifer Jacobs 7/27/2020 5:03 PM



Deleted:

Unknown

Formatted: Font:9 pt, Bold, Font color: Black

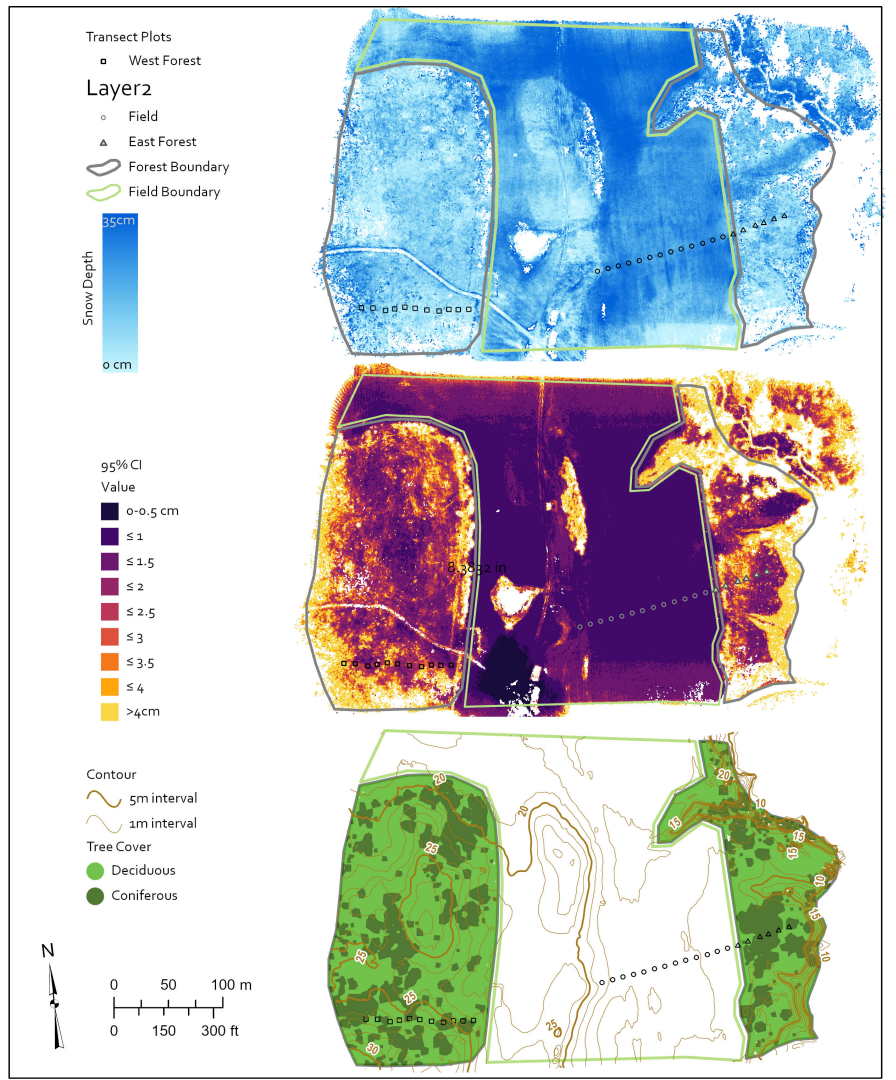


**Figure 5.** Average (top) snow depth values, (middle) one sided confidence intervals, and (bottom) topography and forest cover type. Snow depth and confidence intervals calculated from the snow-on and snow-off lidar point clouds for 1 m<sup>2</sup> cells at Thompson Farm, Durham, NH. Topography and forest cover type determined from snow-off lidar point clouds on snow-off flight for 1 m<sup>2</sup> cells conducted on April 11, 2019.

570



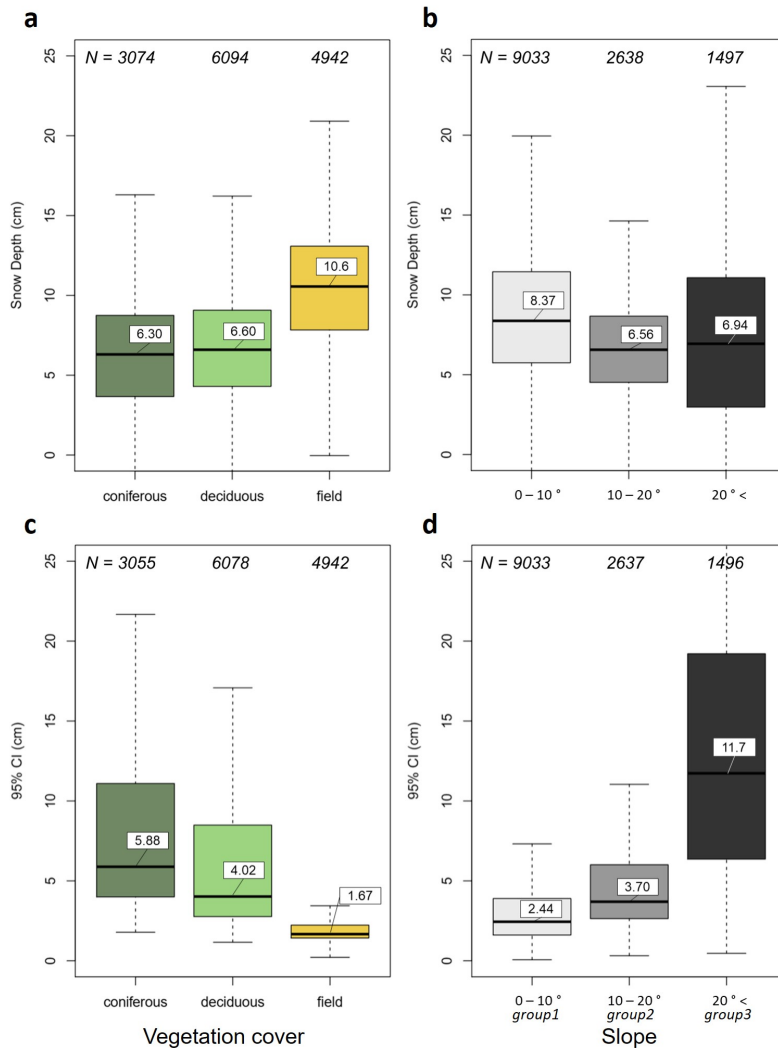


**Figure 6.** Snow depths (a,b) and their one sided confidence intervals (c,d) from the random sample points of the field and forest at Thompson Farm, Durham, NH on January 23, 2019 from the individual cells for 1 m<sup>2</sup> cells by vegetation cover (a,c) and slope group (b,d). Boxplots show the lower quartile, median, upper quartile, and whiskers with the median value noted. Because of missing values in the raster images, not all random points extracted values and resulted in different numbers of samples points for vegetation cover classes.

Unknown

Formatted: Font:9 pt, Bold, Font color:

Jennifer Jacobs 7/13/2020 12:04 PM

95% CI

- 0-0.5 cm
- ≤ 1
- ≤ 1.5
- ≤ 2
- ≤ 2.5
- ≤ 3
- ≤ 3.5
- ≤ 4
- >4cm

Forest Boundary

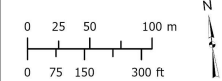
Field Boundary

Transect Plots

West Forest

Field

East Forest



Deleted:

Snow depth precision was examined in light of the point cloud density and the spatial resolution at which lidar returns were aggregated. The ability to precisely estimate mean snow depth of a 1 m<sup>2</sup> area increases dramatically as the lidar point cloud density increases (Figure 5a). Except for the cells with fewer than 10 point/m<sup>2</sup>, forest cells have less precise estimates of the mean depths than field cells for a given sample size. When the density exceeds 25 point/m<sup>2</sup> in the field and 50 point/m<sup>2</sup> in the forest, precision is typically 2 cm. The cells with the highest point cloud densities have one-sided confidence intervals of about 1 and 1.5 cm for the field and forest cells, respectively. The field cells with more than 50 point/m<sup>2</sup> did not have noticeably smaller confidence intervals, but the increased density did reduce the number of cells with anomalously low precision. Given the high lidar point cloud density for the field cells, it is possible that reasonably precise estimates of snow depth can be made at scales finer than 1 m (Figure 5b).

Jennifer Jacobs 7/13/2020 12:00 PM

**Moved up [3]: 3.4 Point Cloud Density and Spatial Resolution**

Snow depth precision was examined in light of the point cloud density and the spatial resolution at which lidar returns were aggregated. The ability to precisely estimate mean snow depth of a 1 m<sup>2</sup> area increases dramatically as the lidar point cloud density increases (Figure 5a). Except for the cells with fewer than 10 point/m<sup>2</sup>, forest cells have less precise estimates of the mean depths than field cells for a given sample size. When the density exceeds 25 point/m<sup>2</sup> in the field and 50 point/m<sup>2</sup> in the forest, precision is typically 2 cm. The cells with the highest point cloud densities have one-sided confidence intervals of about 1 and 1.5 cm for the field and forest cells, respectively. The field cells with more than 50 point/m<sup>2</sup> did not have noticeably smaller confidence intervals, but the increased density did reduce the number of cells with anomalously low precision. Given the high lidar point cloud density for the field cells, it is possible that reasonably precise estimates of snow depth can be made at scales finer than 1 m (Figure 5b).

Unknown

Formatted: Font:9 pt, Font color: Black



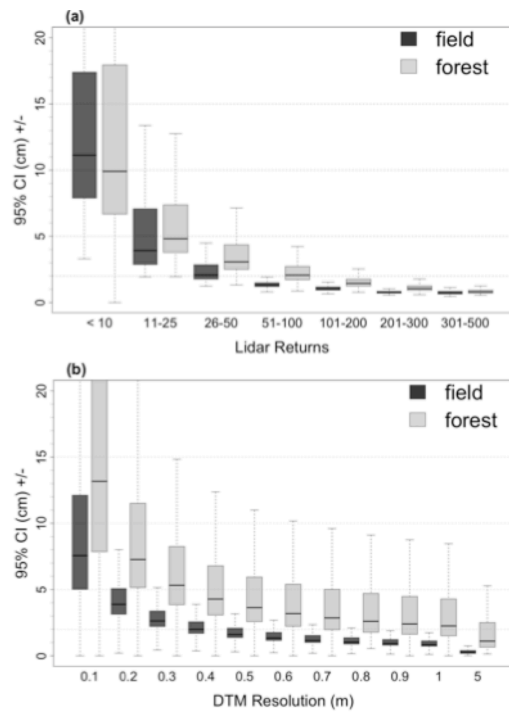
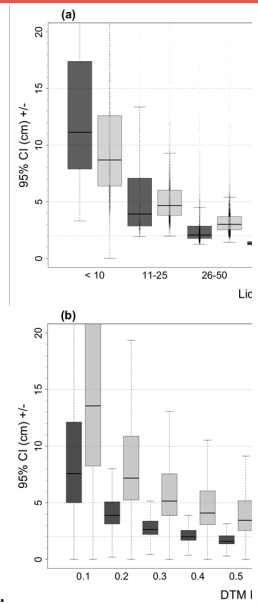


**Figure 5.** One sided confidence intervals of the mean snow depth values in the field and forest at Thompson Farm, Durham, NH on January 23, 2019 from the individual cells for 1 m<sup>2</sup> cells by land cover and point cloud density (a) and for grid resolutions ranging 0.1 to 5 m (b). Boxplots show the lower quartile, median, upper quartile, and whiskers.

In addition to the lidar point cloud density, the ability to capture the snow depth also depends on the ground surface variability within a cell as well as the lidar performance. For this site and its shallow snowpack, the local scale variability of the ground surface elevation was estimated by calculating the standard deviation of the lidar elevation values and found to depend primarily on the cell size and, to a more limited extent, on land cover and snow cover (Figure 8a). Snow cover reduces the within cell variability in field by about 1 cm, but has a limited effect in the forest. It is possible that the modest snowpack was able to flatten the higher grass in the field, while the forest's vegetation and terrain features that dominate the within cell variability are only minimally compacted by the snow. Within the 1 m grid cells, snow depth variability was much lower in the field than the forest (Figure 6b). Both distributions had a positive skew. Typical standard deviations of the lidar surface elevation values within a 10 cm cell are on the order of 1.5 and 2 cm for the field and forest, respectively. That variability doubles for a 20 cm cell. The within cell variability increases gradually to about 3 to 4 cm in the field, and to about 6 cm in the forest.

Thus, confidence intervals largely depend on the point per cell in the lidar cloud because the standard deviation of a cell's surface elevation is relatively constant for spatial scales from 0.5 to 1 m (Figure 8a). In the field, reducing the cell size from 1 m to 0.5 m still yields about 100 points/m<sup>2</sup> and provides snow depth estimates within +/- 1.5 cm. Because the forest cells require a higher ground return density to capture these snow depths within a 1 cm precision, any reduction in cell size below 1 m greatly increase the cell mean snow depth's confidence intervals.

Jennifer Jacobs 7/13/2020 12:05 PM



Deleted:

Unknown

Formatted: Font:9 pt, Bold, Font color: Black

Jennifer Jacobs 7/13/2020 12:05 PM

Deleted: top

Jennifer Jacobs 7/13/2020 12:05 PM

Formatted: Superscript

Jennifer Jacobs 7/13/2020 12:05 PM

Deleted: bottom

Jennifer Jacobs 7/13/2020 12:06 PM

Deleted: precisely

Jennifer Jacobs 7/13/2020 12:06 PM

Deleted: on the within cell variability

Jennifer Jacobs 7/13/2020 12:06 PM

Deleted: 6a

Jennifer Jacobs 7/13/2020 12:07 PM

Deleted: Snow cover reduces the within cell variability in field cells by about 1 cm, but has limited effect in the forest.

Jennifer Jacobs 7/13/2020 12:07 PM

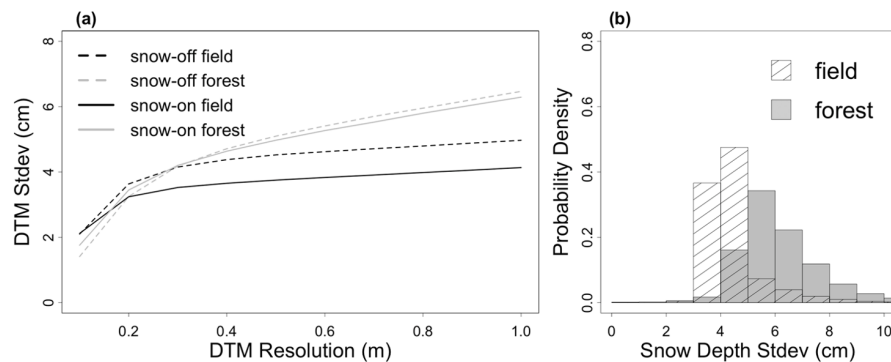
Deleted: precision

Jennifer Jacobs 7/13/2020 12:08 PM

Deleted: s

Jennifer Jacobs 7/13/2020 12:08 PM

Deleted: 6a



660 **Figure 8.** Lidar surface elevation standard deviations by (a) cell size and land cover (top). (b) Probability density function of the pooled  
snow depth standard deviation for each 1 m<sup>2</sup> cell in the forest (gray) and field (hashed) (bottom).

#### 4. Challenges and Recommended Improvements to UAS Lidar Snow Depth Mapping

Despite UAS-based lidar's increasing use in the natural sciences and capacity to make high resolution snow maps, there are many operational and technical challenges that require consideration prior to successfully conducting UAS-based lidar surveys that produce research grade, high-resolution snow depth data. Even though the UAVs are modest in size (i.e., weighing less than 25 kg), the hardware and supporting software analysis tools can be expensive and require trained pilots and lidar data analysis specialists. In this section, we present some general considerations regarding validation of the lidar snow depth maps, selection and deployment of a lidar sensor on a UAV for snow depth mapping as well as specific insights that we experienced when using our system.

##### 4.1 *In Situ* and UAS Sampling

While UAS-based lidar surveys can measure snow depth to within a centimeter at high spatial resolutions, validation of those observations is challenging. A time consuming collection of high accuracy GNSS survey points was required to co-locate magnaprobe and lidar observations. Surveying in sample locations prior to the winter season might reduce this effort. It is also challenging to make *in situ* snow depth measurements that provide centimeter accuracy. In this study, the magnaprobe *in situ* snow depth observations made in the forest were considerably higher than the lidar observations as compared to the open field where the magnaprobe and lidar measurements were within 1 cm. Previous studies also found that snow depth observations from ALS measurements are biased lower than those from snow-probe observations in the forest (Hopkinson et al., 2004; Currier et al., 2019; Harder et al., 2020). In past studies, the causes of these differences have been partially attributed to the snow probe's ability to penetrate the soil and vegetation, human observers tending to make snow depth measurements in locations with relatively high snow (Sturm and Holmgren, 2018) and the reduced accuracy of the GNSS. Our study suggests additional issues in forest sampling including enhanced terrain variability in forested areas relative to adjacent field areas and reduced lidar returns in forested areas as compared to field areas combine with sampling issues to contribute to the higher uncertainty in the forest snow depths observed in our study.

In this study, the cold temperatures and snow-free conditions prior to the January 19<sup>th</sup> and 20<sup>th</sup> snowfall event resulted in deeper frozen soils (23.5 to 25.5 cm) in the field and shallower soil frost depth (5.5 to 8.5 cm) in the west forest, which would have limited the probe penetration into soils at both sites. However, the forest has a 1-4 cm thick organic leaf litter

Jennifer Jacobs 7/13/2020 12:08 PM

**Deleted:** decreases the precision of the cell mean snow depth.

Jennifer Jacobs 7/13/2020 12:10 PM

**Formatted:** Normal1, Space After: 10 pt, Border:Top: (No border), Bottom: (No border), Left: (No border), Right: (No border), Between : (No border)

Jennifer Jacobs 7/13/2020 12:10 PM

**Deleted:** 6

Jennifer Jacobs 7/13/2020 12:10 PM

**Deleted:** .

... (7)

Jennifer Jacobs 7/13/2020 12:11 PM

**Deleted:** data for snow hydrology. Large UAVs and supporting software analysis tools can be expensive and require trained pilots and lidar data analysis specialists. In this section, we present some preliminary insights regarding the deployment of a lidar sensor on a UAV for snow depth mapping.

layer that may have been penetrated by the magnaprobe. The average Federal snow sampler tube depths (13.1 cm) were not as deep as the magna probe (15.2 cm) and thus more closely match the lidar snow depth (7.8 cm; see Figure 3), though a considerable low bias (~5.3 cm) similar to that found by Harder et al. (2020) persists in the lidar snow depth relative to the federal snow sampler snow depths. Additional factors such as downed logs, thick understory, and fine-scale topographic features (ie: small boulders and hummocky terrain) as well as reduced ground return density may contribute to the lidar snow depth errors in a forest, whereas these factors are absent in the field.

An improved understanding of forest canopies impacts on lidar returns is also warranted. Recent work has demonstrated that lidar pulses are “lost” at a much higher rate in forest canopies than open ground terrain due to interception, absorption, and scattering through canopy transmission, with the loss ratio largely influenced by the range of the target from the sensor (Liu et al., 2020). The data that we presented in this paper were acquired using constant flight speed and at consistent altitude above target areas. Because of this, it is feasible that forest canopy conditions and variable understory vegetation density may have resulted in lost pulses and increased uncertainty in our data set. Indeed, we did observe lower return densities for both ground and all returns in forested areas in our data set (Figure 4).

One possible outcome of these lidar sampling issues in forests was a significant difference in snow depth confidence intervals between field and forest types and among slope groups. Confidence intervals were highest in conifer stands and on steep slopes and lowest in the field. While this result is not entirely surprising, it is likely partially the result of lower ground return density in forests due to the combined effects of lost pulses and canopy occlusion in forested areas. Additionally, this observation may be driven by increased variability in snow depth due to pockets of duff and woody debris, and due to higher variability in subnivean terrain in the forested areas of the study site. Areas of high terrain relief are expected to have more variability in ground return elevations over shorter distances, which would partially drive higher confidence intervals of ground surface elevation for pixels located in high relief areas. High relief areas of the study site were more common in forested areas of the study site, and the uncertainty resulting around high slopes also carries through snow depth estimation. Snow depth was significantly different between field and forested areas, as well as between conifer and deciduous forest types, despite the relatively high uncertainty. This indicates the possible influence of tree canopies on snow accumulation due to enhanced snow interception in forests, and particularly in conifer stands, but also could be the result of an under-sampled ground surface in forested areas relative to field areas. Snow depth also was significantly different among the three slope groups, possibly due to wind-driven snow displacement and sloughing on slopes during accumulation.

#### 4.2 Flight Planning

Because larger UAVs that can carry heavier payloads have challenges that may differ from small UAVs, a well-formulated flight plan that addresses weather conditions, logistics of flying at proposed site, flight lines, UAS equipment, and personnel is clearly needed. Weather impacts operations. UAS surveys cannot be conducted when there is any type of precipitation or in dense fog/clouds because moisture can cause electronic components to malfunction and moisture build-up on the propellers can also adversely affect lift production. Depending on the UAV, wind speeds exceeding 7 to 10 m/s may make flights more difficult. This project’s Eagle XF high lift capacity UAS cannot be flown comfortably in winds greater than 8 m/s. At the study site, wind speeds often exceeded this threshold in the days immediately following snowfall except early in the morning. High wind speeds can also significantly reduce battery life as well as impact the accuracy of sensor observations. Low air temperatures can cause batteries to rapidly discharge. For winter UAS surveys, all flight and operational batteries were kept warm in a building, vehicle, or insulated cooler prior to the UAS survey. This also applies to the computer used to upload flight lines and relay telemetry information. A MIL-STD-810 certified Panasonic Toughbook

was used in this study to handle the anticipated cold temperatures. Additionally, cold temperatures can severely limit the dexterity of the person manipulating the flight controls.

High lift UAVs capable of carrying a lidar sensor package have the potential to cause significant damage to person and property. The selection of a survey site not only needs to meet the scientific objectives of the UAV survey, but also must have the proper attributes for safe and legal UAV operation including permission to operate the UAV at the site. Visual line of sight (VLOS) of the UAV needs to be maintained throughout the flight. When it is difficult to maintain VLOS (e.g., flying over forested or mountainous sites), spotters can be used if there is constant two-way communication between the spotters and the person operating the flight controls. For this study, an on-site, walk up tower with a spotter was necessary while the UAV was flown over the forest.

The deployment of a UAV lidar system requires additional flight patterns designed for boresighting to ensure that point clouds are aligned (Painter et al., 2016). Provided that GNSS data are accurate, the most common reason for misalignment of point clouds is boresight angle errors (Li et al., 2019). Boresighting is the process of calculating the differences between lidar sensor and IMU roll, pitch, and yaw angle measurements to correct those errors in point clouds. Due to battery flight time limitations, we were unable to complete the flight pattern that is commonly used for boresighting alignment. Because of this, we leveraged our first two antiparallel flight lines for boresighting calibration. Additional details on boresighting calibration, our technique due to the flight time limitations, and examples of roll and pitch alignment errors observed during this field campaign appear in the supplemental materials.

#### 4.3 UAS Sampling Strategies

While lidar calibration and data post-processing requirements are quite similar for UAS and airborne surveys, the UAS lidar surveys presented in this study have key differences from previous ALS surveys. As noted above, UAS flight durations are considerably shorter, resulting in limited spatial coverage as compared to previous ALS snow depth surveys. An advantage of UAS over ALS surveys is that the average point cloud density is much higher and has fewer missing pixels in the forest. This study's sampling densities and the proportion of areas with no ground returns are quite different from previous airborne lidar SD studies. This study had ground returns of 90 and 364 points/m<sup>2</sup> in the forest and field, respectively, and had no ground returns in only 0.086% and 0.95% of the 1 m resolution field and forest cells, respectively. In contrast, ALS surveys typically report surface model densities between 8 to 16 points/m<sup>2</sup> (Broxton et al., 2015; 2019; Currier et al., 2019; Kirchner et al., 2014) and ground returns between 3 and 6 points/m<sup>2</sup> (Broxton et al., 2019; Kirchner et al., 2014). ALS derived snow depth maps have a much greater proportion of areas that are masked due to no ground returns, particularly under trees, with masking areas ranging from less to 10% to more than 23% (Harpold et al., 2014; Mazzotti et al., 2019). While gap filling is possible, interpolation using measured snow depth values to fill under tree can overestimate snow depth (Zheng et al., 2016). Based on our work comparing field and forest lidar collections from a UAS, we suggest testing alternative flight plans, including reduced flight speed over forest canopies to account for lost pulses and canopy returns to produce ground return density that is comparable to field ground return density and to further reduce the number of missing pixels in an acquisition area.

A well understood challenge exists when developing a spatial sampling strategy in which, for given resources, there is a trade-off between spatial extent and sampling density (Clark et al. 2011). Increasing flight altitude can expand the spatial extent of an aerial survey. However, flying at higher altitudes results in a decreased point density. In theory, a higher point density could be achieved by slower speeds and increased swath overlap. The targeted spatial extent of an aerial survey dictates whether a manned aircraft or a UAV platform should be used. If the targeted area has a limited domain then using a

785 manned airborne platform is probably overkill and inefficient for many studies and the use of a UAV would be more cost  
effective. However, as the domain increases in size, additional batteries would be required, much of the battery power would  
be used to reach the outer limits of the domain, and the ability to maintain the required line of sight could be difficult. Thus,  
there are end-members for survey site or regions where it is self-evident as to whether a UAV or an airborne platform should  
be used, but that leaves considerable gray areas where an appropriate choice of UAV platform with a well designed mission  
790 could stretch the domain. Future research and technological advances are needed to offer insights for snow science  
observation platforms and trade-offs.

## 5. Conclusions

This paper describes and demonstrates a UAV lidar system for snow depth mapping using commercially available  
components. The UAS was assessed in a mixed deciduous and coniferous forest and open field with little relief over a thin  
795 snowpack. The UAS includes an Eagle X8 UAV manufactured by UAV America, a small, light-weight VLP-16 lidar  
(Velodyne, Inc.), and an Applanix APX-15 UAV INS. The INS has a measurement rate of 200 Hz, allowing returns to be  
georeferenced without ground control points. Data, post-processed to a SBET file, resulted in approximately 3 cm positional  
accuracy. Flights were conducted at an altitude of 81 m and flight speed of 7 m/s, with a total of 12 parallel flight lines with  
targeted overlap of 40 percent. Once the point clouds were classified as ground and non-ground points, the flights yielded an  
800 average of 90 and 364 ground points/m<sup>2</sup> in a forest canopy and field, respectively, with 6.7% of the forest and 0.03% of the  
field cells having less than 5 point/m<sup>2</sup>.

The snow depth map, generated by subtracting snow-off from snow-on DTMs derived from the resultant point clouds,  
reveals a snowpack whose depth ranges from less than 2 cm to over 18 cm. For both snow depth and confidence intervals,  
805 differences were found between vegetation cover types and slope, indicating complex snow-vegetation interaction that can  
be observed by UAV lidar return numbers. For 0.4 x 0.4 m cells, the *in situ* and lidar mean snow depths in the field were  
nearly identical with the MAD and RMSD values of approximately 1 cm. In the forest, the *in situ* mean snow depths from a  
magnaprobe were twice as large as the lidar snow depths with a correspondingly high RMSD. These forest differences have  
numerous possible explanations: 1) the snow probe's ability to penetrate the soil and vegetation resulting in random errors,  
810 2) higher uncertainty in areas with canopy cover and areas of high terrain relief that occur more commonly in forested areas,  
3) reduced total and ground return density in forests due to occlusion and lost pulses. Nevertheless, the results support  
previous findings indicating that there are limits to lidar snow depth validation at high horizontal and vertical spatial  
resolutions in some land covers and conditions. Mapped at 1 m<sup>2</sup> cells, a 0.5 to 1 cm snow depth confidence interval was  
achieved consistently in the field with confidence intervals increasing to median values of 4.0 cm in the deciduous forest and  
815 5.9 cm in the coniferous forest. In the field, snow depth can be mapped at finer spatial resolutions with limited reduction in  
performance when reducing the cell size to 0.5 x 0.5 m and still achieving snow depth precision of less than 5 cm for a 0.2 x  
0.2 m. Performance depends on both the point cloud density, which can be increased or decreased by changing the flight  
plan, and the within cell variability that depends on site surface conditions.

## Acknowledgements

820 This material is based upon work supported by the Broad Agency Announcement Program and the Cold Regions Research  
and Engineering Laboratory (ERDC-CRREL) under contract number W913E5-18-C-005. Any opinions, findings and  
conclusions or recommendations in this material are those of the author(s) and do not necessarily reflect the views of the  
Broad Agency Announcement Program and the Cold Regions Research and Engineering Laboratory.

Jennifer Jacobs 7/13/2020 12:12 PM

**Deleted:** Because larger UAVs that can carry heavier payloads have challenges that may differ from small UAVs, a well-formulated flight plan is critical. Flight planning should address weather conditions, logistics of flying at proposed site, flight lines, UAS equipment, and personnel. Protocols should be developed and used consistently for each step of flight planning. Weather conditions influence the safety and success of a UAS survey. UAS should not be operated when there is any type of precipitation or in dense fog/clouds. Moisture can cause electronic components to malfunction. Moisture build-up on the propellers can also adversely affect lift production. This project's Eagle X8 high lift capacity UAS cannot be flown comfortably in winds greater than 7.8 m/s. High wind speeds can also significantly reduce battery life as well as impact the accuracy of sensor observations. Cold air temperatures can cause batteries to rapidly discharge. For winter UAS surveys, all flight and operational batteries should be kept warm prior to the UAS survey. This also applies to the computer used to upload flight lines and relay telemetry information. A MIL-STD-810 certified Panasonic Toughbook was used in this study to handle the anticipated cold temperatures. Additionally, cold temperatures can severely limit the dexterity of the person manipulating the flight controls. Proper gloves/clothing are required to effectively operate the flight controls in cold weather. ... [8]

Jennifer Jacobs 7/13/2020 12:12 PM

**Deleted:** (590 g)

Jennifer Jacobs 7/13/2020 12:13 PM

**Deleted:** inertial navigation system

Jennifer Jacobs 7/13/2020 12:13 PM

**Deleted:** (

Jennifer Jacobs 7/13/2020 12:13 PM

**Deleted:** )

Jennifer Jacobs 7/13/2020 12:14 PM

**Deleted:** additional

Jennifer Jacobs 7/13/2020 12:13 PM

**Deleted:** Smoothed Best-Estimate Trajectory (

Jennifer Jacobs 7/13/2020 12:13 PM

**Deleted:** )

Jennifer Jacobs 7/13/2020 12:15 PM

**Deleted:** shallow

Jennifer Jacobs 7/13/2020 12:15 PM

**Deleted:** These forest differences, which appear to be caused by the snow probe's ability to penetrate the soil and vegetation resulting in random errors, support previous findings indicating that there are limits to lidar snow depth validation at high horizontal and vertical spatial resolutions in some land covers and conditions.

Jennifer Jacobs 7/13/2020 12:16 PM

**Deleted:** snow depth precision

Jennifer Jacobs 7/13/2020 12:17 PM

**Deleted:** with modestly reduced accuracy in the forest and heavily vegetated areas.

875 The authors are grateful to Lee Friess for providing a technical review of the draft manuscript, Mahsa Moradi Khaneghahi for supporting manuscript preparation, and Ronny Schroeder contributing to the field data collection.

#### Data Availability

The UAS-based lidar point clouds and in-situ snow observations are available from the corresponding author upon reasonable request.

#### 880 Author Contributions

JJ, AH, FS, and MP designed research and performed analysis. JJ, AH, FS, MP, EB, and EC conducted field work to obtain lidar and/or in-situ snow observations. AH, FS, CH, and EC produced figures. JJ wrote the initial draft. All authors contributed to manuscript revisions, reviews, and editing.

#### Competing Interests

885 The authors declare that they have no conflict of interest.

#### References

- Aanderud, Z. T., Jones, S. E., Schoolmaster Jr, D. R., Fierer, N., and Lennon, J. T.: Sensitivity of soil respiration and microbial communities to altered snowfall, Soil Biology and Biochemistry, 57, 217-227, 2013.
- Aase, J. K. and Siddoway, F. H.: Crown-Depth Soil Temperatures and Winter Protection for Winter Wheat Survival, Soil Science Society of America Journal, 43, 1229-1233, 1979.
- Adams, M. S., Bühler, Y., and Fromm, R.: Multitemporal accuracy and precision assessment of unmanned aerial system photogrammetry for slope-scale snow depth maps in Alpine terrain, Pure and Applied Geophysics, 175, 3303-3324, 2018.
- Adolph, A. C., Albert, M. R., Lazarcik, J., Dibb, J. E., Amante, J. M., and Price, A.: Dominance of grain size impacts on seasonal snow albedo at open sites in New Hampshire, Journal of Geophysical Research: Atmospheres, 122, 121-139, 2017.
- Broxton, P., Harpold, A., Biederman, J., Troch, P. A., Molotch, N., and Brooks, P.: Quantifying the effects of vegetation structure on snow accumulation and ablation in mixed - conifer forests, Ecohydrology, 8, 1073-1094, 2015.
- Broxton, P. D., van Leeuwen, W. J., and Biederman, J. A.: Improving Snow Water Equivalent Maps With Machine Learning of Snow Survey and Lidar Measurements, Water Resources Research, 2019, 2019.
- Bühler, Y., Adams, M. S., Bösch, R., and Stoffel, A.: Mapping snow depth in alpine terrain with unmanned aerial systems (UASs): potential and limitations, The Cryosphere, 10, 1075-1088, 2016.
- Bühler, Y., Adams, M. S., Stoffel, A., and Boesch, R.: Photogrammetric reconstruction of homogenous snow surfaces in alpine terrain applying near-infrared UAS imagery, International journal of remote sensing, 38, 3135-3158, 2017.
- Burakowski, E., Tawfik, A., Ouimette, A., Lepine, L., Novick, K., Ollinger, S., Zarzycki, C., and Bonan, G.: The role of surface roughness, albedo, and Bowen ratio on ecosystem energy balance in the Eastern United States, Agricultural and Forest Meteorology, 249, 367-376, 2018.
- Burakowski, E. A., Ollinger, S. V., Lepine, L., Schaaf, C. B., Wang, Z., Dibb, J. E., Hollinger, D. Y., Kim, J., Erb, A., and Martin, M.: Spatial scaling of reflectance and surface albedo over a mixed-use, temperate forest landscape during snow-covered periods, Remote Sensing of Environment, 158, 465-477, 2015.
- Cimoli, E., Marcer, M., Vandecrux, B., Bøggild, C. E., Williams, G., and Simonsen, S. B.: Application of low-cost UASs and digital photogrammetry for high-resolution snow depth mapping in the Arctic, Remote Sensing, 9, 1144, 2017.
- Clark, M. P., Hendriks, J., Slater, A. G., Kavetski, D., Anderson, B., Cullen, N. J., Kerr, T., Örn Hreinnsson, E., and Woods, R. A.: Representing spatial variability of snow water equivalent in hydrologic and land - surface models: A review, Water Resources Research, 47, 2011.
- Cook, B. D., Corp, L. A., Nelson, R. F., Middleton, E. M., Morton, D. C., McCorkel, J. T., Masek, J. G., Ranson, K. J., Ly, V., and Montesano, P. M.: NASA Goddard's LiDAR, Hyperspectral and Thermal (G-LiHT) Airborne Imager, Remote Sensing, 5, 4045-4066, 2013.
- Currier, W. R. and Lundquist, J. D.: Snow depth variability at the forest edge in multiple climates in the western United States, Water Resources Research, 54, 8756-8773, 2018.

Jennifer Jacobs 7/13/2020 12:18 PM

Deleted:

Currier, W. R., Pflug, J., Mazzotti, G., Jonas, T., Deems, J. S., Bormann, K. J., Painter, T. H., Hiemstra, C. A., Gelvin, A., and Uhlmann, Z.: Comparing aerial lidar observations with terrestrial lidar and snow - probe transects from NASA's 2017 SnowEx campaign, *Water Resources Research*, 2019, 2019.

925 De Michele, C., Avanzi, F., Passoni, D., Barzaghi, R., Pinto, L., Dosso, P., Ghezzi, A., Gianatti, R., and Della Vedova, G.: Using a fixed-wing UAS to map snow depth distribution: an evaluation at peak accumulation, *Cryosphere*, 10, 511-522, 2016.

Deems, J. S., Fassnacht, S. R., and Elder, K. J.: Fractal distribution of snow depth from LiDAR data, *Journal of Hydrometeorology*, 7, 285-297, 2006.

930 Deems, J. S., Painter, T. H., and Finnegan, D. C.: Lidar measurement of snow depth: a review, *J. Glaciol.*, 59, 467-479, 2013.

Dickinson, W. and Whiteley, H.: A sampling scheme for shallow snowpacks, *Hydrological Sciences Journal*, 17, 247-258, 1972.

935 Dolgun, A. and Demirhan, H.: Performance of nonparametric multiple comparison tests under heteroscedasticity, dependency, and skewed error distribution, *Communications in Statistics-Simulation and Computation*, 46, 5166-5183, 2017.

Fernandes, R., Prevost, C., Canisius, F., Leblanc, S. G., Maloley, M., Oakes, S., Holman, K., and Knudby, A.: Monitoring snow depth change across a range of landscapes with ephemeral snowpacks using structure from motion applied to lightweight unmanned aerial vehicle videos, *The Cryosphere*, 12, 3535-3550, 2018.

940 Fey, C., Schattan, P., Helfricht, K., and Schöber, J.: A compilation of multitemporal TLS snow depth distribution maps at the Weisssee snow research site (Kaunertal, Austria), *Water Resources Research*, 2019, 2019.

Friggens, M. M., Williams, M. I., Bagne, K. E., Wixom, T. T., and Cushman, S. A.: Effects of climate change on terrestrial animals [Chapter 9], In: Halofsky, Jessica E.; Peterson, David L.; Ho, Joanne J.; Little, Natalie, J.; Joyce, Linda A., eds. *Climate change vulnerability and adaptation in the Intermountain Region [Part 2]*. Gen. Tech. Rep. RMRS-GTR-375, Fort Collins, CO: US Department of Agriculture, Forest Service, Rocky Mountain Research Station, p. 264-315, 375, 264-315, 2018.

945 Gabrlik, P., Janata, P., Zalud, L., and Harcarik, J.: Towards Automatic UAS-Based Snow-Field Monitoring for Microclimate Research, *Sensors*, 19, 1945, 2019.

Gandahl, R.: Determination of the depth of soil freezing with a new frost meter (text in Swedish). Report 30, Statensaginsitutit Stockholm (SIP 16347), 1957.

950 Gichamo, T. Z. and Tarboton, D. G.: Ensemble Streamflow Forecasting using an Energy Balance Snowmelt Model Coupled to a Distributed Hydrologic Model with Assimilation of Snow and Streamflow Observations, *Water Resources Research*, 2019, 2019.

955 Goetz, J. and Brenning, A.: Quantifying uncertainties in snow depth mapping from structure from motion photogrammetry in an alpine area, *Water Resources Research*, 55, 7772-7783, 2019.

Groffman, P. M., Driscoll, C. T., Fahey, T. J., Hardy, J. P., Fitzhugh, R. D., and Tierney, G. L.: Colder soils in a warmer world: A snow manipulation study in a northern hardwood forest ecosystem, *Biogeochemistry*, 56, 135-150, 2001.

Grünewald, T., Schirmer, M., Mott, R., and Lehning, M.: Spatial and temporal variability of snow depth and SWE in a small mountain catchment, *The Cryosphere*, 4, 215-225, 2010.

960 Harder, P., Pomeroy, J. W., and Helgason, W. D.: Improving sub-canopy snow depth mapping with unmanned aerial vehicles: lidar versus structure-from-motion techniques, *The Cryosphere*, 14, 1919-1935, 2020.

Harder, P., Schirmer, M., Pomeroy, J., and Helgason, W.: Accuracy of snow depth estimation in mountain and prairie environments by an unmanned aerial vehicle, *The Cryosphere*, 10, 2559, 2016.

965 Harpold, A., Guo, Q., Molotch, N., Brooks, P., Bales, R., Fernandez - Diaz, J., Musselman, K., Swetnam, T., Kirchner, P., and Meadows, M.: LiDAR - derived snowpack data sets from mixed conifer forests across the Western United States, *Water Resources Research*, 50, 2749-2755, 2014.

Hatchett, B. J. and Eisen, H. G.: Brief Communication: Early season snowpack loss and implications for oversnow vehicle recreation travel planning, *The Cryosphere*, 13, 21-28, 2019.

Helsel, D. R. and Hirsch, R. M.: *Statistical methods in water resources*, Elsevier, 1992.

970 Henry, H. A. L.: Climate change and soil freezing dynamics: historical trends and projected changes, *Climatic Change*, 87, 421-434, 2008.

Hopkinson, C., Chasmer, L., Young-Pow, C., and Treitz, P.: Assessing forest metrics with a ground-based scanning lidar, *Canadian Journal of Forest Research*, 34, 573-583, 2004.

Horn, B. K.: Hill shading and the reflectance map, *Proceedings of the IEEE*, 69, 14-47, 1981.

975 Isard, S. A. and Schaeztl, R. J.: Effects of winter weather conditions on soil freezing in southern Michigan, *Physical Geography*, 19, 71-94, 1998.

Jagt, B. V., Lucieer, A., Wallace, L., Turner, D., and Durand, M.: Snow Depth Retrieval with UAS Using Photogrammetric Techniques, *Geosciences*, 5, 264-285, 2015.

Keyetieu, R. and Seube, N.: Automatic Data Selection and Boresight Adjustment of LiDAR Systems, *Remote Sensing*, 11, 1087, 2019.

980 Kirchner, P., Bales, R., Molotch, N., Flanagan, J., and Guo, Q.: LiDAR measurement of seasonal snow accumulation along an elevation gradient in the southern Sierra Nevada, California, *Hydrology and Earth System Sciences*, 18, 4261-4275, 2014.



985 Kraatz, S., Jacobs, J. M., Schröder, R., Cho, E., Cosh, M., Seyfried, M., Prueger, J., and Livingston, S.: Evaluation of SMAP freeze/thaw retrieval accuracy at core validation sites in the contiguous united states, *Remote Sensing*, 10, 1483, 2018.

Kraus, K. and Pfeifer, N.: Advanced DTM generation from LiDAR data, *International Archives of Photogrammetry, Remote Sensing and Spatial Information Sciences*, 34, 23–30, 2011.

990 Kwok, R., Kacimi, S., Webster, M., Kurtz, N., and Petty, A.: Arctic Snow Depth and Sea Ice Thickness From ICESat - 2 and CryoSat - 2 Freeboards: A First Examination, *Journal of Geophysical Research: Oceans*, 125, e2019JC016008, 2020.

Li, Z., Tan, J., and Liu, H.: Rigorous boresight self-calibration of mobile and UAV LiDAR scanning systems by strip adjustment, *Remote Sensing*, 11, 442, 2019.

995 López-Moreno, J. I., Revuelto, J., Alonso-González, E., Sanmiguel-Valladolid, A., Fassnacht, S. R., Deems, J., and Morán-Tejeda, E.: Using very long-range terrestrial laser scanner to analyze the temporal consistency of the snowpack distribution in a high mountain environment, *Journal of Mountain Science*, 14, 823-842, 2017.

Marti, R., Gascoin, S., Berthier, E., De Pinel, M., Houet, T., and Laffly, D.: Mapping snow depth in open alpine terrain from stereo satellite imagery, *Cryosphere*, 10, 2016.

1000 Maune, D. F. and Nayegeandhi, A.: Digital elevation model technologies and applications: the DEM users manual, Asprs Publications, 2018.

Mazzotti, G., Currier, W. R., Deems, J. S., Pflug, J. M., Lundquist, J. D., and Jonas, T.: Revisiting Snow Cover Variability and Canopy Structure Within Forest Stands: Insights From Airborne Lidar Data, *Water Resources Research*, 55, 6198-6216, 2019.

1005 McGrath, D., Webb, R., Shean, D., Bonnell, R., Marshall, H. P., Painter, T. H., Molotch, N. P., Elder, K., Hiemstra, C., and Brucker, L.: Spatially extensive ground - penetrating radar snow depth observations during NASA's 2017 SnowEx campaign: Comparison with In situ, airborne, and satellite observations, *Water Resources Research*, 55, 10026-10036, 2019.

Meyer, J. and Skiles, S. M.: Assessing the Ability of Structure From Motion to Map High - Resolution Snow Surface Elevations in Complex Terrain: A Case Study From Senator Beck Basin, CO, *Water Resources Research*, 55, 6596-6605, 2019.

1010 Monson, R. K., Lipson, D. L., Burns, S. P., Turnipseed, A. A., Delany, A. C., Williams, M. W., and Schmidt, S. K.: Winter forest soil respiration controlled by climate and microbial community composition, *Nature*, 439, 711, 2006.

Mott, R., Schirmer, M., and Lehning, M.: Scaling properties of wind and snow depth distribution in an Alpine catchment, *Journal of Geophysical Research: Atmospheres*, 116, 2011.

1015 Mott, R., Vionnet, V., and Grünewald, T.: The seasonal snow cover dynamics: review on wind-driven coupling processes, *Frontiers in Earth Science*, 6, 197, 2018.

Muir, J., Goodwin, N., Armston, J., Phinn, S., and Scarth, P.: An accuracy assessment of derived digital elevation models from terrestrial laser scanning in a sub-tropical forested environment, *Remote Sensing*, 9, 843, 2017.

1020 Nolan, M., Larsen, C., and Sturm, M.: Mapping snow-depth from manned-aircraft on landscape scales at centimeter resolution using Structure-from-Motion photogrammetry, *Cryosphere Discussions*, 9, 2015.

Painter, T. H., Berisford, D. F., Boardman, J. W., Bormann, K. J., Deems, J. S., Gehrke, F., Hedrick, A., Joyce, M., Laidlaw, R., and Marks, D.: The Airborne Snow Observatory: Fusion of scanning lidar, imaging spectrometer, and physically-based modeling for mapping snow water equivalent and snow albedo, *Remote Sensing of Environment*, 184, 139-152, 2016.

1025 Palace, M., Keller, M., Asner, G. P., Hagen, S., and Braswell, B.: Amazon forest structure from IKONOS satellite data and the automated characterization of forest canopy properties, *Biotropica*, 40, 141-150, 2008.

Palace, M. W., McMichael, C., Braswell, B. H., Hagen, S. C., Bush, M. B., Neves, E., Tamanaha, E., Herrick, C., and Frolking, S.: Ancient Amazonian populations left lasting impacts on forest structure, *Ecosphere*, 8, e02035, 2017.

1030 Pauli, J. N., Zuckenberg, B., Whiteman, J. P., and Porter, W.: The subnivium: a deteriorating seasonal refugium, *Frontiers in Ecology and the Environment*, 11, 260-267, 2013.

Perron, C.J., Bennett, K., & Lee, T.D.: Forest stewardship plan: Thompson farm. NH: University of New Hampshire. Produced by Ossipee Mountain Land Company, West Ossipee, <https://colsa.unh.edu/sites/default/files/thompson-farm-plan.pdf>, 2004.

1035 Prince, M., Roy, A., Royer, A., and Langlois, A.: Timing and spatial variability of fall soil freezing in boreal forest and its effect on SMAP L-band radiometer measurements, *Remote Sensing of Environment*, 231, 111230, 2019.

Reinmann, A. B. and Templer, P. H.: Increased soil respiration in response to experimentally reduced snow cover and increased soil freezing in a temperate deciduous forest, *Biogeochemistry*, 140, 359-371, 2018.

1040 Ricard, J. A., Tobiasson, W., and Greatedorex, A.: The field assembled frost gage. Technical Note. Cold Regions Research and Engineering Laboratory, U.S. Army Corps of Engineers, Hanover, New Hampshire, 1976, 1976.

Schweizer, J., Jamieson, J. B., and Schneebeli, M.: Snow avalanche formation, *Rev. Geophys.*, 41, 25, 2003.

Seyfried, M. S., Wilcox, B. P., and Cooley, K. R.: Environmental conditions and processes associated with runoff from frozen soil at Reynolds Creek Watershed, *Frozen soil impacts on agricultural, range, and forest lands*, 1990, 125-134, 1990.

1045 Sharratt, B. S. and McCool, D. K.: Frost Depth. In: *Micrometeorology in Agricultural Systems*, Hatfield, J. L. and Baker, J. M. (Eds.), 2005.

Shaw, T. E., Gascoin, S., Mendoza, P. A., Pellicciotti, F., and McPhee, J.: Snow Depth Patterns in a High Mountain Andean Catchment from Satellite Optical Tristereoscopic Remote Sensing, *Water Resources Research*, 56, e2019WR024880, 2020.

Singh, P., Wu, J. Q., McCool, D. K., Dun, S., Lin, C.-H., and Morse, J. R.: Winter hydrologic and erosion processes in the US Palouse region: Field experimentation and WEPP simulation, *Vadose Zone Journal*, 8, 426-436, 2009.

Sorensen, P. O., Finzi, A. C., Giasson, M.-A., Reinmann, A. B., Sanders-DeMott, R., and Templer, P. H.: Winter soil freeze-thaw cycles lead to reductions in soil microbial biomass and activity not compensated for by soil warming, *Soil Biology and Biochemistry*, 116, 39-47, 2018.

Starkloff, T., Stolte, J., Hessel, R., and Ritsema, C.: Investigating the development of shallow snowpacks on arable land, using comprehensive field observations and spatially distributed snow modelling, *Hydrology Research*, 49, 41-59, 2017.

Sturm, M. and Holmgren, J.: An automatic snow depth probe for field validation campaigns, *Water Resources Research*, 54, 9695-9701, 2018.

Sullivan, F. B., Ducey, M. J., Orwig, D. A., Cook, B., and Palace, M. W.: Comparison of lidar and allometry-derived canopy height models in an eastern deciduous forest, *Forest Ecology and Management*, 406, 83-94, 2017.

Tonkin, T. N. and Midgley, N. G.: Ground-Control Networks for Image Based Surface Reconstruction: An Investigation of Optimum Survey Designs Using UAV Derived Imagery and Structure-from-Motion Photogrammetry, *Remote Sensing*, 8, 8, 2016.

Tucker, C. L., Tamang, S., Pendall, E., and Ogle, K.: Shallow snowpack inhibits soil respiration in sagebrush steppe through multiple biotic and abiotic mechanisms, *Ecosphere*, 7, e01297, 2016.

Tuttle, S. E., Cho, E., Restrepo, P. J., Jia, X., Vuyovich, C. M., Cosh, M. H., and Jacobs, J. M.: Remote sensing of drivers of spring snowmelt flooding in the North Central US. In: *Remote sensing of hydrological extremes*, Springer, 2017.

Vander Jagt, B., Lucieer, A., Wallace, L., Turner, D., and Durand, M.: Snow depth retrieval with UAS using photogrammetric techniques, *Geosciences*, 5, 264-285, 2015.

Wallace, L., Lucieer, A., Watson, C., and Turner, D.: Development of a UAV-LiDAR system with application to forest inventory, *Remote Sensing*, 4, 1519-1543, 2012.

Wallace, L., Lucieer, A., and Watson, C. S.: Evaluating tree detection and segmentation routines on very high resolution UAV LiDAR data, *IEEE Transactions on Geoscience and Remote Sensing*, 52, 7619-7628, 2014.

Watanabe, K. and Osada, Y.: Comparison of hydraulic conductivity in frozen saturated and unfrozen unsaturated soils, *Vadose Zone Journal*, 15, 2016.

Wever, N., Jonas, T., Fierz, C., and Lehning, M.: Model simulations of the modulating effect of the snow cover in a rain-on-snow event, *Hydrology and Earth System Sciences*, 18, 4657-4669, 2014.

Yi, Y., Kimball, J. S., Chen, R. H., Moghaddam, M., and Miller, C. E.: Sensitivity of active-layer freezing process to snow cover in Arctic Alaska, *The Cryosphere*, 13, 197, 2019.

Zhang, K., Chen, S.-C., Whitman, D., Shyu, M.-L., Yan, J., and Zhang, C.: A progressive morphological filter for removing nonground measurements from airborne LIDAR data, *IEEE transactions on geoscience and remote sensing*, 41, 872-882, 2003.

Zhu, L., Ives, A. R., Zhang, C., Guo, Y., and Radeloff, V. C.: Climate change causes functionally colder winters for snow cover-dependent organisms, *Nature Climate Change*, 9, 886-893, 2019.

Jennifer Jacobs 7/13/2020 12:18 PM

Deleted: References

... [9]

-In many regions, shallow snowpacks, i.e., snow depth less than 20 cm, are typical throughout the winter. Even in mountainous regions with deep seasonal snowpacks, snowpacks can be shallow and nonuniform during the accumulation and melt periods as well as in areas with high winds. Shallow snowpacks impact many hydrologic, agricultural, and ecosystem processes. Shallow snowpack characteristics effect the location and condition of suitable habitats in animal populations (Friggens et al., 2018). Meltwaters from shallow snowpacks can be a major contributor to streamflow and spring floods in many regions (Tuttle et al., 2017) and intensify overland nutrient transport and soil erosion (Seyfried et al., 1990; Singh et al., 2009). Thin, ephemeral snowpacks allow the underlying soils to freeze more readily in the winter because they lack the insulating properties of deeper packs and the shallower snow's higher albedo may increase deep-freezing (Starkloff et al. 2017). Soil frost severity impacts soil respiration, carbon sequestration, nutrient retention, and microbial communities as well as a plant root health and tree growth (Aase and Siddoway, 1979; Isard and Schaetzel, 1998; Monson et al., 2006; Henry, 2008; Aanderud et al., 2013; Tucker et al., 2016; Sorensen et al., 2018; Reinmann and Templer, 2018). When the frozen soils impede meltwater infiltration, flooding and erosion may increase (Watanabe and Osada, 2016). Winter recreation is also affected by shallow snowpacks. In some regions, minimum snow depth restrictions for recreational activities are required (e.g., 30.5 cm for snowmobiling on US Forest Service lands) or being considered to reduce impacts to sensitive ecosystems (Hatchett and Eisen, 2019).

Shallow snowpacks are highly dynamic, accumulating and ablating throughout the winter with associated changes in snowpack density, grain size, and albedo (Adolph et al., 2017) as well as ice formation. Wind redistribution, sloughing of snow off slopes, trapping of snow by vegetation, and forest canopy interception also result in a range of spatial features at varying scales (Clark et al., 2011; Mott et al., 2011; Mott et al., 2018). These variations cause shallow snowpacks to more readily ripen during winter rain events and warmer air temperature than deeper snowpacks (Wever et al., 2014) and, in combination with the transport and refreeze of meltwaters (Watanabe and Osada, 2016) make modeling and mapping of shallow snowpacks extremely challenging (Hall et al., 2010; Gichamo and Tarboton 2019; Starkloff et al., 2017). Despite their prevalence, complexity, and importance, shallow snowpacks have received relatively little attention for measurement, modelling, and mapping efforts.

Because shallow snowpacks have considerable spatiotemporal variability, a large number of snow depth measurements are often needed to characterize the snowpack (Dickinson and Whiteley, 1972). Using traditional point measurements with its limited sample size requires a balance between the sampling extent and sample spacing; this impacts the ability to capture spatial variability that naturally increases with spatial scale as compared to capturing small-scale spatial structures (Clark et al. 2011).

The payload is equipped with an Applanix APX-15 UAV inertial navigation system (INS), which has 2-5 cm positional, 0.025-degree roll and pitch, and 0.08-degree true heading uncertainties following post-processing. The INS has a measurement rate of 200 Hz, allowing for a timestamp to associate each lidar pulse with the closest data for latitude, longitude, altitude, and perspective information (roll/pitch/yaw), which is required for georeferencing returns.

<b>Page 7: [3] Deleted</b>	<b>Jennifer Jacobs</b>	<b>7/13/20 11:47 AM</b>
----------------------------	------------------------	-------------------------

Error statistics were calculated and the results were summarized by forest and field locations. At each magnaprobe location, the average and standard deviation of the five magnaprobe samples were calculated. The average lidar snow depth was determined for a 0.4 x 0.4 m cell centered on the center magnaprobe location. The mean absolute difference (MAD) and root mean square difference (RMSD) were used to characterize the differences between the magnaprobe snow depths and the lidar snow depths.

The uncertainty of the lidar estimate of the snow depth mean value was calculated for each cell as the one-sided 95% confidence interval of the snow depth.

<b>Page 10: [4] Deleted</b>	<b>Jennifer Jacobs</b>	<b>7/13/20 11:52 AM</b>
-----------------------------	------------------------	-------------------------

4

<b>Page 10: [4] Deleted</b>	<b>Jennifer Jacobs</b>	<b>7/13/20 11:52 AM</b>
-----------------------------	------------------------	-------------------------

4

<b>Page 10: [5] Deleted</b>	<b>Jennifer Jacobs</b>	<b>7/13/20 11:56 AM</b>
-----------------------------	------------------------	-------------------------

In the field, the precision of the mean snow depth estimate is

<b>Page 10: [5] Deleted</b>	<b>Jennifer Jacobs</b>	<b>7/13/20 11:56 AM</b>
-----------------------------	------------------------	-------------------------

In the field, the precision of the mean snow depth estimate is

<b>Page 10: [5] Deleted</b>	<b>Jennifer Jacobs</b>	<b>7/13/20 11:56 AM</b>
-----------------------------	------------------------	-------------------------

In the field, the precision of the mean snow depth estimate is

<b>Page 10: [5] Deleted</b>	<b>Jennifer Jacobs</b>	<b>7/13/20 11:56 AM</b>
-----------------------------	------------------------	-------------------------

In the field, the precision of the mean snow depth estimate is

<b>Page 10: [5] Deleted</b>	<b>Jennifer Jacobs</b>	<b>7/13/20 11:56 AM</b>
-----------------------------	------------------------	-------------------------

In the field, the precision of the mean snow depth estimate is

<b>Page 10: [5] Deleted</b>	<b>Jennifer Jacobs</b>	<b>7/13/20 11:56 AM</b>
-----------------------------	------------------------	-------------------------

In the field, the precision of the mean snow depth estimate is

<b>Page 10: [5] Deleted</b>	<b>Jennifer Jacobs</b>	<b>7/13/20 11:56 AM</b>
-----------------------------	------------------------	-------------------------

In the field, the precision of the mean snow depth estimate is

<b>Page 10: [6] Deleted</b>	<b>Jennifer Jacobs</b>	<b>7/13/20 12:00 PM</b>
-----------------------------	------------------------	-------------------------

Snow depth precision was

<b>Page 10: [6] Deleted</b>	<b>Jennifer Jacobs</b>	<b>7/13/20 12:00 PM</b>
-----------------------------	------------------------	-------------------------

Snow depth precision was

<b>Page 10: [6] Deleted</b>	<b>Jennifer Jacobs</b>	<b>7/13/20 12:00 PM</b>
-----------------------------	------------------------	-------------------------

Snow depth precision was

<b>Page 10: [6] Deleted</b>	<b>Jennifer Jacobs</b>	<b>7/13/20 12:00 PM</b>
-----------------------------	------------------------	-------------------------

Snow depth precision was

<b>Page 10: [6] Deleted</b>	<b>Jennifer Jacobs</b>	<b>7/13/20 12:00 PM</b>
-----------------------------	------------------------	-------------------------

Snow depth precision was

<b>Page 10: [6] Deleted</b>	<b>Jennifer Jacobs</b>	<b>7/13/20 12:00 PM</b>
-----------------------------	------------------------	-------------------------

Snow depth precision was

<b>Page 10: [6] Deleted</b>	<b>Jennifer Jacobs</b>	<b>7/13/20 12:00 PM</b>
-----------------------------	------------------------	-------------------------

Snow depth precision was

<b>Page 10: [6] Deleted</b>	<b>Jennifer Jacobs</b>	<b>7/13/20 12:00 PM</b>
-----------------------------	------------------------	-------------------------

Snow depth precision was

<b>Page 14: [7] Deleted</b>	<b>Jennifer Jacobs</b>	<b>7/13/20 12:10 PM</b>
-----------------------------	------------------------	-------------------------

Because larger UAVs that can carry heavier payloads have challenges that may differ from small UAVs, a well-formulated flight plan is critical. Flight planning should address weather conditions, logistics of flying at proposed site, flight lines, UAS equipment, and personnel. Protocols should be developed and used consistently for each step of flight planning. Weather conditions influence the safety and success of a UAS survey. UAS should not be operated when there is any type of precipitation or in dense fog/clouds. Moisture can cause electronic components to malfunction. Moisture build-up on the propellers can also adversely affect lift production. This project's Eagle X8 high lift capacity UAS cannot be flown comfortably in winds greater than 7.8 m/s. High wind speeds can also significantly reduce battery life as well as impact the accuracy of sensor observations. Cold air temperatures can cause batteries to rapidly discharge. For winter UAS surveys, all flight and operational batteries should be kept warm prior to the UAS survey. This also applies to the computer used to upload flight lines and relay telemetry information. A MIL-STD-810 certified Panasonic Toughbook was used in this study to handle the anticipated cold temperatures. Additionally, cold temperatures can severely limit the dexterity of the person manipulating the flight controls. Proper gloves/clothing are required to effectively operate the flight controls in cold weather.

High lift UAVs capable of carrying a lidar sensor package have the potential to cause significant damage to person and property. The selection of a survey site not only needs to meet the objectives of the UAV survey, but also must have the proper attributes for safe and legal UAV operation. It is important that permission to operate the UAV at the site has been granted and that the land owner/public is aware of the UAV survey operations. Visual line of sight (VLOS) of the UAV needs to be maintained throughout the flight. It can be difficult to maintain VLOS while flying over forested or mountainous sites. Spotters can be used if there is constant two-way communication between the spotters and the person operating the flight controls. For this study, an on-site, walk up tower allowed a spotter to maintain VLOS while the UAV was flown over the forest. Two-way communication was maintained throughout the flight.

In the first season, the project team experienced more than one situation that required the pilot to manually land the UAV. Flying using first person view (FPV) by an experienced pilot is highly recommended for a UAS platform that is capable of handling large payloads such as this study's VLP-16 lidar. If an emergency occurs and the UAS needs to land as quickly as possible, FPV will help the pilot to orientate the UAV, safely land, and limit damage to the payload. For this study, the UAV was equipped with low quality linearly polarized FPV antennas. The FPV signal was easily lost as the orientation of the drone relative to the base station changed. The FPV signal was also not able to penetrate the forest. Circular polarized FPV antennas are generally recommended for drones because they are not affected by transmitter/receiver orientation changes and are better at avoiding obstacle interference.

The deployment of a lidar system mounted on a UAV platform for snow depth monitoring requires flight patterns designed for bore sighting alignment and post-processing to ensure that point clouds are aligned (Painter et al., 2016). Provided that GNSS data are accurate, the most common reason for misalignment of point clouds is boresight angle errors (Li et al., 2019). Traditionally, boresighting calibration is performed using antiparallel flight lines and a perpendicular flight line to calculate IMU offsets (Keyetieu and Seube, 2019). Due to battery flight time limitations, we were unable to complete the flight pattern that is commonly used for boresighting alignment. Because of this, we leveraged our first two antiparallel flight lines for boresighting calibration. To determine roll offset, we used broad (10 m) along-path cross-sections over flat terrain, and to determine pitch offset we used narrow (1 m) across-path cross-sections in sloped terrain where the point clouds overlapped (Figure 7). Though not shown here, we additionally leveraged unique features within our data acquisition region, including barn roofs and deciduous tree branches to assess the resulting boresight angles (Kumari et al., 2011; Li et al., 2005). For this particular study, we performed boresight calibration manually. Methods often require extensive user input (Li et al., 2005), however boresight calibration is an increasingly automated process with wide variation in algorithms and approaches (e.g. Maas, 2000; Kumari et al., 2011; Zhang et al., 2019). In future work, we plan to explore automated boresight calibration methods to improve the accuracy of point cloud data sets.

While lidar calibration and data post-processing requirements are quite similar for UAS and airborne surveys, lidar surveys by the UAS platform deployed in this study have key differences from previous ALS surveys. A limitation noted above is that the UAS flight duration is considerably shorter causing the spatial extent to be much more limited than previous ALS snow depth surveys. An advantage is that the UAS's average point cloud density is much higher and has fewer missing pixels in the forest than previous ALS surveys. This study had ground returns of 90 and 364 points/m<sup>2</sup> in the forest and field, respectively, and had no ground returns in only 0.086% and 0.95% of the 1 m resolution field and forest cells, respectively. In contrast, ALS surveys typically report surface model densities between 8 to 16 points/m<sup>2</sup> (Broxton et al., 2015; 2019; Currier et al., 2019; Kirchner et al., 2014) and ground returns between 3 and 6 points/m<sup>2</sup> (Broxton et al., 2019; Kirchner et al., 2014). ALS derived snow depth maps have a much greater proportion of areas that are masked due to no ground returns, particularly under trees, with masking areas ranging from less to 10% to more than 23% (Harpold et al., 2014; Mazzotti et al., 2019). While gap filling is possible, interpolation using measured snow depth values to fill under tree can overestimate snow depth (Zheng et al., 2016).



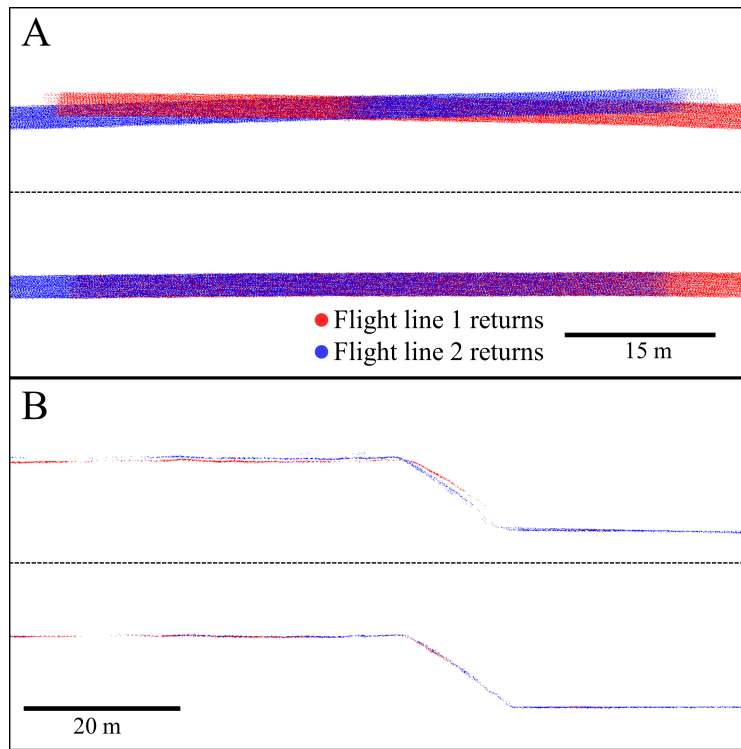


**Figure 7.** Uncalibrated boresight angles between the INS and lidar sensor can result in poorly aligned point clouds (A top and B top). Roll offsets present as crossed planes of data acquired from anti-parallel flight lines and are most clearly observed over flat terrain (A), while pitch offsets typically present as crossed planes of data acquired from perpendicular flight lines. Following boresight calibration, point clouds aligned well in both directions (A bottom and B bottom).

While UAS-based lidar surveys can measure snow depth to within a centimeter at high spatial resolutions, validation of those observations is challenging. A time consuming collection of high accuracy GNSS survey points was required to co-locate magnaprobe and lidar observations. Surveying in sample locations prior to the winter season might reduce this effort. It is also challenging to make *in situ* snow depth measurements that provide centimeter accuracy. In this study, the magnaprobe *in situ* snow depth observations made in the forest were considerably higher than the lidar observations as compared to the open field where the magnaprobe and lidar measurements were within 1 cm. Previous studies also found that snow depth observations from ALS measurements are biased lower than those from snow-probe observations in the forest (Currier et al., 2019; Hopkinson et al., 2004). The cause of these differences is attributed to the snow probe's ability to penetrate the soil and vegetation, human observers tending to make snow depth measurements in locations with relatively high snow (Sturm and Holmgren, 2018) and the reduced accuracy of the GNSS. Sturm and Holmgren (2018) indicate "The degree of penetration below the snow base is highly dependent on the nature of ground. For snow over sea, lake, or river ice, penetration is virtually zero and recorded depths are accurate to better than  $\pm 0.1$  cm. Over hard soils, rocks, and vegetation wetted in the fall and then frozen, the depth accuracy is nearly as high." In this study, the cold temperatures and no snow conditions prior to the January 19<sup>th</sup> and 20<sup>th</sup> snowfall event resulted in deeper

frozen soils (23.5 to 25.5 cm) in the field and thinner soil frost layers (5.5 to 8.5 cm) in the west forest, which would have limited the probe penetration into soils at both sites. However, the forest has a 1-4 cm thick loose leaf litter layer that may have been penetrated by the magnaprobe. The snow tube depths were not as deep as the magna probe and more closely match the lidar snow depth, further supporting that “over-probe” by the magnaprobe is responsible for the forest snow depth differences. A simple penetration test under similar snow depth and soil frost conditions revealed that the probe penetration into soil and leaf litter ranged from 0 to 10 cm, averaging 5 cm over-probe bias over ten sample locations in the forest.

## References

- Aanderud, Z. T., Jones, S. E., Schoolmaster Jr, D. R., Fierer, N., and Lennon, J. T.: Sensitivity of soil respiration and microbial communities to altered snowfall. *Soil Biol.*, 57, 217-227, 2013.
- Adams, M. S., Bühler, Y. and Fromm, R.: Multitemporal accuracy and precision assessment of unmanned aerial system photogrammetry for slope-scale snow depth maps in Alpine terrain. *Pure Appl. Geophys.*, 175, 3303-3324, 2018.
- Adolph, A. C., Albert, M. R., Lazarcik, J., Dibb, J. E. Amante, J. M. and Price, A.: Dominance of grain size impacts on seasonal snow albedo at open sites in New Hampshire. *J. Geophys. Res.-Atmos.*, 122, 121-139, 2017.
- Broxton, P., Harpold, A., Biederman, J., Troch, P. A., Molotch, N., and Brooks, P.: Quantifying the effects of vegetation structure on snow accumulation and ablation in mixed conifer forests. *Ecohydrol.*, 8, 1073-1094. 2015.
- Broxton, P. D., van Leeuwen, W. J., and Biederman, J. A.: Improving snow water equivalent maps with machine learning of snow survey and lidar measurements. *Water Resour. Res.*, 55(5), 3739-3757, 2019.
- Bühler, Y., Adams, M. S., Bösch, R., and Stoffel, A.: Mapping snow depth in alpine terrain with unmanned aerial systems (UASs): potential and limitations. *The Cryosphere*, 10, 1075-1088, 2016.
- Bühler, Y., Adams, M. S., Stoffel, A., and Boesch, R.: Photogrammetric reconstruction of homogenous snow surfaces in alpine terrain applying near-infrared UAS imagery. *Int. J. Remote Sens.*, 38, 3135-3158, 2017.
- Cimoli, E., Marcer, M., Vandecrux, B., Bøggild, C. E., Williams, G., and Simonsen, S. B.: Application of low-cost UASs and digital photogrammetry for high-resolution snow depth mapping in the Arctic. *Remote Sens.*, 1144, 2017.
- Clark, M. P., and Coauthors: Representing spatial variability of snow water equivalent in hydrologic and land-surface models: A review. *Water Resour. Res.*, 47. 2011.
- Cook, B. D., and Coauthors: NASA Goddard's LiDAR, Hyperspectral and Thermal (G-LiHT) Airborne Imager. *Remote Sens.*, 5, 4045-4066, 2013.
- Currier, W. R., and Lundquist, J. D.: Snow depth variability at the forest edge in multiple climates in the western United States. *Water Resour. Res.*, 54, 8756-8773, 2018.
- Currier, W.R., Pflug, J., Mazzotti, G., Jonas, T., Deems, J.S., Bormann, K.J., Painter, T.H., Hiemstra, C.A., Gelvin, A., Uhlmann, Z. and Spaete, L.: Comparing aerial lidar observations with

terrestrial lidar and snow-probe transects from NASA's 2017 SnowEx campaign. *Water Resour. Res.*, 55(7), 6285-6294, 2019.

De Michele, C., and Coauthors: Using a fixed-wing UAS to map snow depth distribution: an evaluation at peak accumulation. *The Cryosphere*, 10, 511–522, doi:10.5194/tc-10-511-2016, 2016.

Deems, J. S., Painter, T. H. and Finnegan, D. C.: Lidar measurement of snow depth: a review. *J. Glaciol.*, 59, 467-479.

Dickinson, W., and Whiteley, H.: A sampling scheme for shallow snowpacks. *Hydrol. Sci. J.*, 17, 247-258, 2013.

Fernandes, R., and Coauthors: Monitoring snow depth change across a range of landscapes with ephemeral snowpacks using structure from motion applied to lightweight unmanned aerial vehicle videos. *The Cryosphere*, 12, 3535-3550, 2018.

Fey, C., Schattan, P., Helfricht, K., and Schöber, J.: A compilation of multitemporal TLS snow depth distribution maps at the Weisssee snow research site (Kaunertal, Austria). *Water Resour. Res.*, 55(6), 5154-5164, 2019.

Friggens, M. M., Williams, M. I., Bagne, K. E., Wixom, T. T., and Cushman, S. A.: Effects of climate change on terrestrial animals [Chapter 9]. In: Halofsky, Jessica E.; Peterson, David L.; Ho, Joanne J.; Little, Natalie, J.; Joyce, Linda A., eds. *Climate change vulnerability and adaptation in the Intermountain Region [Part 2]*. Gen. Tech. Rep. RMRS-GTR-375. Fort Collins, CO: US Department of Agriculture, Forest Service, Rocky Mountain Research Station. 375, 264-315, 2018.

Hatchett, B. J., and Eisen, H. G.: Brief Communication: Early season snowpack loss and implications for oversnow vehicle recreation travel planning. *The Cryosphere*, 13, 21-28, 2019.

Gabrlík, P., Janata, P., Zalud, L., and Hrcarik, J.: Towards automatic uas-based snow-field monitoring for microclimate research. *Sensors*, 19(8), 1945, 2019.

Gichamo, T. Z., and Tarboton, D. G.: Ensemble streamflow forecasting using an energy balance snowmelt model coupled to a distributed hydrologic model with assimilation of snow and streamflow observations. *Water Resour. Res.*, 55(12), 10813-10838, 2019.

Goetz, J., and Brenning, A.: Quantifying uncertainties in snow depth mapping from structure from motion photogrammetry in an alpine area. *Water Resour. Res.*, 55, 7772-7783, 2019.

Grünwald, T., Schirmer, M., Mott, R., and Lehning, M.: Spatial and temporal variability of snow depth and SWE in a small mountain catchment. *The Cryosphere*, 4, 215-225, 2010.

Hall, D. K., Riggs, G. A., Foster, J. L., and Kumar, S. V.: Development and evaluation of a cloud-gap-filled MODIS daily snow-cover product. *Remote Sens. Environ.*, 114(3), 496-503, 2010.

Harder, P., Schirmer, M., Pomeroy, J. and Helgason, W.: Accuracy of snow depth estimation in mountain and prairie environments by an unmanned aerial vehicle. *The Cryosphere*, 10, 2559, 2016.

Harpold, A., and Coauthors: LiDAR derived snowpack data sets from mixed conifer forests across the Western United States. *Water Resour. Res.*, 50, 2749-2755, 2014.

Hopkinson, C., Chasmer, L., Young-Pow, C., and Treitz, P.: Assessing forest metrics with a ground-based scanning lidar. *Can. J. For. Res.*, 34, 573-583, 2004.

Keyetieu, R., and Seube, N.: Automatic Data Selection and Boresight Adjustment of lidar Systems. *Remote Sensing*, 11, 1087, 2019.

Kirchner, P., Bales, R., Molotch, N., Flanagan, J., and Guo, Q.: LiDAR measurement of seasonal snow accumulation along an elevation gradient in the southern Sierra Nevada, California. *Hydrol. Earth Syst. Sci.*, 18, 4261-4275, 2014.

Kraus, K., and Pfeifer, N.: Advanced DTM generation from LiDAR data. *International Archives of Photogrammetry, Remote Sensing and Spatial Information Sciences*, 34, 23-30, 2011.

Kumari, P., Carter, W. E., & Shrestha, R. L.: Adjustment of systematic errors in ALS data through surface matching. *Adv. Space Res.*, 47(10), 1851-1864, 2011.

Li, Z., Tan, J., & Liu, H.: Rigorous boresight self-calibration of mobile and UAV LiDAR scanning systems by strip adjustment. *Remote Sens.*, 11(4), 442, 2019.

López-Moreno, J. I., Revuelto, J., Alonso-González, E., Sanmiguel-Valladolid, A., Fassnacht, S. R., Deems, J., and Morán-Tejeda, E.: Using very long-range terrestrial laser scanner to analyze the temporal consistency of the snowpack distribution in a high mountain environment. *J. Mt. Sci.*, 14, 823-842, 2017.

Maas, H. G.: Least-squares matching with airborne laserscanning data in a TIN structure. *International Archives of Photogrammetry and Remote Sensing*, 33(B3/1; PART 3), 548-555, 2000.

Mazzotti, G., Currier, W. R., Deems, J. S., Pflug, J. M., Lundquist, J. D., and Jonas, T.: Revisiting snow cover variability and canopy structure within forest stands: insights from airborne lidar data. *Water Resour. Res.*, 55, 6198-6216, 2019.

Meyer, J., and Skiles, S. M.: Assessing the ability of structure from motion to map high resolution snow surface elevations in complex terrain: A case study from Senator Beck Basin, CO. *Water Resour. Res.*, 55, 6596-6605, 2019.

Monson, R. K., Lipson, D. L., Burns, S. P., Turnipseed, A. A., Delany, A. C., Williams, M. W., and Schmidt, S. K.: Winter forest soil respiration controlled by climate and microbial community composition. *Nature*, 439, 711, 2006.

Mott, R., Schirmer, M., and Lehning, M.: Scaling properties of wind and snow depth distribution in an Alpine catchment. *J. Geophys. Res.-Atmos.*, 116, 2011.

Mott, R., Vionnet, V., and Grünewald, T.: The seasonal snow cover dynamics: review on wind-driven coupling processes. *Front. Earth Sci.*, 6, 197, 2018.

Muir, J., Goodwin, N., Armston, J., Phinn, S., and Scarth, P.: An accuracy assessment of derived digital elevation models from terrestrial laser scanning in a sub-tropical forested environment. *Remote Sens.*, 9, 843, 2017.

Nolan, M., Larsen, C., and Sturm, M.: Mapping snow-depth from manned-aircraft on landscape scales at centimeter resolution using Structure-from-Motion photogrammetry. *The Cryosphere*, 9, 1445–1463, 2015.

Painter, T. H., Berisford, D. F., Boardman, J. W., Bormann, K. J., Deems, J. S., Gehrke, F., Hedrick, A., Joyce, M., Laidlaw, R., Marks, D. and Mattmann, C.: The Airborne Snow Observatory: Fusion of scanning lidar, imaging spectrometer, and physically-based modeling for mapping snow water equivalent and snow albedo. *Remote Sensing of Environment*, 184, 139-152, 2016.

Palace, M., Sullivan, F. B., Ducey, M., & Herrick, C.: Estimating tropical forest structure using a terrestrial lidar. *PLoS One*, 11(4), 2016.

Perron, C.J., Bennett, K., & Lee, T.D.: Forest stewardship plan: Thompson farm. NH: University of New Hampshire. Produced by Ossipee Mountain Land Company, West Ossipee, <https://colsa.unh.edu/sites/default/files/thompson-farm-plan.pdf>, 2004.

Reinmann, A. B., and Templer, P. H.: Increased soil respiration in response to experimentally reduced snow cover and increased soil freezing in a temperate deciduous forest. *Biogeochemistry*, 140, 359-371, 2018.

Schweizer, J., Jamieson, J. B., and Schneebeli, M.: Snow avalanche formation. *Rev. Geophys.*, 41, 25, 2003. Starkloff, T., Stolte, J., Hessel, R., and Ritsema, C.: Investigating the development of shallow snowpacks on arable land, using comprehensive field observations and spatially distributed snow modelling. *Hydrol. Res.*, 49, 41-59, 2017.

Sturm, M., and Holmgren, J.: An automatic snow depth probe for field validation campaigns. *Water Resour. Res.*, 54, 9695-9701, 2018.

Team, R. C.: *R: A language and environment for statistical computing*; 2018.

Tonkin, T. N., and Midgley, N. G.: Ground-Control Networks for Image Based Surface Reconstruction: An Investigation of Optimum Survey Designs Using UAV Derived Imagery and Structure-from-Motion Photogrammetry. *Remote Sens.*, 8, 8, 2016.

Tucker, C. L., Tamang, S., Pendall, E., and Ogle, K.: Shallow snowpack inhibits soil respiration in sagebrush steppe through multiple biotic and abiotic mechanisms. *Ecosphere*, 7, e01297, 2016.

Tuttle, S. E., Cho, E., Restrepo, P. J., Jia, X., Vuyovich, C. M., Cosh, M. H., & Jacobs, J. M.: Remote sensing of drivers of spring snowmelt flooding in the north central US. In V. Lakshmi (Ed.), *Remote Sensing of Hydrological Extremes* (pp. 21–45). Switzerland: Springer International Publishing. [https://doi.org/10.1007/978-3-319-43744-6\\_2](https://doi.org/10.1007/978-3-319-43744-6_2), 2017.

Vander Jagt, B., Lucieer, A., Wallace, L., Turner, D., and Durand, M.: Snow depth retrieval with UAS using photogrammetric techniques. *Geosci.*, 5(3), 264-285, 2015.

Wallace, L., Lucieer, A., and Watson, C. S.: Evaluating tree detection and segmentation routines on very high resolution UAV LiDAR data. *IEEE T. Geosci. Remote*, 52, 7619-7628, 2014.

Wallace, L., Lucieer, A., Watson, C., and Turner, D.: Development of a UAV-LiDAR system with application to forest inventory. *Remote Sens.*, 4, 1519-1543, 2012.

Watanabe, K., and Osada, Y.: Comparison of hydraulic conductivity in frozen saturated and unfrozen unsaturated soils. *Vadose Zone J.*, 15, 2016.

Wever, N., Jonas, T., Fierz, C., and Lehning, M.: Model simulations of the modulating effect of the snow cover in a rain-on-snow event. *Hydrol. Earth Syst. Sci.*, 18, 4657-4669, 2014.

Zhang, K., Chen, S.-C., Whitman, D., Shyu, M.-L., Yan, J., and Zhang, C.: A progressive morphological filter for removing nonground measurements from airborne LIDAR data. *IEEE T. Geosci. Remote*, 41, 872-882, 2003.

Zhang, Z., Sun, L., Zhong, R., Chen, D., Xu, Z., Wang, C., ... & Li, R.: 3-D deep feature construction for mobile laser scanning point cloud registration. *IEEE Geosci. Remote S.*, 16(12), 1904-1908, 2019.